

University of Nottingham
UK | CHINA | MALAYSIA

Design, Optimisation, *In Vitro* and *In Vivo* Evaluation of Promising Once-A-Day Tablet Formulations of the Novel Antihypertensive Drug MT-1207

Napoleon Nikolaos Vrettos, MSc

Submitted to the University of Nottingham for the degree of

Doctor of Philosophy

January 2022

Publications related to this thesis

Vrettos NN, Wang P, Wang Y, Roberts CJ, Xu J, Yao H, Zhu Z. *Novel gastroretentive bilayer tablets based on a combination of hydrophilic and hydrophobic polymers: Preparation, in vitro/in vivo characterisation, and pH effect investigation*. Under review.

Vrettos NN, Roberts CJ, Zhu Z. *Gastroretentive Technologies in Tandem with Controlled-Release Strategies: A Potent Answer to Oral Drug Bioavailability and Patient Compliance Implications*. Pharmaceutics. 2021. 13(10), 1591. DOI: https://doi.org/10.3390/pharmaceutics13101591

Vrettos NN, Wang P, Zhou Y, Roberts CJ, Xu J, Yao H, Zhu Z. *In vitro and in vivo evaluation of a sustained-release once-a-day formulation of the novel antihypertensive drug MT-1207*. Pharmaceutical Development and Technology. 2021. 26(3): 349-361. DOI: https://doi.org/10.1080/10837450.2021.1872087

Author's Declaration

The research work presented in this Thesis entitled "Design, Optimisation, *In Vitro* and *In Vivo* Evaluation of Promising Once-A-Day Tablet Formulations of the Novel Antihypertensive Drug MT-1207" has been entirely performed by me, unless otherwise cited and acknowledged. I hereby declare that this work is original and has not been submitted in part, or full, for any other degree or diploma at any other University or Institution. All contributions of others are indicated in references to the literature.

Acknowledgements

I would like to start by expressing my gratitude towards my primary supervisor, Dr Zheying Zhu, for giving me the opportunity to work on this amazing project. She continuously supported me throughout my PhD journey, was always there for me with great suggestions and ideas, and forged me into an independent researcher, a PhD. I am most grateful for her unconditional support and the opportunity to work under her supervision.

I would like to thank my second supervisor, Professor Clive J Roberts, for his supervision and support throughout my PhD. His critical thinking, comments and suggestions helped me improve as a person and as a scientist and elevated the quality of my work. His door was always open for me, and for that, I will always be grateful. He and Dr Zheying Zhu made a great supervision team that rendered my supervision meetings pleasant and most fruitful.

Furthermore, I would like to thank Yuhan Wang (MRes student) whom I was task supervisor during her research project during the period October 2020 – September 2021. She was a great person to work with and provided valuable help and support during the execution of the *in vitro* release testing of the gastroretentive bilayer tablets. It was wonderful supervising her, and I wish her all the best for her PhD.

I would like to thank Shenyang Haiwang Biotechnology Co. Ltd. (Shenyang, China), the company that fully funded my PhD tuition fees and monthly stipends, as well as the animal studies conducted during my PhD project. Without the financial support of this company, the present thesis would have never been written and this PhD would have never been undertaken. Furthermore, Mr Peng Wang, the project collaborator from the company, was always there for me to provide any help and support I needed, including any possible information on MT-1207, even, though, most of it was confidential at the time.

Additionally, I would like to thank my parents and family for their emotional support throughout these 3 years. They were always there for me, always available to listen to any worries or issues I had at different periods. Without them to support me when things got very hard, I am not sure whether I would be able to complete my PhD.

In addition to the above, I would like to express my gratitude towards my partner, Wenshi He. Since the very start of our relationship, Wenshi was always there for me. During my PhD, she endured quite a few of my mental breakdowns and she provided support without the slightest of complaints. The first lockdown of the pandemic created a distance of 1,716 miles between us (distance between Nottingham, UK and Tripoli, Greece), but, still, she was there for me and endured the whole situation. I do not think there are any words in which I could express my gratitude towards her. Her advice and example triggered a shift of my mindset that probably saved my PhD and my view towards it.

Finally, I would like to thank my friends both inside and outside the University, both inside and outside Nottingham, both inside and outside the UK. They were always there to share good moments with me and have a good laugh and a good cup of coffee or pint!

Abstract

Hypertension is the most common cardiovascular disease characterised by elevated systolic and diastolic blood pressure. Globally, around 1.28 billion adults have hypertension with only about 21 % having it under control. Prevalence depends on a range of different factors. Currently, there are many different drugs that are used to manage hypertension through different mechanisms of action. In recent years, guidelines suggest that hypertension should be treated with a combinatory therapy from its onset, instead of monotherapy, so that many different receptors can be targeted. However, the administration of many different drugs to hypertensive patients (polypharmacy) can in itself impede patient compliance to the treatment, reducing the desired effectiveness of this approach.

MT-1207 is a new promising antihypertensive agent that targets multiple different receptors, namely, calcium channels, α_1 and serotonin (5-Hydroxytryptamine) 5-HT_{2A} receptors. Its safety and efficacy have been indicated in preclinical animal studies and phase I clinical trials in healthy human subjects. Immediate-release tablets of MT-1207 have been developed and are currently being tested in phase Ib/IIa clinical trials.

The aim of the present study was to develop sustained-release tablet formulations of MT-1207 that could be administered as a once-a-day dosing regimen, thereby providing improved patient compliance and better control of the drug plasma levels. Initially, to achieve this, single-layer hydroxypropyl methylcellulose (HPMC) matrix tablets were prepared and characterised *in vitro*. Based on the results, an optimised HPMC matrix tablet formulation was selected and was forwarded to a pharmacokinetic study in Beagle dogs.

Based on the *in vivo* study results, further formulation optimisation was carried out by developing non-effervescent gastroretentive bilayer tablets that consisted of a novel gastroretentive layer and an MT-1207-containing layer. As part of the gastroretentive layer

optimisation, a factorial experiment was designed and executed to determine the factors affecting the *in vitro* buoyancy behaviour of the tablets. Based on the factorial experiment results, an optimised gastroretentive layer was designed which was easy to prepare, ensured an immediate floatation of the tablets, and maintained tablet buoyancy over more than 24 hours in fasted state simulated gastric fluid (FaSSGF) pH 1.6, regardless of the drug layer composition. It was also shown that the media pH influenced the total floating time of the tablets. Based on scanning electron microscopy (SEM) imaging and viscosity analysis, a statistically significant difference in the total floating time values of the bilayer tablets over the pH range 1.0 – 6.0 was attributed to pH-dependent degradation of polyethylene oxide (PEO) in acidic conditions at temperatures above 36 °C. With regards to the drug layer, ethylcellulose was incorporated as an additional release retardant. The *in vitro* release testing demonstrated that the presence of the gastroretentive layer was the main factor that significantly retarded the release of MT-1207 from the bilayer tablets, rather than the amount of ethylcellulose incorporated into the drug layer. Ultimately, two bilayer formulations were developed that provided a complete sustained release of MT-1207 maintained over 24 hours.

The non-effervescent gastroretentive bilayer tablet formulations were forwarded to a second pharmacokinetic study in Beagle dogs in fed conditions. The study results demonstrated the potential of those formulations to be used for the once-a-day oral delivery of MT-1207. The bilayer tablet formulations will be the subject of clinical trials.

Table of Contents

Publications related to this thesis i

Author's Declaration ii

Acknowledgements iii

Abstract v

List of Abbreviations xii

List of Figures xvii

List of Tables xxii

1 Chapter 1: General Introduction 1

1.1 Hypertension 1

1.1.1 Definition 1

1.1.2 Aetiology of hypertension 1

1.1.3 Diagnosis and risks of hypertension 2

1.1.4 Treatment of hypertension 3

1.2 Controlled-release formulations 4

1.2.1 Matrix systems 4

1.2.2 Gastroretentive systems 11

1.3 MT-1207 as a new choice for hypertension treatment 28

1.3.1 Physicochemical properties 28

1.3.2 Animal studies 29

1.3.3 Phase I clinical trials 36

1.4 Thesis Aim and Hypothesis 37

2 Chapter 2: Materials and Methods 40

2.1 Materials 40

2.2 HPLC-UV method for the quantitation of MT-1207 samples 40

2.3 Flowability characterisation of the tablet blends....41
2.4 Hardness and friability of tablets....42
2.5 Tablet weight variation....42
2.6 Differential scanning calorimetry (DSC) analysis of MT-1207 and tablet samples....42
2.7 Fourier-Transform Infrared (FTIR) spectrophotometric studies....43
2.8 X-ray powder diffraction (XRPD) analysis of MT-1207 and tablet samples....43
2.9 Kinetics and mechanism of drug release....43
2.10 Bioanalytical method....45
3 Chapter 3: Preparation, *In Vitro* Characterisation and *In Vivo* Evaluation of MT-1207 Sustained-Release HPMC Matrix Tablets....47
3.1 Introduction....48
3.1.1 Experimental aim....48
3.2 Experimental Techniques....49
3.2.1 Validation of HPLC and dissolution methods....50
3.2.2 Scanning electron microscopy (SEM) analysis of MT-1207 reference standard and micronised MT-1207....52
3.2.3 Solubility measurements of MT-1207:colloidal silicon dioxide 5:1 mixture....52
3.2.4 Preparation of MT-1207 tablet formulations....53
3.2.5 Flowability characterisation of the powder mixtures....54
3.2.6 In vitro release of MT-1207 from sustained-release tablets....54
3.2.7 Swelling and erosion studies....55
3.2.8 *In vivo animal study*....56
3.2.9 *In vitro and in vivo data analysis*....57
3.3 Results and Discussion....58

3.3.1 HPLC method development for the quantitation of MT-1207 agent in dissolution samples 58

3.3.2 HPLC and dissolution method validation 59

3.3.3 Scanning electron microscopy and solubility characterisation of MT-1207 61

3.3.4 Characterisation of flowability and compressibility of the tablet powder blends 63

3.3.5 Post-compression parameters of tablet formulations 65

3.3.6 DSC analysis 67

3.3.7 FTIR analysis 69

3.3.8 XRPD analysis 70

3.3.9 In vitro release of MT-1207 from sustained-release tablets 71

3.3.10 Swelling and erosion study 74

3.3.11 Kinetics and mechanism of MT-1207 release from formulation F4 75

3.3.12 In vivo animal study 76

3.4 Conclusions 79

4 Chapter 4: Preparation, Optimisation and *In Vitro* Characterisation of Non-Effervescent Gastroretentive Bilayer Tablet Formulations For Once-a-Day Delivery of MT-1207 82

4.1 Introduction 83

4.1.1 Experimental aim 84

4.2 Experimental Techniques 86

4.2.1 Validation of HPLC and dissolution methods 86

4.2.2 Preparation of preliminary gastroretentive layer tablets and MT-1207 gastroretentive bilayer tablets 88

4.2.3 Design of the factorial experiment for the gastroretentive layer 91

4.2.4 In vitro buoyancy 93

4.2.5 Tablet dimension and wet strength measurements 94

4.2.6 Tablet density and porosity determination 94

4.2.7 SEM analysis of the optimised gastroretentive layer of the tablets in different media…… 95

4.2.8 Viscosity study 95

4.2.9 In vitro release of MT-1207 from gastroretentive bilayer tablets 96

4.2.10 Data analysis 96

4.3 Results and Discussion 97

4.3.1 Flowability testing of gastroretentive and drug layer powder mixtures 97

4.3.2 In vitro buoyancy and wet strength testing of the gastroretentive layer tablets 98

4.3.3 Factorial experiment 102

4.3.4 Post-compression characterisation of tablets 110

4.3.5 Physicochemical characterisation of MT-1207 and the optimised tablets 112

4.3.6 Tablet density and porosity characterisation 116

4.3.7 In vitro buoyancy in media of different pH values 117

4.3.8 In vitro release study 127

4.3.9 Kinetics and mechanism of drug release from bilayer F_{HE6005} and bilayer A1 tablets… 134

4.4 Conclusions 136

5 Chapter 5: *In Vivo* Pharmacokinetic Study of the Optimised Gastroretentive Bilayer Tablet Formulations in Beagle Dogs 138

5.1 Introduction 138

5.1.1 Experimental aim 138

5.2 Methodology 138

5.3 Results and Discussion 139

5.4 Conclusions 144
6 Chapter 6: General Conclusions 145
7 Chapter 7: Limitations and Future Work 148
7.1 Limitations 148
7.2 Future Work 149
Appendix 150
Chapter 3 HPLC and dissolution method validation 150
- Linearity 150
- LOD and LOQ determination 153
- Specificity 154
- Accuracy, intra-day and inter-day precision 155
Chapter 4 HPLC and dissolution method validation 157
- Linearity 157
- LOD and LOQ determination 160
- Specificity 161
- Accuracy, intra-day and inter-day precision 162
References 164

List of Abbreviations

2K1C – Two-kidney one-clip

5-HT – 5-Hydroxytryptamine

% v/v – % volume/volume

% w/v – % weight/volume

% w/w – % weight/weight

ACE – Angiotensin-converting enzyme

ADME – Absorption, distribution, metabolism and excretion

AGS – Adenocarcinoma gastric

ANOVA – Analysis of variance

API – Active pharmaceutical ingredient

AUC – Area under the curve

BP – Blood pressure

CHF – Coronary heart failure

CL – Clearance

cm – Centimeter(s)

DBP – Diastolic blood pressure

DSC – Differential scanning calorimetry

EMA – European Medicines Agency

ESC/ESH – European Society of Cardiology/European Society of Hypertension

ESI – electron spray ionisation

FaSSGF – Fasted state simulated gastric fluid

FDA – Food and Drug Administration

FDC – Fixed-dose combination

FTIR – Fourier-transform infrared

g – Gram(s)

GIT – Gastrointestinal tract

GRDDS – Gastroretentive drug delivery system(s)

GRT – Gastric residence time

h – Hour(s)

HBS – Hydrodynamically balanced system(s)

HCl – Hydrochloric acid

HCSO – Hydrogenated cottonseed oil

HPC – Hydroxypropyl cellulose

HPLC – High-performance liquid chromatography

HPMC – Hydroxypropyl methylcellulose

IBS-D – Irritable bowel syndrome with diarrhoea

ICH – The International Council for Harmonisation of Technical Requirements for Pharmaceuticals for Human Use

IPA – Isopropyl alcohol

IR – Immediate-release

kg – Kilogram(s)

kN – Kilonewton(s)

kPa – Kilopascal(s)

kV – Kilovolt(s)

L – Litre(s)

LOD – Limit of Detection

LOQ – Limit of Quantitation

MCC – Microcrystalline cellulose

mg – Milligram(s)

min – Minute(s)

mL – Millilitre(s)

mm – millimetre(s)

M – molarity

MMC – Migrating motor complex

MRM – Multiple response monitoring

MRT – Mean residence time

MS – Mass spectrometry/Mass spectrometer

N – Newton(s)

NaCl – Sodium chloride

NADPH – Nicotinamide adenine dinucleotide phosphate

ng – Nanogram(s)

NICE – National Institute for Health and Care Excellence

o.d. – Once daily

PEO – Polyethylene oxide

psi – Pounds per square inch

PVP – Polyvinylpyrrolidone

rpm – Revolutions per minute

RSD – Residual standard deviation

S – Slope

s – Second

SBP – Systolic blood pressure

SD – Sprague Dawley (rats)

SD – Standard deviation

SDL – Spray-dried lactose

SDS – Sodium dodecyl sulfate

SEM – Scanning electron microscopy

SHR – Spontaneously hypertensive rat(s)

SHR-SP – Stroke-prone spontaneously hypertensive rat(s)

SR – Sustained-release

THCPSi – Thermally hydrocarbonised porous silicon

t.i.d – Three times a day

UPLC – Ultra-performance liquid chromatography

US – United States

USP – United States Pharmacopoeia

UV – Ultraviolet

WHO – World Health Organisation

XRPD – X-ray powder diffraction

μL – Microlitre(s)

μm – Micrometer

List of Figures

Figure 1-1: *The matrix system where drug particles are distributed in a polymer matrix. The figure was created using BioRender (https://www.biorender.com/).* 5

Figure 1-2: *Intragastric location of the floating drug delivery systems. The figure was created using BioRender (https://www.biorender.com/).* 13

Figure 1-3: *Schematic localisation of high-density systems in the stomach. The figure was created using BioRender (www.biorender.com).*.....21

Figure 1-4: *Localisation of mucoadhesive/bioadhesive drug delivery systems in the stomach. The figure was created using BioRender (www.biorender.com).*.....22

Figure 1-5: *Intragastric behaviour of (a) expandable and (b) superporous hydrogel systems. The figure was created using BioRender (www.biorender.com).*.....26

Figure 1-6: *Application of magnetic drug delivery systems for gastric retention purposes. The figure was prepared using BioRender (www.biorender.com).* 27

Figure 1-7: *The chemical structure of MT-1207 hydrochloride (207).*.....28

Figure 1-8: *Possible metabolic pathways of MT-1207 in SD rats. No changes were made to the original figure (208).*.....32

Figure 3-1: *Chromatogram of MT-1207 0.05 mg/mL standard solution in 0.1 M phosphate pH 6.8 with 0.2% w/v SDS. The MT-1207 peak was eluted at around 5.0 minutes. The solvent front was eluted at around 2.5 minutes.*.....58

Figure 3-2: *Calibration curve of MT-1207 in 0.1 M phosphate pH 6.8 with 0.2% w/v SDS at a concentration range of 0.001 − 0.05 mg/mL.* 59

Figure 3-3: *SEM image of (A) MT-1207 reference standard and (B) micronised MT-1207:silicon dioxide 5:1 mixture.* 63

Figure 3-4: *DSC thermogram of MT-1207 hydrochloride reference standard.*.....68

Figure 3-5: *DSC thermograms of (A) Formulation F1, (B) Formulation F2, (C) Formulation F3 and (D) Formulation F4.*.....68

Figure 3-6: *Fourier-Transform Infrared (FTIR) spectra of (A) MT-1207 hydrochloride reference standard, (B) HPMC K15M, (C) colloidal silicon dioxide and (D) pulverised tablets [Transmittance vs Wavenumber (cm^{-1})]*.....69

Figure 3-7: *Diffractograms of (A) MT-1207 hydrochloride reference standard, (B) formulations F1 (red) and F4 (blue) and (C) MT-1207 hydrochloride reference standard (red), F4 (blue) and alpha-D-lactose monohydrate (green) combined [Intensity (Counts) vs Position(˚2Theta)]*.....71

Figure 3-8: *In vitro release profiles of MT-1207 from immediate-release tablets, and formulations F1, F2, F3, F4 and A1 in 0.1 M phosphate pH 6.8 with 0.2% w/v SDS (n = 3).* 72

Figure 3-9: *In vitro release profiles of MT-1207 (% of MT-1207 released vs time) from the three F4 batches in 0.1 M phosphate pH 6.8 with 0.2% w/v SDS (n = 3).*.....73

Figure 3-10: *In vitro swelling and erosion profiles of formulation F4 in 0.1 M phosphate pH 6.8 with 0.2% w/v SDS (% swelling and % erosion vs time, n = 3).* 74

Figure 3-11: *Plasma concentration of MT-1207 in Beagle dogs after oral administration of 30 mg SR tablet o.d., 10 mg IR tablet t.i.d. and 3 × 10 mg IR tablet o.d. (n = 4).* 78

Figure 4-1: *DSC thermograms of (A) MT-1207 hydrochloride reference standard and (B) optimised drug layer of the bilayer tablets.* 113

Figure 4-2: *Diffractograms of MT-1207 hydrochloride reference standard (red), alpha-D-lactose monohydrate (green) and the drug layer of the optimised bilayer* F_{HE6005} *tablets (blue).* 115

Figure 4-3: *FTIR spectra of (A) MT-1207 hydrochloride reference standard and (B) drug layer of the optimised bilayer* F_{HE6005} *tablets.* 116

Figure 4-4: *SEM images of the optimised gastroretentive layer of the dry bilayer tablets.*..120

Figure 4-5: *SEM images of the optimised gastroretentive layer of the bilayer tablets after 12 hours of in vitro buoyancy testing in (A) HCl pH 1.0, (B) phosphate pH 3.0, and (C) phosphate pH 6.0.* 121

Figure 4-6: *SEM images of the optimised gastroretentive layer of the bilayer tablets after 22 hours of in vitro buoyancy testing in (A) HCl pH 1.0, (B) phosphate pH 3.0, and (C) phosphate pH 6.0.* 122

Figure 4-7: *SEM images of the optimised gastroretentive layer of the bilayer tablets after 31 hours of in vitro buoyancy testing in (A) phosphate pH 3.0, and (B) phosphate pH 6.0.*.....123

Figure 4-8: *SEM images of the optimised gastroretentive layer of the bilayer tablets after 43.5 hours of in vitro buoyancy testing in phosphate pH 6.0.* 124

Figure 4-9: *Viscosity of HCl pH 1.0, phosphate pH 3.0 and phosphate pH 6.0 media during in vitro buoyancy testing of the optimised gastroretentive bilayer tablets (n = 3). Results are presented as mean ± standard deviation.* 125

Figure 4-10: *In vitro drug release profiles of A1, single-layer F_{HE6005} and the bilayer tablet formulations in 0.1 M acetate pH 4.0 at 75 rpm (n = 3 tablets). Results are presented as mean ± standard deviation.*.....130

Figure 4-11: *In vitro release profiles of MT-1207 from bilayer F_{HE6005} and bilayer A1 tablets at paddle rotation speeds of 75 rpm and 200 rpm (n = 3 tablets). Results are presented as mean ± standard deviation.*.....133

Figure 5-1: *Plasma concentration of MT-1207 in Beagle dogs after oral administration of bilayer F_{HE6005} tablet o.d., bilayer A1 tablet o.d., and 3 × 10 mg IR tablet o.d. (n = 4).* 141

Figure A-1: *MT-1207 calibration curve in 0.1 M phosphate pH 6.8 with 0.2% w/v SDS:methanol 95:5 (% v/v) replicate 1 (Peak Area vs Concentration)*…….149

Figure A-2: *MT-1207 calibration curve in 0.1 M phosphate pH 6.8 with 0.2% w/v SDS:methanol 95:5 (% v/v) replicate 2 (Peak Area vs Concentration)*…….150

Figure A-3: *MT-1207 calibration curve in 0.1 M phosphate pH 6.8 with 0.2% w/v SDS:methanol 95:5 (% v/v) replicate 3 (Peak Area vs Concentration)*…….151

Figure A-4: *MT-1207 calibration curve in 0.1 M phosphate pH 6.8 with 0.2% w/v SDS:methanol 95:5 (% v/v) that was used for the LOD and LOQ determination (Peak Area vs Concentration). Peak area results are presented as mean ± standard deviation.* ……152

Figure A-5: *Chromatogram of specificity sample (n = 3)*……..152

Figure A-6: *MT-1207 calibration curve in 0.1 M acetate buffer pH 4.0 replicate 1 (Peak Area vs Concentration)*……155

Figure A-7: *MT-1207 calibration curve in 0.1 M acetate buffer pH 4.0 replicate 2 (Peak Area vs Concentration)*……156

Figure A-8: *MT-1207 calibration curve in 0.1 M acetate buffer pH 4.0 replicate 3 (Peak Area vs Concentration)*……157

Figure A-9: *MT-1207 calibration curve in 0.1 M acetate buffer pH 4.0 (Peak Area vs Concentration) (n = 3). Results are shown as mean ± standard deviation*……...……..158

Figure A-10: *Chromatogram of specificity sample (n = 3)*……159

List of Tables

Table 1-1: *MT-1207 pharmacokinetic parameter values after (i) oral administration of 0.75, 1.5, and 3 mg/kg of the drug in Beagle dogs during fasted state, (ii) after oral administration of 1.5 mg/kg MT-1207 during fed state, and (iii) after oral administration of 1.5 mg/kg MT-1207 twice daily over seven consecutive days (208).* 30

Table 1-2: *MT-1207 pharmacokinetic parameter values after oral administration of 1, 3, and 9 mg/kg of the drug in Sprague Dawley rats during fasted state (208).*.....31

Table 3-1: *Compositions of the MT-1207 sustained-release tablets.* 54

Table 3-2: *Solubility values of non-micronised MT-1207 hydrochloride reference standard and micronised MT-1207 hydrochloride:colloidal silicon dioxide 5:1 mixture in HCl pH 1.2 (n = 9) and 0.1 M phosphate buffer pH 6.8 (n = 9). Results are expressed as mean ± standard deviation.*.....62

Table 3-3: *Flowability characterisation results.* 64

Table 3-4: *Tablet hardness and friability testing results (n = 10 tablets for each formulation). Results are presented as mean ± standard deviation.*.....66

Table 3-5: *Tablet weight variation testing results (n = 10 tablets per formulation).*.....67

Table 3-6: *Formulation F4 kinetic analysis results.*.....75

Table 3-7: *Pharmacokinetic parameters of MT-1207 after oral administration of a single MT-1207 30 mg sustained-release tablet (30 mg SR o.d.), 10 mg immediate-release tablets (one tablet at a time) three times a day (10 mg IR t.i.d.) and three 10 mg immediate-release tablets administered at the same time (3 × 10 mg IR o.d.) to Beagle dogs (n = 4).*.....77

Table 4-1: *Compositions of the gastroretentive layers G1 − G20.* 90

Table 4-2: *Compositions of the bilayer tablet ethylcellulose-containing drug layers.*.....90

Table 4-3: *Experimental layout of the gastroretentive layer factorial experiment.* 92

Table 4-4: *Bulk/Tapped density testing results for the gastroretentive layer powder mixtures of the preliminary gastroretentive layer experiments (G1 − G20).* 97

Table 4-5: *Flowability characterisation results of the different gastroretentive layer powder mixtures of the factorial experiment.* 98

Table 4-6: *Flowability characterisation results of the different drug layer powder mixtures.*98

Table 4-7: *In vitro buoyancy, wet strength and swollen dimension measurement data of the gastroretentive layer tablets (G1 − G20) compressed using a force of 7.5 kN (n = 3 tablets). Results are presented as mean ± standard deviation.*.....100

Table 4-8: *In vitro buoyancy, wet strength and swollen dimension measurement data of the gastroretentive layer tablets compressed using a force of 8.5 kN (G10 – G12 and G14 – G18) (n = 3 tablets). Results are expressed as mean ± standard deviation.* 101

Table 4-9: *Factorial experiment results for the different formulations, regarding their floating lag time and total floating time (n = 3 tablets). Results are expressed as mean ± standard deviation.* 103

Table 4-10: *Post-compression parameters of the factorial experiment bilayer tablets and wet strength characterisation results after the in vitro buoyancy run (n = 3 tablets). Results are reported as mean ± standard deviation.* 106

Table 4-11: *Hardness and friability testing results for the bilayer tablets containing different drug layers (n = 10 tablets). The thickness, hardness and tensile strength results are presented as mean ± standard deviation.* 111

Table 4-12: *Tablet weight variation testing results for the bilayer tablets containing different drug layers (n = 10 tablets).* 112

Table 4-13: *In vitro buoyancy testing results for the optimised gastroretentive bilayer* F_{HE6005} *tablets in HCl pH 1.0, phosphate pH 3.0, and phosphate pH 6.0. Results are presented as mean ± standard deviation.*.....118

Table 4-14: *The optimised bilayer tablet formulation (*F_{HE6005} *and A1) details.* 134

Table 4-15: *Bilayer* F_{HE6005} *kinetic analysis results.* 135

Table 4-16: *Bilayer A1 kinetic analysis results.* 136

Table 5-1: *Pharmacokinetic parameters of MT-1207 after oral administration of a single MT-1207 30 mg gastroretentive bilayer* F_{HE6005} *tablet (*F_{HE6005} *o.d.), a single MT-1207 30 mg gastroretentive bilayer A1 tablet (Bilayer A1 o.d.), and three MT-1207 10 mg immediate-release tablets administered at the same time (3 × 10 mg IR o.d.) to Beagle dogs (n = 4).* .141

Table A-1: Concentration and peak area values of MT-1207 calibration curve in 0.1 M phosphate pH 6.8 with 0.2% w/v SDS:methanol 95:5 (% v/v) replicate 1. ……...148

Table A-2: *Concentration and peak area values of MT-1207 calibration curve in 0.1 M phosphate pH 6.8 with 0.2% w/v SDS:methanol 95:5 (% v/v) replicate 2*……149

Table A-3: *Concentration and peak area values of MT-1207 calibration curve in 0.1 M phosphate pH 6.8 with 0.2% w/v SDS:methanol 95:5 (% v/v) replicate 3*……150

Table A-4: *Data of the calibration curve that occurred from calculating the mean of the peak area values from the linearity calibration curves for the respective concentration points (n = 3). Peak area results are presented as mean ± standard deviation*……151

Table A-5: *MT-1207 dissolution method accuracy and intra-day precision validation results at 20 %, 50 %, 80 %, 100 % and 120 % concentration level of MT-1207*……153

Table A-6: *MT-1207 dissolution method inter-day precision validation results at 20 %, 50 %, 80 %, 100 % and 120 % concentration level of MT-1207*……..154

Table A-7: *Concentration and peak area values of MT-1207 calibration curve in 0.1 M acetate buffer pH 4.0 replicate 1*……155

Table A-8: *Concentration and peak area values of MT-1207 calibration curve in 0.1 M acetate buffer pH 4.0 replicate 2*……156

Table A-9: *Concentration and peak area values of MT-1207 calibration curve in 0.1 M acetate buffer pH 4.0 replicate 3*……157

Table A-10: *Data of the calibration curve that occurred from calculating the mean of the peak area values from the linearity calibration curves for the respective concentration points (n = 3). Peak area results are presented as mean ± standard deviation*……....158

Table A-11: *MT-1207 dissolution method accuracy and intra-day precision validation results at 20 %, 50 %, 80 %, 100 % and 120 % concentration level of MT-1207 (n = 3)*……160

Table A-12: *MT-1207 dissolution method inter-day precision validation results at 20 %, 50 %, 80 %, 100 % and 120 % concentration level of MT-1207 (n = 3)*……161

1 Chapter 1: General Introduction

Part of this chapter (Section 1.2.2) has been published in the following review article:

Vrettos NN, Roberts CJ, Zhu Z. *Gastroretentive Technologies in Tandem with Controlled-Release Strategies: A Potent Answer to Oral Drug Bioavailability and Patient Compliance Implications*. Pharmaceutics. 2021. 13(10), 1591. DOI: https://doi.org/10.3390/pharmaceutics13101591

1.1 Hypertension

1.1.1 Definition

Hypertension is the most common cardiovascular disease (1). In the United Kingdom, the National Institute for Health and Care Excellence (NICE) defines the cut-off point between normal blood pressure (BP) and hypertension in adults as sustained systolic blood pressure (SBP) ≥ 140 mm Hg and/or diastolic blood pressure (DBP) ≥ 90 mm Hg following repeated tests (2). According to World Health Organisation (WHO), approximately 1.28 billion adults aged 30-79 years globally have hypertension and only about 21 % of them have it under control (3). Many variables influence the prevalence of this disease, including race, age, and education (4-6). Hypertension presents a significant challenge in therapeutics as it is usually a lifelong disease that causes few symptoms until its advanced stage. It is the most common risk factor of coronary heart failure (CHF) (7, 8).

1.1.2 Aetiology of hypertension

A specific cause of hypertension can only be established in 5 % of patients. Patients in whom no specific cause of hypertension can be found are said to have essential or primary hypertension, while patients with specific aetiology are said to have secondary hypertension (9). It is important, though, to consider specific causes since some of them are amenable to

definitive surgical treatment, e.g coarctation of the aorta, renal artery constriction, pheochromocytoma, Cushing's disease and primary aldosteronism (10-14).

In most cases, elevated BP is connected to an overall increase in resistance to the flow of blood through arterioles, whereas the cardiac output is usually normal. Elevated BP is usually caused by a combination of several (multifactorial) abnormalities, such as genetic factors, psychological stress, along with environmental and dietary factors (increased salt and decreased potassium or calcium intake) that are believed to contribute to hypertension (15-18). Furthermore, as the population ages, increases its body weight and adopts a more sedentary lifestyle, the prevalence of hypertension will continue to rise globally (19).

The heritability of essential hypertension is estimated to be about 30 – 50 % (20). Mutations in several genes have been linked to various rare causes of hypertension. Functional variations of the genes for angiotensinogen, angiotensin-converting enzyme (ACE), the β adrenoceptor and α adducin (a cytoskeletal protein) appear to contribute to some cases of essential hypertension (21-24).

1.1.3 Diagnosis and risks of hypertension

The diagnosis of hypertension is based on repeated, reproducible measurements of elevated BP (25). The diagnosis is mostly used to predict the consequences for the patient, rather than to find the cause of hypertension (1).

Hypertension is the leading preventable risk factor for premature death and disability globally (26). The risks of damage to the kidney, heart and brain are directly related to the extent of BP elevation as seen from epidemiologic studies. Even mild hypertension (140/90 mm Hg) increases the risk of eventual end-organ damage. Both systolic hypertension and diastolic hypertension are related to end-organ damage; so-called isolated systolic hypertension is not benign (27, 28). Hypertension is linked to an increased probability of

sudden cardiac death, angina pectoris, kidney disease, vascular dementia, ophthalmologic disorders, and other events (29). The risks increase in proportion to the magnitude of BP elevation. Other factors that increase risks include smoking (30), metabolic syndrome (including obesity) (31), dyslipidemia (32), diabetes (33), and family history (34).

The diagnosis of hypertension depends on measurements of BP and not on symptoms reported by the patient. Hypertension is usually asymptomatic until end-organ damage is imminent or has occurred (1, 35).

1.1.4 Treatment of hypertension

A therapeutic regimen must be carefully designed once a decision to treat hypertension is made. A properly designed antihypertensive drug therapy has been shown to significantly reduce the probability of new coronary events, stroke, and CHF (29, 36, 37).

Many drugs are used to treat hypertension through different mechanisms of action, such as angiotensin-receptor blockers, ACE inhibitors, beta blockers, calcium channel blockers, diuretics, and alpha-receptor antagonists (19, 38, 39). It is mainly the level of BP and the presence and severity of end-organ damage that dictates the selection of drugs for the therapeutic regimen. In recent years, the paradigm regarding the start of antihypertensive therapy was shifted from monotherapy to drug combinations since they have proved more effective in achieving management of hypertension (25). The use of many different drugs targeting different receptors is called polypharmacy (the concurrent use of multiple medications by a patient) (19, 40). However, the need to take many separate medicines can lead to reduced patient compliance. Therefore, according to the European Society of Cardiology/European Society of Hypertension (ESC/ESH) guidelines, it would be best to initiate antihypertensive treatment using a fixed-dose combination (FDC) to ensure patient compliance to the treatment and to speed up the process towards reaching the target BP (19).

Since hypertension is a chronic disorder, a steady-state concentration of the drug(s) is required throughout the time of treatment (41). Controlled-release formulations are very frequently used to achieve drug release in the desired gastrointestinal tract site at a predetermined rate. For this reason, a few antihypertensive drugs are available in the market as controlled-release products. Typical examples include Coreg® CR (carvedilol), Coracten® SR (nifedipine), Calan® SR (verapamil), and Toprol® XL (metoprolol).

1.2 Controlled-release formulations

Controlled-release formulations are dosage forms from which drugs can be released in a controlled manner over time. There are many different categories of controlled-release formulations, depending on the technology and the consequent release mechanism(s) applied. This thesis will focus on sustained-release matrix systems, as well as gastroretentive formulations.

1.2.1 Matrix systems

In a matrix system (Figure 1-1), the most commonly used system in the pharmaceutical industry, the drug is homogeneously distributed throughout a polymer matrix (42). Drugs may be released through diffusion and/or erosion mechanisms based on the properties of drugs and matrix polymers (43-45). In a matrix dissolution-controlled system, as the polymer matrix dissolves, drug molecules are released. This is also referred to as "erosion-controlled release". This is a usual case for hydrophobic drugs incorporated into hydrophilic polymer matrices (44). Since the size of the matrix decreases as more drug is released, the amount of drug released is also decreased, resulting in a non-zero-order release. In the matrix diffusion-controlled systems, drug molecules may mainly be released via diffusion mechanism through a polymer matrix (42).

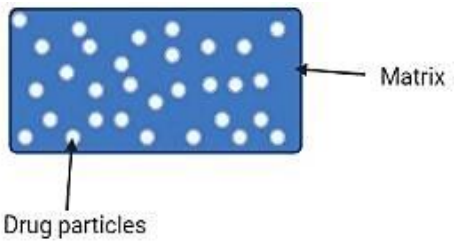


Figure 1-1: *The matrix system where drug particles are distributed in a polymer matrix. The figure was created using BioRender (https://www.biorender.com/).*

1.2.1.1 Dissolution-controlled matrix formulations

The desired controlled-release profile from dissolution-controlled matrix systems is achieved easily through their use, they are cost-effective and have the United States (US) Food and Drug Administration (FDA) acceptance (46). Many different polymers are used in controlled-release systems where release is controlled by the dissolution rate of the polymer matrix. Hydrophilic matrix systems are matrix systems where the release retardant is a hydrophilic polymer. A typical hydrophilic polymer matrix system consists of the drug, the hydrophilic polymer(s) and other excipients distributed throughout the matrix. This system is dependent on polymer wetting, hydration and dissolution with regards to achieving controlled release of the drug (46). Drug release from hydrophilic matrices is believed to be affected by water diffusion through the matrix, drug diffusion through the matrix, as well as the erosion of the hydrated matrix (47).

Many different hydrophilic polymers can be used to prepare oral controlled-release matrix systems. The most commonly used polymers are cellulose ether derivatives which include hydroxypropyl methylcellulose (HPMC), hydroxypropyl cellulose (HPC), and sodium carboxymethylcellulose (48-50). HPMC is a partly O-methylated and O-(2-hydroxypropylated) cellulose (51). Its hydration rate depends on the molecular structure and degree of substitution of these substituents. More specifically, the hydration rate of HPMC increases with increasing hydroxypropyl content (52). It forms swellable matrices that lead to

the formation of viscous solutions, instead of true gels (53). When HPMC of a lower molecular weight is used, such as K15M, the erosion of the swollen polymer matrices control drug release, while HPMC K100M can form stable gels which are more resistant to erosion (47). When HPMC polymers of different molecular weights are used, the effect on the release profile is more obvious for water-insoluble drugs the release of which is governed by erosion than for water-soluble drugs the release of which is governed by diffusion in hydrophilic matrix tablets (54). Furthermore, polyethylene oxide (PEO) is a hydrophilic polymer used in controlled-release tablet preparations and is considered an alternative to HPMC for controlled drug delivery (55, 56). It is a non-ionic polymer, stable over a wide range of physiological pH values. Like HPMC, PEO can swell rapidly forming a homogeneous viscous gel layer and a viscous solution, thus controlling drug release (57, 58). Other polymers, such as chitosan, polyacrylic acid, sodium alginate, gums can also be used as controlled-release matrices (59-63).

Hydrophilic polymers have been used either as sole release retardants or in combinations to achieve controlled release of drugs. Savaşer et al. carried out a study where HPMC K4M, sodium carboxymethylcellulose, Carbopol® and chitosan were used as the sole release retardants or in different combinations to develop a once-a-day tablet formulation of metoclopramide (64). All the tablets that were tested in the study indicated that an increase in the concentration of the gelling polymer in the matrix led to slower drug release. The effect of the dissolution medium in terms of pH was especially observed for Carbopol® and chitosan formulations. The sodium carboxymethylcellulose-based matrices exhibited very fast drug release which was probably due to the higher aqueous solubility of the polymer, along with the fact that it was less ionised in acidic medium and, thus, less viscous. The release of the drug from HPMC-based formulations seemed independent of the pH of the dissolution medium. This was probably because when the polymer comes in contact with

water or other aqueous fluids, it absorbs water and swells or hydrates regardless of the pH of the medium. Matrix tablets that contained a blend of HPMC and chitosan at equal ratio were chosen as the optimised formulation to be forwarded to further studies (64).

Apart from the material properties, formulation and technological factors, such as polymer:drug ratio, polymer and drug particle size, and compression force, also need to be considered. Velasco et al. studied the effects of these factors on the release of diclofenac sodium from HPMC matrix tablets (65). The polymer:drug ratio was found to be the important factor affecting drug release. Increasing polymer concentration potentially resulted in an increased viscosity of the polymer and increased diffusion path of the drug in the gel layer which reduced the rate of drug release, whilst also reducing the gel erosion. With regards to drug particle size, smaller sizes resulted in higher dissolution rates which favoured diffusion mechanism and kinetics of drug release. An increase in the polymer particle size resulted in a reduction or elimination of lag time in drug release which showed that a certain amount of the drug underwent burst release at the beginning of dissolution, prior to the formation of the gel (65). In another study, it has also been found that the effect of polymer particle size is less important at higher polymer contents (66). Since the porosity of the hydrated matrix was independent of the initial tablet porosity, the compression force did not have a significant effect on drug release (65). Additionally, when lactose is used as a diluent in the formulation, the ratio of lactose to HPMC needs to be considered since it has been defined as a key parameter in controlling the hydration and swelling behaviour of the matrix (67).

With regards to matrix erosion, various parameters need to be considered. The polymer content and molecular weight can affect the erosion rate. Jain et al. have reported that the *in vivo* erosion variability decreases with increasing content of high-molecular-weight HPMC in the matrix (68). Also, the erosion rate from hydrophilic matrix tablets could

be expected to vary between different regions in the GI tract due to variations in motility and fluids. The erosion rate in the small intestine tended to be somewhat higher than in the large intestine. Since no correlation could be established between the HPMC release and the movement velocity of the tablets neither in the whole gastrointestinal tract (GIT) nor in the stomach, small intestine, and colon, it was assumed that the variability in the erosion rate could be attributed to the inhomogeneous distribution of fluid (water pockets) in the intestine than to motility (68, 69). The same differences in swelling and erosion behaviour have also been recorded for tablets based on PEO of different molecular weights (70).

The use of multiple grades of polymers should be considered for the development of effective controlled-release formulations. Korner et al. prepared tablets consisting of a single grade of PEO or a mixture of various grades in different ratios (71). It was concluded that the ratio of high/low molecular weight PEO controlled the release rate, and the fraction of high molecular weight polymers dominated the effect on the overall release rate in mixed PEO tablets. Furthermore, the release rate was probably not a single function of the average molecular weight of the polymer. Polydispersity also affected the rate of drug release (71).

1.2.1.2 Diffusion-controlled matrix formulations

Diffusion-controlled matrix formulations utilise water-insoluble, hydrophobic polymers as matrix formers for controlled-release applications. Many different hydrophobic polymers have been used in the literature for the preparation of sustained-release tablet formulations.

Ethylcellulose is a partially ethoxylated cellulose polymer (51). It is non-toxic, stable at varying pH, compressible, inert, and is used in formulations as a binder, film-forming agent, coating material, as well as a matrix material (72-78). Ethylcellulose is available commercially in different viscosity grades (7, 10, 100 mPa.s). However, since it is a water-

insoluble polymer, polymer viscosity grade does not have a significant effect on drug release when it is used in the form of a matrix (72). However, different viscosity grades have different particle size values. The higher the viscosity grade the higher the particle size of the polymer solid particles (72). Particle size seems to affect drug release with smaller particle size values resulting in lower drug release rates, probably because the pores of the matrix are smaller and, thus, drug release is retarded more effectively (72, 79, 80). Also, smaller particle size seems to lead to better compressibility of tablets prepared with ethylcellulose of low viscosity grades, potentially due to greater interparticle cohesion which contributes to slower drug release (72). Furthermore, burst release of drugs has been recorded in cases where ethylcellulose was used as a sole matrix former in matrix tablets. This is probably due to the diffusion of the drug(s) through the pores and cracks in the polymer matrix structure, along with the fact that the gel effect of ethylcellulose is very little, due to its hydrophobicity (81, 82). Additionally, the tablets seem to break rapidly, and the drug is released in few hours when ethylcellulose is used as a sole matrix former. However, when used in combination with other polymers, such as HPMC or methacrylic acid copolymers (Eudragit® RL/RS), it can modulate the tablet *in vitro* release profile (47). Blending of ethylcellulose with HPMC has proved to lead to the formation of an extended-release matrix, especially when the percentage of HPMC is higher than that of ethylcellulose (81). The increased retardation of drug release could be due to the reduced solvent penetration in the matrix caused by the presence of a hydrophobic polymer, thus leading to reduced drug diffusion i.e drug release is monitored by the permeability of the matrix structure (83, 84). Ethylcellulose has also been used in the form of suspension (Surelease®) as a granulating liquid, leading to the formation of granules with improved flowability and compatibility, compared to the respective physical mixtures, whilst also reducing drug release from the resulting matrix tablets (85).

Methacrylic acid copolymers (commercially available as Eudragit®) are hydrophobic polymers that are widely used in oral controlled-release formulations. They are synthesized via free-radical polymerisation from acrylate and methacrylate derivatives that are incorporated into the polymer structure via chain growth reactions (86). The polymerisation reaction can take place in solvent, emulsion, bulk, or suspension. The properties of the final methacrylate copolymer depend on the selection of monomers and determine their application. Eudragit® RL and RS are polymers that are used as both coating agents and hydrophobic matrices. Between the two, Eudragit® RS seems to be the most effective in retarding drug release from polymer matrices containing the two polymers. The permeability of the polymer matrix significantly increases with increasing Eudragit® RL content. This is probably because the latter contains more quaternary ammonium groups than Eudragit® RS, it is more hydrophilic, more permeable to water and, thus, takes up more water and swells to a higher extent (83, 87, 88). Consequently, the polymer chain mobility increases with increasing Eudragit® RL content, resulting in increased drug mobilities within the polymeric network. In matrices containing Eudragit® RS and RL polymer blends, drug release can be easily monitored by changing the polymer ratios within the blend (89). Both Eudragit® RL and RS are water-insoluble and their behaviour is pH independent (88). Furthermore, Eudragit® RS can be used effectively as a binding agent within the matrix for the preparation of granules with characteristics desirable for compaction using an organic solvent, such as ethanol, as the granulating fluid (90).

Apart from polymers, waxes have also been used as matrix formers in the development of hydrophobic sustained-release matrices. Waxy matrices are considered suitable for high-solubility drugs (84). Hydrogenated cottonseed oil (HCSO) consists of triglycerides of hydroxy stearic acid. It has the ability to melt and re-solidify during compression, thus enhancing the bonding capacity of tablets (51). Sudha et al. prepared

hydrophobic tablets based on tramadol-HCSO solid dispersion which was prepared via a hot fusion method. The drug release was reduced significantly with increasing wax concentration in the matrix, while the addition of hydrophilic excipients and/or surfactants enhanced drug release. The drug release from the HCSO tablets best fitted the Higuchi model (91). Furthermore, sustained-release matrix formulations based on cetyl alcohol and stearyl alcohol have been prepared in the literature and provided sustained drug release which best fitted the Higuchi model (82, 92, 93). The use of waxy matrices in sustained-release formulations, however, comes with disadvantages. Even though these matrices can modulate drug release, the procedures that must be carried out, such as hot fusion and thermal treatment, highlight the length of the manufacturing process that would be required to form such tablets. This can potentially be a deterrent for manufacturing companies that would prefer a more economical method of producing sustained-release formulations (94). Furthermore, the use of waxy materials in tablets has been associated with sticking problems which can be detrimental for tablet appearance and quality (95).

Apart from the dissolution- and diffusion-controlled matrix systems, matrix formulations containing combinations of hydrophilic and hydrophobic polymers have been reported in the literature. It is believed that the incorporation of a hydrophobic polymer into a hydrophilic matrix system could contribute to further retardation of the release of drugs, through a reduction in the matrix porosity (96), and/or a reduction in water penetration due to their hydrophobic nature (97).

1.2.2 Gastroretentive systems

Gastroretentive drug delivery systems (GRDDS) were developed as an alternative approach for the oral controlled-release delivery of drugs (98-101). These systems can be retained in the stomach long enough to completely release the active drug from the dosage form in the gastric fluids. Their application comes with several advantages, including

improved absorption of drugs and reduced fluctuation in drug blood levels that lead to increased therapeutic efficacy and minimised adverse effects, as well as their potential to enable stomach-specific activity. These systems can ensure the controlled delivery of drugs for an extended period at the desired rate and absorption site (102-105). Suitable candidates for GRDDS include drugs with poor absorption in the distal GIT, a narrow absorption window in the proximal small intestine, stability and/or solubility issues at the alkaline intestinal pH, a short half-life and/or a local activity at the upper part of the GIT for the eradication of *Helicobacter pylori* (101, 106-114).

GRDDS can either be controlled-release systems intrinsically or coupled with such technologies to ensure a controlled release of drugs. Controlled-release applications promote enhanced patient compliance to the treatment, due to less frequent administration, and minimised adverse effects, thereby promoting therapeutic efficacy (115-120).

Several strategies have been developed for gastric retention purposes. These include floating systems (106, 107, 109), high-density systems (121), bio/mucoadhesive (112, 113, 122-125), expandable (108), superporous hydrogels (126, 127), and magnetic systems (128-130).

1.2.2.1 Floating Systems

Floating systems are the most extensively studied gastroretentive dosage forms. The bulk density of such formulations is lower than 1.004 g/cm^3 which enables its buoyancy in the gastric fluids for an extended period while the drug is released (Figure 1-2) (102, 103, 131-133). A major advantage of this approach is that dosage form floatation results in the formulation presence not affecting the gastric motility or causing harm to the gastric mucosa (114, 134). This category includes non-effervescent floating systems, such as hydrodynamically balanced systems and non-effervescent tablets, effervescent floating systems, and raft-forming systems.

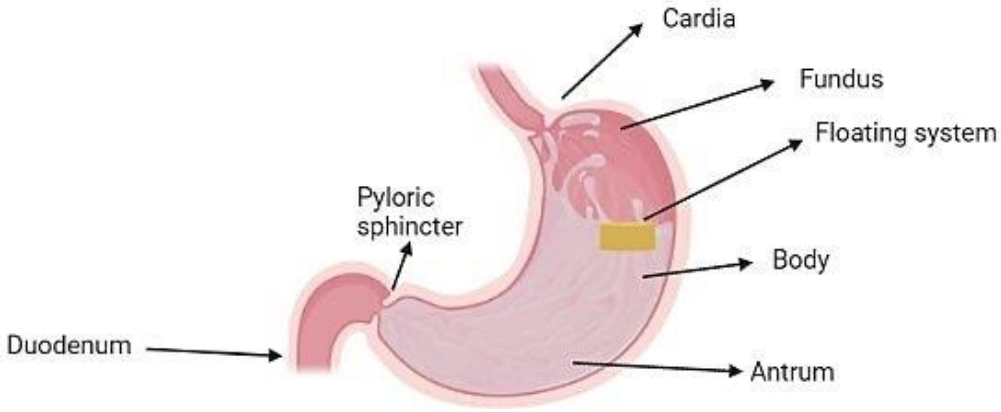


Figure 1-2: *Intragastric location of the floating drug delivery systems. The figure was created using BioRender (https://www.biorender.com/).*

1.2.2.1.1 Non-effervescent floating systems

In non-effervescent floating systems, highly swellable or gel-forming polymers are employed to achieve floatation. This category includes hydrodynamically balanced systems, floating tablets (single-layer or bilayer), and low-density systems (eg. microballoons) (103). The use of non-effervescent floating systems comes with notable advantages, including independence of the floating mechanism of variable gastric pH and avoiding problems in patients with achlorhydria. Furthermore, the exclusion of acidic and/or basic gas-generating agents can ensure better stability of acid- or base-labile drugs, respectively (106).

- Hydrodynamically balanced systems

Hydrodynamically balanced systems (HBS) are single-unit dosage forms composed of one or more gel-forming hydrophilic polymers. The key element in the development of this form is the appropriate selection of hydrophilic polymer(s) to ensure adequate flotation and release of the drug (135). These include HPMC, HPC, sodium carboxymethylcellulose, hydroxyethylcellulose, chitosan, tamarind, xanthan, carrageenan, agar, and alginic acid. These systems are mainly formulated in gelatin capsules (136-139). In this approach, the drug is mixed with the gel-forming polymer which hydrates and swells upon contact with the fluids, thus maintaining the density of the system below 1 g/cm^3 (103). Hydrophilic polymers

such as HPMC, PEO, HPC, and cellulose acetate phthalate, are the most commonly used. Madopar® HBS is a typical example of an HBS capsule. It contains a combination of levodopa and benserazide and is used for the treatment of Parkinson's syndrome. HPMC is used as the gel-forming polymer and hydrogenated vegetable oil as a low-density fatty excipient. Valrelease® is another example that contains diazepam as the API in a similar formulation and is used in patients suffering from anxiety, muscle spasms and seizures.

Since HBSs are single-unit dosage forms and gel-forming hydrophilic polymers are major components of this type of formulation, HBSs are by default controlled-release systems, as well as being gastroretentive. Hydrophilic polymers are used alone or in combinations to ensure tablet floatation and retard drug release (140). Furthermore, hydrophobic polymers and substances can also be included in HBS formulations to further retard the release of drugs. These include ethylcellulose or liquid paraffin (141).

A drawback of HBS is that it is not possible to change the release kinetics of the drug without changing the floating behaviour of the system since it is a matrix comprised of a mix of the drug and low-density hydrophilic polymers (103). As floatation behaviour is passive and has a strong dependence on the air sealed in the dry mass centre and the swelling of the polymer surface, changes in polymer amount significantly affect system behaviour (139).

- Non-effervescent tablets

Single-layer and bilayer floating tablets are another category of non-effervescent floating systems. For gastric retention, usually hydrophilic polymers, such as HPMC, HPC, sodium alginate, PEO, are used (106, 110, 142-144).

Non-effervescent single-layer floating tablets have been reported in the literature and their use is associated with novel work. Like HBS, single-layer floating tablets combine both gastroretentive and controlled-release properties since the polymers are responsible for both

tablet floatation and controlled drug release. Glucophage® XR is an example of this type of gastroretentive formulation that contains metformin and is used to treat type 2 diabetes.

Hwang et al. developed highly porous cilostazol gastroretentive tablets using a manufacturing method that included a sublimation step. Menthol was incorporated into the tablets as the sublimating agent and, after compression, the tablets were placed in a vacuum oven for 12 hours, so that sublimation may occur. The resultant highly porous formulations floated immediately without any lag time, while the percolation threshold of HPMC was an important factor in determining the release mechanism of cilostazol (107). Other formulation excipients can also affect the buoyancy behaviour of non-effervescent single-layer tablets. Kim et al. developed pregabalin gastroretentive tablets containing HPMC, HPC and PEO as swelling hydrophilic polymers and demonstrated that the selection of a super-disintegrant, such as crospovidone, resulted in a prolonged tablet buoyancy, compared to using microcrystalline cellulose (MCC). The super-disintegrant was thought to have contributed to a significant expansion of the tablet volume upon contact with the dissolution media, compared to MCC which, due to its relatively weak disintegrant properties, absorbed water and hindered buoyancy (106).

Apart from hydrophilic polymers, hydrophobic materials and proteins, such as zein (an amphiphilic protein derived from corn), have also been used for gastric retention (145). Additionally, single-layer tablets containing stearyl alcohol as a floating-assistance material due to its low bulk density have been reported (95, 142). However, sticking problems may hinder development. In general, tabletability is a factor that needs to be considered when using fatty excipients (95).

Non-effervescent formulations have also been reported in the form of bilayer tablets. Bilayer tablets can be fixed-dose combinations where a single dosing unit can contain two or more APIs in different layers (146). Also, one layer can be an immediate-release layer of a

drug, while the other may be a sustained-release layer of the drug which is also responsible for the floating of the tablet. In other cases, the tablet can be comprised of a drug-free gastroretentive layer and a sustained-release drug layer (114). To avoid long floating lag times, low-density materials are used in the gastroretentive layer to achieve rapid buoyancy of tablets. Additionally, rapid buoyancy can result from low compression force values that allow for a higher tablet porosity and lower tablet density and, hence, a rapid polymer wetting and swelling that further reduces the density of the dosage form (110). Furthermore, materials such as camphor and L-menthol that can undergo sublimation may be used. These materials are sublimed upon tablet heating, leading to increased tablet porosity and reduced density that enable tablets to float immediately (107, 145, 147). Among these materials, camphor is the most frequently used. Nguyen et al. prepared gastroretentive bilayer tablets based on Kollidon® SR which was used in the gastroretentive layer along with camphor as a sublimation agent. Due to the inherently low density of Kollidon® SR and the improved wet strength of the gastroretentive layer linked to the presence of a hydrophobic polymer, along with the further reduction in the tablet density from camphor sublimation, a 12-hour floating was successfully reached *in vitro*, even at a rotation rate of 200 rpm (134). This high paddle rotation speed is designed to create conditions that better simulate the *in vivo* conditions in fasted Beagle dogs, compared to typically used lower rotation speed values (134, 148).

- Low-density systems

Most floating gastroretentive formulations tend to have a lag time prior to floating in stomach contents. During that time, a premature evacuation of the dosage form from the stomach may take place via the pyloric sphincter (101). Low-density systems are formulations that have an inherent density lower than 1.004 g/cm^3 which enables their immediate floatation in the stomach. These include drug-loaded microballoons/hollow microspheres, sponges, and are multiple-unit floating systems (149, 150).

Microballoons have a low-density, hollow core, and are made of materials that can entrap oil or air (151-155). Commonly used polymers in these systems are polycarbonate, calcium alginate, Eudragit® S, cellulose acetate, agar and low-methoxylated pectin. They can be prepared through simple solvent evaporation or solvent diffusion techniques (138).

There are certain limitations to the application of low-density gastroretentive systems. Since they are multiple-unit systems, the release rate can be different between different doses and units. Furthermore, if system integrity is compromised, a consequent burst release of drug could lead to adverse effects since drug loadings tend to be higher in controlled-release formulations (149).

1.2.2.1.2 Effervescent floating systems

Effervescent systems contain a gas-forming agent and/or volatile liquids that contribute to their floatation. In a gas-generating floating system, swellable polymers are mixed with effervescent agents, such as sodium bicarbonate, calcium carbonate, tartaric acid, and citric acid, used alone or in combinations (103, 109, 156). Upon contact of the system with gastric fluids, the gas-generating agent reacts with hydrochloric acid and CO_2 gas is generated. CO_2 causes the floatation of the tablet and helps maintain tablet buoyancy by getting trapped in the hydrocolloid matrix of the system. It also influences drug release properties (95, 157-159). One disadvantage of effervescent systems is the fact that, unless low-density materials are used, they show long floating lag times if the generation of gas bubbles that will promote buoyancy is not fast enough and are, therefore, under the risk of premature gastric emptying (160). Furthermore, they are not suitable to be administered to patients with achlorhydria since the low excretion of gastric acid in these patients can lead to a higher gastric pH, thus resulting in extended floating lag times of the effervescent systems which can be problematic for their gastric retention (106).

Effervescent floating systems can be single-layer and bilayer floating tablets, and multiple-unit systems (103, 110, 131). Single-layer tablets can be prepared by mixing the drug with the gas-generating agent(s), polymer(s), and other excipients. In bilayer tablets, different strategies can be followed. One layer may contain the drug, polymer(s), and gas-generating agent(s), whereas the other layer could constitute an immediate-release one consisting of drug and excipients without gas-forming agents and release-retarding polymer(s) (103). The amount of a gas-generating agent, such as sodium bicarbonate, can significantly affect the total hydration volume of a tablet, along with its floatability. The higher the percentage of the gas-generating agent, the greater and faster-growing hydration volumes can be, along with reduced floating lag times (110). Also, the presence of sodium bicarbonate can overcome tablet floatability issues in cases where high tablet compaction forces result in low tablet porosity values that are insufficient for floatation (110). Also, in other cases, one layer consists of the drug, release retardant(s) and other excipients, while the other layer is the gastroretentive layer containing the gas-generating agent(s) and hydrophilic polymer(s) (143). Cifran® OD is a ciprofloxacin commercial product that constitutes effervescent single-layer gastroretentive tablets coated with a polymer film that is responsible for tablet buoyancy.

Apart from hydrophilic polymers, in other cases, a hydrophobic protein, such as zein, has been used in effervescent tablets for gastric retention. Raza et al. reported the preparation of zein-based compression coated single-layer tablets. The tablet core contained zein matrix as a release retardant, while the compression coating was comprised of zein and sodium bicarbonate. The tablets showed a short floating lag time and a total floating time longer than 12 hours, along with a 12-hour controlled release of captopril (159). Increasing amounts of sodium bicarbonate accelerated drug release rate from the matrix, probably due to higher pore formation that allowed for increased penetration of the dissolution medium into the matrix.

The floating mechanism was a combination of rapid formation of pores the size of which grew over time (confirmed via scanning electron microscopy and porosity studies) and CO_2 entrapment in the swelling matrix (159).

Recently, studies have reported the use of nanofibre technology for gastric retention purposes. Nanofibres are generally produced via electrospinning and can be tuned to provide controlled release of drugs through different mechanisms (161-164). Nanofibres can offer specific benefits as part of an effervescent GRDDS. These include their high porosity that can promote the penetration of gastric hydrochloric acid into the effervescent film within the nanofibre, as well as their ability to entrap the generated CO_2 gas which, not being able to diffuse out of the system, significantly prolongs the floatation of GRDDS (165). Furthermore, alongside their high porosity, the high surface-area-to-volume ratio of nanofibres results in an intrinsically low bulk density which helps ensure their immediate buoyancy upon contact with the gastric fluids (166).

Multiple-unit effervescent floating systems may consist of sustained-release cores surrounded by one or more layers. The layer(s) can contain gas-forming agents along with polymers with swelling properties (103, 131, 157).

1.2.2.1.3 Raft-forming systems

Raft-forming system is comprised of effervescent excipient(s) and gel-forming polymers to achieve system floatation and sustained release of drugs. These systems are tablets or liquids at room temperature that can undergo gelation when in contact with gastric fluids, due to an increased temperature, or as a response to pH change. Therefore, their behaviour can be either temperature-dependent or characterised by cation-induced gelation. Either way, the formation of a gel that is thick enough to remain intact for hours within the stomach contents leads to their buoyancy and controlled drug release applications (131, 167, 168). This system is mostly used to achieve localised effects. Floating rafts can act as a

blockade between the oesophagus and the stomach. This property renders these formulations ideal for the management of gastric oesophageal reflux disease. Furthermore, when an antacid is incorporated into the raft-forming system in significant amounts, the system can aid in the treatment of both indigestion and heartburn via acid neutralisation in both the stomach and the oesophagus (169, 170). Upon contact with the gastric fluids, these systems swell and form a viscous cohesive gel layer termed a raft (103, 131, 171). Raft systems are used for the delivery of antacids, such as simethicone, aluminium hydroxide, and calcium carbonate. However, the mechanical strength of the raft is weak which could result in its premature disruption by the migrating motor complex (MMC) (167, 171). Gaviscon® is a commercial raft-forming formulation that is available as tablets or liquids. It is used to treat indigestion and heartburn. Its raft-forming mechanism is based on a combination of sodium alginate, sodium bicarbonate and calcium carbonate. Topalkan® is an antacid formulation containing aluminium and magnesium as active components, while alginic acid is the raft-forming excipient.

In general, the use of floating systems comes with certain potential issues. These include the possibility that system units may stick together (for multiple-unit systems) or be obstructed in the GIT, which could cause gastric irritation. Therefore, drugs that may have an irritating effect on the gastric mucosa are not considered suitable candidates for floating systems (103, 131, 172).

1.2.2.2 High-Density Systems

High-density systems have a density greater than that of gastric fluids (1.004 g/cm^3) and, therefore, sink to the bottom of the stomach fluids and achieve gastric retention, probably via increased resistance to the gastric contractions that is linked to their high density (Figure 1-3) (173). Excipients that are commonly used to ensure a sufficiently high density of these systems include barium sulfate, zinc oxide, iron oxide, iron powder and titanium

dioxide. Usually, the dosage forms reported in the literature are high-density pellets or tablets (121, 174).

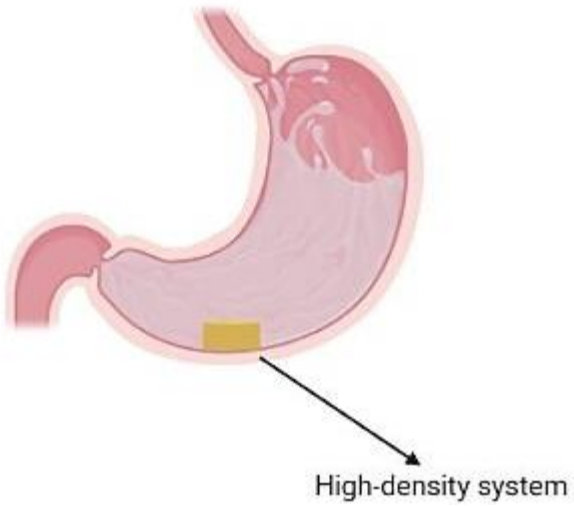


Figure 1-3: *Schematic localisation of high-density systems in the stomach. The figure was created using BioRender (www.biorender.com).*

Even though such systems are promising in achieving long gastric residence times (GRTs), it is difficult to design high-density pellets containing high doses of drugs. Furthermore, the clinical significance of these systems is yet to be proved since only a few animal studies have been carried out (103, 175).

1.2.2.3 Mucoadhesive/Bioadhesive Systems

Adhesion is the process by which two surfaces are "fixed" to one another (176). When adhesion happens in a biological setting, it is referred to as "bioadhesion", while if it occurs on mucosal surfaces it is termed "mucoadhesion" (124). Regarding gastric retention applications, this system can adhere to the surface of the gastric mucosa and prolong the GRT of drug compounds (Figure 1-4) (113, 131). In these systems, the drug is incorporated into one mucoadhesive agent or a combination of them that can be natural or synthetic hydrophilic polymer(s). Xifaxan® is a commercial bioadhesive tablet formulation containing rifaximin as

an antibiotic and is used to treat traveller's diarrhoea, hepatic encephalopathy, and irritable bowel syndrome with diarrhoea (IBS-D).

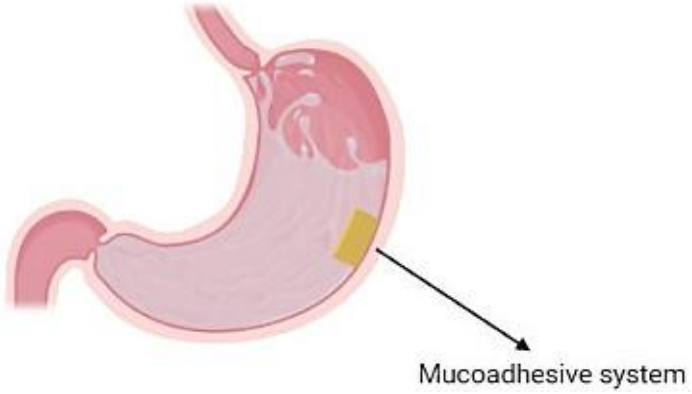


Figure 1-4: *Localisation of mucoadhesive/bioadhesive drug delivery systems in the stomach. The figure was created using BioRender (www.biorender.com).*

Many different mucoadhesive dosage forms have been reported in the literature, including beads, microspheres, films, capsules, and tablets (122). Polymers such as chitosan, sodium alginate, HPMC, polyethylene glycol and polyacrylic acid have mucoadhesive properties that render them suitable for use in these systems (101, 131). These polymers bind to the mucosal surfaces and, thus, maintain the drug in continuous contact with the mucus and increase the residence time of the drug at the application site. These polymers should be inert, non-irritating to the mucosa, non-toxic, adhering to the mucosal surface, and site-specific (103).

Chitosan hydrogels have been used extensively in gastroretentive drug delivery system applications. Chitosan can form gels with improved mechanical strength through chemical cross-linking using glutaraldehyde, glyoxal or other substances as cross-linkers, or through physical cross-linking as ionically cross-linked chitosan gels with multi-valent phosphates or as polyionic complexes of positively charged chitosan with a negatively charged polymer, such as alginate or polylactic acid. Chitosan-based hydrogels have been used for mucoadhesive and other gastroretentive, as well as controlled-release, applications (177-189).

Additionally, poly(acrylic acid) and its derivatives have been reported as excellent mucoadhesive agents (190).

Nanoparticles are in general known to suffer from a rapid passage through the stomach and intestine, thus being unable to release drugs in a controlled manner and to an acceptable extent (113). This limits their oral applications. To address this challenge, Sarparanta et al. developed thermally hydrocarbonised porous silicon (THCPSi) nanoparticles (113). Porous silicon was used since it is known for its biocompatibility and biodegradability, as well as variable particle size, pore size and degree of porosity (191, 192). The nanoparticles were coated with hydrophobin class II which ensured the efficient dispersal of the nanoparticles in aqueous media with minimal aggregation. During an *in vitro* study on human gastric adenocarcinoma (AGS) cells, the nanoparticles demonstrated a gradual adhesion to the cells over time with 35 % of the nanoparticles being retained for at least 4 hours on the cells. However, it took 30 − 60 minutes for the nanoparticles to be attached to the cells with the mucoadhesion achieved probably via hydrophobic and electrostatic interactions. Nevertheless, an *in vivo* biodistribution study in rats demonstrated that the nanoparticles were able to be retained in the rat stomach for 3 hours, prior to their emptying from the stomach towards the duodenum, where the hydrophobin class II coating would be expected to be shed, due to the presence of surfactants (113).

The use of mucoadhesive systems comes with certain limitations. Site targeting can be challenging, due to differences in the composition of the mucus across the mucosal membrane. Furthermore, the constant turnover of the mucus, along with high stomach hydration, can contribute to a reduced bioadhesion of the systems. Finally, there is a risk of adhesion of the system to the oesophagus which could result in collateral lesions (101, 193).

1.2.2.4 Expandable Systems

Expandable drug delivery systems are designed to grow in size or reconfigure their geometry within the stomach to prevent passage through the pyloric sphincter and have a longer GRT (108). These systems need to have a small size for easy oral intake, expand in the stomach and attain dimensions larger than the diameter of the pyloric sphincter, and have their size reduced after drug release is completed, for them to be evacuated from the stomach (101, 102, 108). Due to their ability to block the pyloric sphincter, these systems are also referred to as "plug-type" systems. It has been suggested that these systems should expand to a size greater than 15-16 mm in the fasted state and greater than 12-13 mm in the fed state to ensure successful gastric retention, based on the resting orifice of the pyloric sphincter (12.8 ± 7 mm) (61, 194). Furthermore, a sufficiently high tablet wet strength is an additional requirement that will ensure the protection of gastroretentive tablets from premature rupture and emptying under the effect of the housekeeper waves (195). The expansion takes place through swelling and/or unfolding which allows for volume and shape modification, respectively (108, 196). Accordion Pill® Levodopa/Carbidopa is a commercial expandable capsule formulation containing carbidopa and levodopa as active components and is used to treat Parkinson's disease. It achieves gastric retention via an unfolding mechanism through the presence of folded multilayer polymeric films. Additionally, Acuform® and Geomatrix® are two expandable system technologies that have been used in commercial gastroretentive formulations, such as Requip® XL (ropinirole), Glumetza® (metformin), Nucynta® ER (tapentadol), Gralise® (gabapentin) and Janumet® XR (Sitagliptin and metformin).

Hydrophilic polymers, such as HPMC, PEO and Carbopol®, are usually utilised in the swelling expandable systems, due to their ability to absorb water and increase volume by swelling. Likewise, in unfolding systems, the drug and polymer can be in a folded/compressed state inside a gelatin capsule. When the capsule comes in contact with the

gastric fluids, it dissolves, and the mechanically preferred expanded configuration is released. In these systems, the critical attributes that need to be considered include the molecular weight, viscosity, swelling or expanding properties and biodegradability of the polymer chosen to maintain gastric retention and sustained release of the drug (101, 197). Xanthan gum has shown promising properties as a swelling and expanding agent either used solely or in combination with other materials, such as guar gum (198).

The applications of expandable systems come with a few limitations. There are difficulties in storing easily hydrolysable and biodegradable polymers, while manufacturing can be challenging, alongside a potential lack of cost-effectiveness. Furthermore, there can be challenges in maintaining the structural integrity of the systems in the stomach. Finally, the application of this type of system may cause adverse effects, such as bowel obstruction, intestinal adhesion, and gastropathy (101, 108, 199).

1.2.2.5 Superporous Hydrogel Systems

These systems have gained high popularity as controlled-release formulations, due to their high mechanical strength and elastic properties (127). Superporous hydrogels are highly cross-linked polymers that can absorb significant amounts of aqueous fluids and swell within relatively short periods to form a stable gel (200, 201). Such systems have a pore size greater than 100 μm. This enables them to rapidly absorb water by capillary wetting and swell to an equilibrium size in a short time (Figure 1-5) (102, 200). While the conventional hydrogel system swelling is a slow process and can result in premature evacuation from the stomach, superporous hydrogels can swell up to 100 times or more and can gain enough mechanical strength to resist pressure from gastric contractions, thereby increasing the GRT. In these systems, highly swellable polymers, such as sodium croscarmellose and sodium alginate, are used (101, 103, 126). However, such polymers have swelling behaviour that depends sensitively on pH changes, and unintended reversal or slowing of polymer swelling can result

in poor mechanical strength of the system structure and its premature evacuation from the stomach (101, 126).

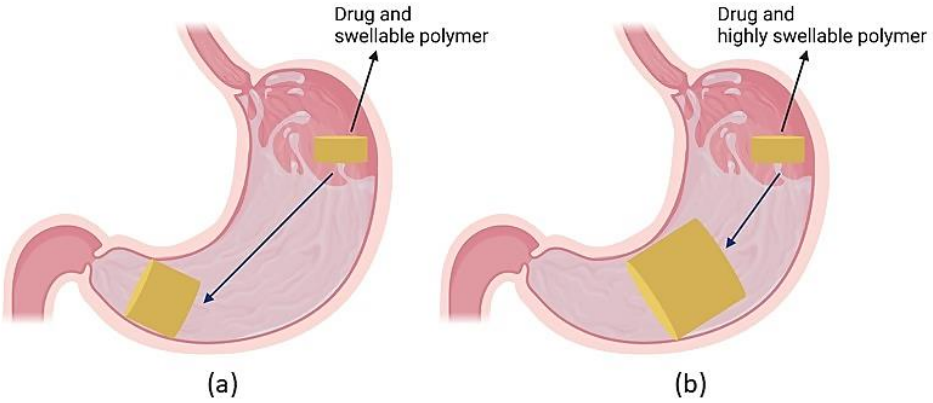


Figure 1-5: *Intragastric behaviour of (a) expandable and (b) superporous hydrogel systems. The figure was created using BioRender (www.biorender.com).*

There are some disadvantages to the use of superporous hydrogels for gastric retention purposes. Since ionic polymers are used to a significant extent in the development of these systems, their swelling behaviour can be heavily dependent on gastric pH and, thus, reversible with any pH changes. Furthermore, sometimes, they may show poor mechanical strength which can be an issue towards achieving effective gastric retention (103, 111).

1.2.2.6 Magnetic Systems

In magnetic systems, the distinct feature in the dosage form is a small amount of internal magnet, apart from API and excipients. An extracorporeal magnet is placed over the stomach to control the position of the dosage form (Figure 1-6) (103). The gastric retention behaviour of the magnetic systems can be affected by the position and magnetic intensity of the extracorporeal magnet (202).

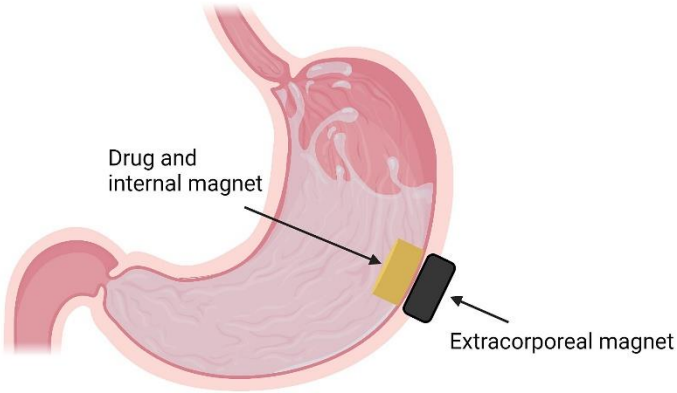


Figure 1-6: *Application of magnetic drug delivery systems for gastric retention purposes. The figure was prepared using BioRender (www.biorender.com).*

In the literature, it has been reported that the GRT and bioavailability of drugs are improved using magnetic tablets (128, 203). Gröning et al. tested the gastric retention capability of acyclovir magnetic depot tablets in human volunteers with and without the application of an external magnetic field. The tablets remained in the stomach for a prolonged period in the presence of the extracorporeal magnet and the area under the concentration curve values were significantly increased (129).

A major challenge associated with the application of magnetic systems is the fact that specific positioning of the magnet can be challenging and could also lead to low patient adherence (202). Therefore, future research studies on these gastroretentive systems need to focus on their clinical significance.

1.2.2.7 Combinatory Approaches

Apart from the abovementioned standalone gastroretentive technologies, combinations have been reported. Combinatory approaches can help tackle the disadvantages of each of the different technologies combined. Also, they can help minimise the variability of GRT and may be less affected by the physiological conditions of the stomach, such as those during fasted and fed state, thus ensuring robust gastric retention (103). These combinations could be floating and expandable systems, mucoadhesive and expandable

systems and floating and mucoadhesive systems. The first two combinations have been indicated to have higher safety and efficacy for clinical applications (204).

1.3 MT-1207 as a new choice for hypertension treatment

MT-1207 hydrochloride is a novel antihypertensive agent that presents combinatory pharmacological actions. More specifically, it exhibits highly inhibitory activities simultaneously towards calcium channels, adrenergic α_{1A}, α_{1B}, α_{1D} and serotonin (5-Hydroxytryptamine) 5-HT_{2A} receptors. Therefore, the mechanism underlying the hypotensive effect of MT-1207 is at least a combination of vasodilation (through the α receptors and vascular smooth muscle relaxation via the calcium channel) and bradycardia (through 5-HT_{2A} receptors) (205, 206).

1.3.1 Physicochemical properties

MT-1207 hydrochloride (molecular formula: $C_{21}H_{24}SN_6 \cdot HCl$) (Figure 1-7) is a weak base with a pK_a value of 7.31. It is a white or white-off crystalline powder that is poorly water-soluble. Its aqueous solubility is pH-dependent with the peak values recorded at pH 3.0 – 4.0. MT-1207 is strongly lipophilic (logP of 4.15), and has a molecular weight of 428.98 g/mol (207).

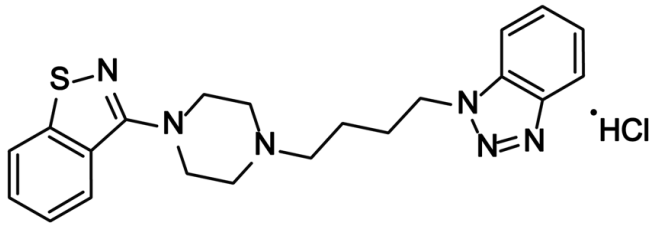


Figure 1-7: *The chemical structure of MT-1207 hydrochloride (207).*

MT-1207 has been isolated in a total of six hydrochloride crystal forms (including the starting sample crystal form) named crystal forms A, B, C, D, E, and F. Forms A, C and D were hydrochloride anhydrate, forms B and F were hydrochloride salt hydrate, while the quantity of form E was small and repeated preparation was difficult. Therefore, the

identification of form E was not completed. To determine the stability relationship between the anhydrous crystal and the hydrate, a suspension competition test was performed for each crystal form. The results demonstrated that the anhydrous crystal A was the most stable one and was selected for further development (207).

1.3.2 Animal studies

1.3.2.1 Pharmacokinetic studies

A series of pharmacokinetic studies was conducted in animals to gain information on the absorption, distribution, metabolism, and excretion (ADME) profile of MT-1207.

A pharmacokinetic study for MT-1207 was initially conducted in Beagle dogs at three different drug doses (0.75, 1.5, and 3 mg/kg) and two different conditions at a certain dose (fasted, fed). After administration of the three different doses of MT-1207 in Beagle dogs during fasted state, a statistically significant difference was demonstrated in the plasma clearance rate (CL/F), the apparent volume of distribution (V_d), and area under the curve (AUC_{0-t}) (one-way ANOVA, $p < 0.05$). However, the ratio of AUC to dose (1:2:4) did not increase in direct proportion. Therefore, it was evident that the absorption of MT-1207 exhibited non-linear kinetics in Beagle dogs in the dose range of 0.75 – 3 mg/kg (208). The values of the pharmacokinetic parameters recorded after administration of the three different doses can be seen in Table 1-1. Furthermore, after administration of 1.5 mg/kg MT-1207 in Beagle dogs during fed state, there was no statistically significant difference in the half-life ($t_{1/2}$), CL/F, V_d and AUC_{0-t} values recorded between the different conditions (fasted, fed) at the same dose (*t*-test, $p > 0.05$) (Table 1-1) (208). Finally, Beagle dogs were orally administered 1.5 mg/kg MT-1207 twice daily for seven consecutive days. The data (Table 1-1) demonstrated no statistically significant differences for any of the pharmacokinetic parameters between their values recorded during the first and last day of the experiment (*t*-test, $p > 0.05$). This indicated that the levels of MT-1207 in Beagle dogs did not increase

significantly after 7 days of continuous administration. Therefore, there was no accumulation or increased metabolism of the drug in Beagle dogs (208).

Table 1-1: *MT-1207 pharmacokinetic parameter values after (i) oral administration of 0.75, 1.5, and 3 mg/kg of the drug in Beagle dogs during fasted state, (ii) after oral administration of 1.5 mg/kg MT-1207 during fed state, and (iii) after oral administration of 1.5 mg/kg MT-1207 twice daily over seven consecutive days (208).*

Beagle Dog	Fasted State			Fed State
Pharmacokinetic Parameters	0.75 mg/kg	1.5 mg/kg	3 mg/kg	1.5 mg/kg
$t_{1/2}$ (h)	N/A	1.47±0.23	N/A	1.61±0.39
CL/F ($L.kg^{-1}.h^{-1}$)	14.7±9.2	6.4±3.3	10.3±6.4	7.1±5.5
V_d ($L. kg^{-1}$)	22.6±10.5	12.8±5.0	32.3±16.5	14.3±5.7
AUC_{0-t} ($ng.h.mL^{-1}$)	78.5±56.5	297.8±152.3	398.7±257.0	281.4±124.4
1.5 mg/kg MT-1207 twice daily over 7 consecutive days				
	First Day		Last Day	
$t_{1/2}$ (h)	2.02±0.39		1.82±0.41	
CL/F ($L.kg^{-1}.h^{-1}$)	8.7±6.3		7.6±5.4	
V_d ($L. kg^{-1}$)	23.0±13.4		17.8±9.6	
AUC_{0-t} ($ng.h.mL^{-1}$)	258.5±150.5		297.1±174.5	

The abovementioned study in Beagle dogs was followed by a pharmacokinetic study in Sprague Dawley (SD) rats. MT-1207 oral preparations were administered to rats during fasted state at three different MT-1207 doses (1, 3, and 9 mg/kg) (208). The results of the study (Table 1-2) were similar to those conducted in Beagle dogs since there were statistically significant differences in the values recorded for the different pharmacokinetic parameters (one-way ANOVA, $p < 0.05$), except for $t_{1/2}$ (one-way ANOVA, $p > 0.05$). Additionally, the absorption of MT-1207 exhibited non-linear kinetics in SD rats in the dose range of 1 – 9 mg/kg (208). Finally, after twice-daily administration of 3 mg/kg MT-1207 over 7 days, the levels of MT-1207 in SD rat plasma did not increase significantly during that time. Therefore, there was no accumulation or increased metabolism of the drug in rats (208).

Table 1-2: *MT-1207 pharmacokinetic parameter values after oral administration of 1, 3, and 9 mg/kg of the drug in Sprague Dawley rats during fasted state (208).*

SD Rats	Fasted State		
Pharmacokinetic Parameters	1 mg/kg	3 mg/kg	9 mg/kg
$t_{1/2}$ (h)	1.50± 0.29	2.15±0.7	1.89±0.79
CL/F ($L.kg^{-1}.h^{-1}$)	23.3±11.8	7.8±4.1	35.2±29.1
V_d ($L. kg^{-1}$)	51.5±28.0	22.4±7.8	78.9±60.3
AUC_{0-t} ($ng.h.mL^{-1}$)	51.7±26.9	421.1±184.6	1,605.4±515.5

The tissue distribution of MT-1207 in male and female SD rats after administration of oral preparation of the drug was investigated. 30 minutes after oral administration of MT-1207 (3 mg/kg) in male SD rats, drug levels in tissues and body fluids were high. The concentration was significantly lower 2 hours and 6 hours after administration. 12 hours after administration the drug concentration in most tissues was extremely low, and drug in some of the tissues was not detected. Since the mode of administration was intragastric administration, the concentration in the gastrointestinal contents was high. The drug concentration in the plasma was lower than in most tissues, indicating that the drug easily entered the tissues. There was a small amount of drug in the brain, meaning that the drug was able to transverse the blood-brain barrier (208). Therefore, the distribution of MT-1207 in the rat body was probably extensive. Furthermore, after administration of MT-1207 in female SD rats, the drug concentration in most tissues was statistically different from the male rats, and the MT-1207 concentration in tissues in female rats was higher than in male rats. So, gender demonstrated a statistically significant effect on the extent of distribution of MT-1207 in the rat body (208).

The *in vivo* metabolic transformation of MT-1207 was investigated in SD rats. The investigators performed mass spectrometry analysis of stool and urine samples in rats after oral administration of MT-1207. Then, they compared the obtained mass spectral information

with the blank matrix sample and combined it with the literature. The researchers found that S was the most active part of the MT-1207 structure since it could react and/or get oxidised. A total of 10 metabolites were found, including metabolites derived from oxidation, methylation, and hydroxylation. The peak area and response of the S-methylated product (M3) were the highest. So, M3 was the main metabolite of MT-1207 (208). The summary of the possible metabolic pathways of MT-1207 in rats are shown in Figure 1-8.

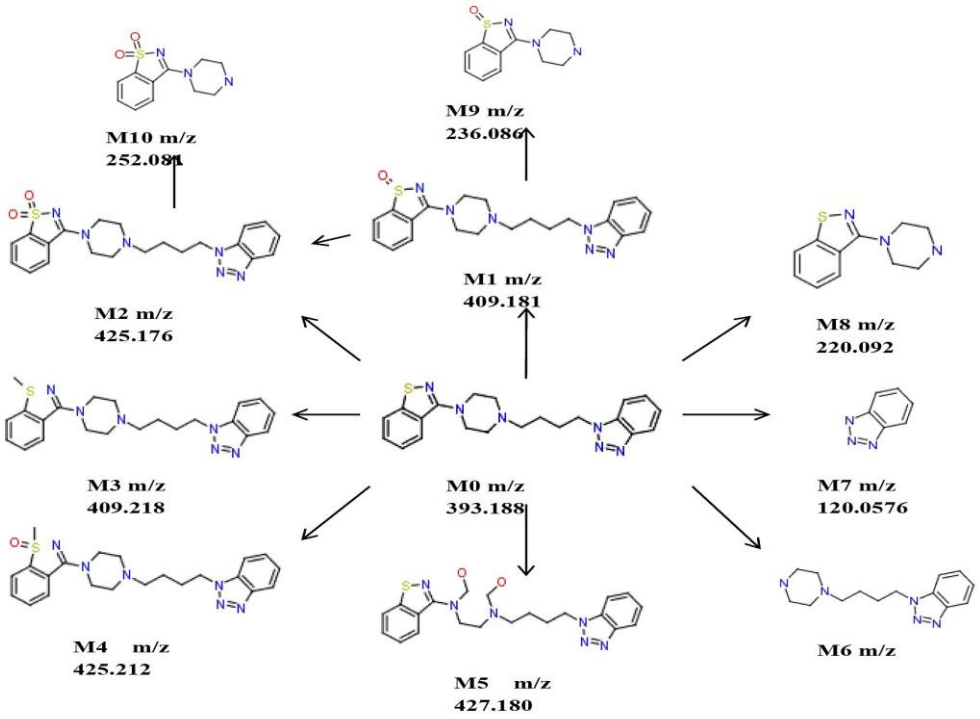


Figure 1-8: *Possible metabolic pathways of MT-1207 in SD rats. No changes were made to the original figure (208).*

An additional study was conducted on rats, Beagle dogs, macaques and humans to gain more information on the organs where the biotransformation of MT-1207 takes place. MT-1207 could not be metabolised in the plasma of rats, beagles, macaques and humans. However, it was rapidly metabolised in the liver microsomes of all four species and its metabolism was NADPH-dependent (208). After MT-1207 was incubated in liver microsomes of the different species, most of the drug dose was linearly eliminated within 0 –

5 min. At 5 min, the remaining percentages of MT-1207 in liver microsomes of rat, beagle, macaque, and human were 21.08 ± 0.41 %, 6.04 ± 0.28 %, 1.50 ± 0.16 %, and 23.90 ± 2.08 %, respectively. The liver clearance rate calculated in combination with physiological parameters (liver weight:drug ratio, blood flow) was 19.2 ± 0.1 (human), 43.2 ± 0.1 (macaque), 36.9 ± 0.0 (Beagles), and 61.7 ± 0.3 $mL.min^{-1}.kg^{-1}$ (rats). Therefore, the clearance rate in the human body was the slowest one among the different species. These results indicated that MT-1207 was biotransformed mainly in the liver of the different species (208).

The excretion of MT-1207 in the bile, urine and faeces of SD rats after oral administration of the drug was investigated. After oral administration of MT-1207 (3 mg/kg) in female SD rats, the drug could be detected in the bile, urine, and faeces. In total, 3.3 ± 0.4 % of the drug dose was retrieved from the bile, urine and faeces in male rats, while a total of 6.8 ± 3.4 % of the MT-1207 dose was retrieved from these routes of elimination in female rats. Therefore, gender may influence the percentage of MT-1207 eliminated through these routes since the cumulative excretion rate in bile, urine and faeces in female rats was higher than that in males. The excretion study data demonstrated that the cumulative excretion rate of MT-1207 in the bile, urine and faeces was low. Therefore, it was speculated that the drug may be excreted mainly in the form of metabolites (208).

To summarise, the pharmacokinetic parameters of MT-1207 in Beagle dogs did not seem to be affected by the absence or presence of food. The absorption of MT-1207 exhibited non-linear kinetics in both Beagle dogs and rats. After absorption, the drug was extensively distributed to many different tissues in male and female SD rats with gender seemingly having a statistically significant effect on the extent of drug distribution. Furthermore, the study demonstrated that MT-1207 was mainly eliminated via enzymatic liver clearance, with S-methylation being the main metabolic pathway. The excretion of the unchanged drug in the bile, urine and faeces was minimal and gender-dependent.

1.3.2.2 Pharmacodynamic studies

Xu et al. examined the pharmacological activity of MT-1207 in spontaneously hypertensive rats (SHR) and two-kidney one-clip (2K1C) dogs. The study researched the pharmacological profile of MT-1207, its acute, subacute and long-term effects on these animal models, as well as its activity on isolated organs and pharmacological targets *in vitro* (205).

The acute effect study in SHR and 2K1C dogs demonstrated a significant dose-dependent relationship with a decline in the systolic and diastolic BP conferred by MT-1207. The maximal reduction was recorded within a much shorter time than amlodipine which was used as a model antihypertensive drug. Furthermore, the effect of MT-1207 on systolic BP lasted longer than 12 hours and, in contrast with amlodipine, did not cause a reflex increase in heart rate, but, on the contrary, reduced it (205).

Similar effects to the above were recorded during the subacute effect study of MT-1207 in SHR and 2K1C dogs which was conducted via multiple administration of the drug for one week. In both animal models, the BP was markedly decreased, alongside a slight reduction in the heart rate. After the withdrawal of MT-1207, both BP and heart rate returned to the levels measured before drug administration (205).

The long-term effect study of MT-1207 in the animal models was conducted over four months in SHR and eight months in stroke-prone spontaneously hypertensive rats (SHR-SP). The effects of MT-1207 administration on BP, baroreflex sensitivity and organ protection were investigated in SHR and an additional survival rate parameter in SHR-SP. In SHR, the BP was reduced by more than 20 mm Hg and remained stable over four months, the baroreflex syndrome improved significantly, and MT-1207 demonstrated protective effects towards the heart, kidneys, brain and aorta. The effects of the drug on these parameters were

similar for SHR-SP, the survival rate of which was significantly higher when treated with MT-1207 or amlodipine. This demonstrated the significant effect of MT-1207 on delaying the occurrence of stroke (205).

Xu et al. conducted further research to attain information on the pharmacological targets of MT-1207. Towards that direction, the effects of the drug on isolated vascular function, as well as pharmacological targets *in vitro,* were investigated. The results of the study on the isolated precontracted aortae indicated a dose-dependent relaxation which suggested an antihypertensive effect of MT-1207, at least through its direct action on blood vessels. Furthermore, the *in vitro* study in different pharmacological targets demonstrated a high inhibition activity of MT-1207 towards α_{1A}, α_{1B}, α_{1D} and 5-HT_{2A} receptors, and a relatively weak inhibition activity towards calcium channels. These pharmacological activities of MT-1207 caused vasorelaxation and slow heart rate, thus contributing to the hypotensive effect of the drug that is responsible for the treatment of hypertension and the delay of end-organ damage (205).

To summarise, Xu et al. demonstrated that MT-1207 was able to effectively reduce BP shortly after its administration in different animals in a dose-dependent manner, whilst reducing the heart rate, instead of increasing it. Furthermore, the drug had a protective effect on different organs by delaying the damage conferred to the heart, kidneys, brain and/or aorta by hypertension. Finally, the understanding of the antihypertensive effect of MT-1207 was increased by identifying the different receptors targeted by the drug, a fact that confirmed its identity as a multi-target drug (205). MT-1207 was deemed a safe and promising antihypertensive agent and was forwarded to phase I clinical trials.

1.3.3 Phase I clinical trials

As part of its development, MT-1207 was forwarded to Phase I clinical trials conducted in healthy human subjects to gain information on the safety, pharmacokinetics and pharmacological activity of the drug. For this purpose, Zhang et al. conducted a single-dose study where four different daily doses of MT-1207 (5 mg, 10 mg, 20 mg, and 40 mg) were administered to healthy individuals and a food effect study where 40 mg MT-1207 were administered daily (206).

No serious adverse effects or deaths were recorded in any of the two studies. The common adverse reactions (incidence ≥ 5 %) were dizziness, vomiting and one case of postural hypotension. Except for the case of postural hypotension which was treated with a rapid intravenous infusion of 0.9 % NaCl, the rest of the adverse reactions were resolved spontaneously without treatment. The incidence of postural hypotension was not increased with the dose. Furthermore, no adverse reactions involving the heart, liver and kidney were recorded. These findings demonstrated the safety and tolerability of MT-1207 in human subjects (206).

Information on the pharmacokinetics of MT-1207 in humans was obtained in both studies. The pharmacokinetics of MT-1207 was consistent with that predicted by the two-compartment model with first-order absorption (206, 209). The drug was rapidly absorbed after single administration at doses 5 – 40 mg during fasting conditions. The C_{max} and AUC parameters showed a dose-dependent increase across that dose range with their geometric means showing a certain linear trend. The mean $t_{1/2}$ of MT-1207 ranged from approximately 4 to 7 hours, with average values of 7.28 (n = 8 subjects) and 7.38 hours (n = 7 subjects) recorded for the 20 mg and 40 mg dosing regimens, respectively. These $t_{1/2}$ values were significantly higher than the ones recorded in the abovementioned animal studies at similar drug doses. With regards to the food effect study, the presence of food did not affect drug

metabolism and plasma exposure (AUC), however, C_{max} decreased to approximately 66 % of the parameter value recorded during fasting conditions. The presence of food probably delayed the absorption of MT-1207 since T_{max} was significantly prolonged in the presence of food. However, the $t_{1/2}$ was not affected by the presence of food which was in alignment with the abovementioned animal study findings. These findings demonstrated that MT-1207 can be administered as a twice-daily dosing regimen without worrying about food ingestion within several hours of drug administration (206).

As part of the assessment of MT-1207 pharmacodynamics, the effects of the drug on systolic BP, diastolic BP and heart after single administration were recorded. The values of all these parameters decreased after drug administration with statistically significant effects recorded 4 – 24 h after administration in the dose range of 10 – 40 mg. These results demonstrated the antihypertensive effect of MT-1207. Due to single-dose administration of the drug, no long-term effects of decreased BP and heart rate were observed (206).

To sum up, the safety and tolerability of MT-1207 in healthy humans were demonstrated in the dose range of 5 – 40 mg, alongside an antihypertensive effect in the dose range of 10 – 40 mg. Since a multi-target therapeutic strategy is essential for the successful management of hypertension, an agent targeting multiple receptors, such as MT-1207, could be a promising choice for the treatment of hypertension. Therefore, the dose range of 10 – 40 mg was selected for phase Ib/IIa clinical trials in hypertensive patients with a suggested twice-daily dosing regimen (206).

1.4 Thesis Aim and Hypothesis

Hypertension is a chronic disease affecting more than 1 billion people around the world. A single drug target treatment is ineffective; therefore, drugs targeting different receptors need to be used in combination to achieve efficient management of the disease. However, the administration of multiple products to patients via polypharmacy may, in turn,

affect patient compliance to the treatment. A few of the drugs approved for hypertension have, therefore, been incorporated into controlled-release formulations to reduce the frequency of administration and, thus, improve patient compliance.

MT-1207 is a multi-target drug that has indicated safety and efficacy in reducing BP in humans. It is currently being tested in phase Ib/IIa clinical trials. Its application could simplify the treatment of hypertensive patients by reducing the number of required medications and, thus, render it more efficient and effective. However, to date, immediate-release tablets of the drug have been developed and are being tested with a suggested twice-daily dosing regimen. This regimen could contribute towards polypharmacy and reduced patient compliance, due to the high frequency of administration of the tablets.

The hypothesis of this thesis proposes the development of viable sustained-release tablet formulations of MT-1207 that could be administered as part of a once-daily dosing regimen. The ability of the drug agent to block many different pharmacological targets and its low frequency of administration, derived from its incorporation into a sustained-release formulation, could provide a promising choice for the effective treatment of hypertension with high patient compliance.

As part of testing this hypothesis, sustained-release HPMC matrix tablets were initially prepared. The required matrix formulations are easy to prepare at lab and industrial scales, and polymer matrices have a proven ability to retard the release of different drugs. HPMC polymers of different viscosities were incorporated into sustained-release tablets and their ability to retard the release of MT-1207 was tested *in vitro*. A promising sustained-release HPMC matrix tablet formulation was selected and was forwarded to a pharmacokinetic study in Beagle dogs. Afterwards, based on the *in vivo* study results for that formulation, further formulation optimisation was conducted through the development of gastroretentive bilayer

tablets consisting of a gastroretentive layer and an MT-1207-containing layer. Based on the tablet *in vitro* testing results, two promising gastroretentive bilayer tablet formulations were selected and forwarded to a final pharmacokinetic study in Beagle dogs.

2 Chapter 2: Materials and Methods

This chapter includes information about the materials used, and the methods that were common across Chapters 3, 4 and 5 of the thesis.

2.1 Materials

MT-1207 hydrochloride reference standard and micronised MT-1207 hydrochloride:colloidal silicon dioxide mixture with a mass ratio of 5:1 were donated by Shenyang Haiwang Biotechnology Co., Ltd (Shenyang, China). Polyethylene oxide average molecular weight 8,000,000 (8M), Kollidon® SR, spray-dried lactose, polyvinylpyrrolidone K30, hydroxypropyl methylcellulose average molecular weight 86,000 (K4M), hydroxypropyl methylcellulose average molecular weight 90,000 (K15M), hydroxypropyl methylcellulose average molecular weight 120,000 (K100M), colloidal silicon dioxide, magnesium stearate, sodium phosphate monobasic dihydrate and sodium acetate anhydrous were purchased from Sigma-Aldrich (Gillingham, United Kingdom). Alpha-D-lactose monohydrate, ethylcellulose 10 cps, iron (III) oxide, sodium dodecyl sulfate (SDS), hydrochloric acid 37 %, acetic acid glacial, sodium hydroxide pellets, orthophosphoric acid, methanol HPLC grade and propan-2-ol HPLC grade were purchased from Fisher Scientific (Loughborough, United Kingdom).

2.2 HPLC-UV method for the quantitation of MT-1207 samples

An HPLC-UV method was developed to quantify MT-1207 samples for solubility and *in vitro* release testing. A Dionex Ultimate 3000 HPLC system was used (Thermo Scientific®, United Kingdom) with an ACE® Generix 3 C18, 150 × 4.6 mm, 3 μm column. The mobile phase consisted of 0.1 M sodium acetate buffer pH 4.0 and methanol at a ratio of 40:60 (% v/v). The mobile phase flow rate was set at 0.7 mL/min. The wavelength maximum of MT-1207 was found to be 230 nm and, therefore, the UV wavelength was set at that value. The

injection volume was 20 µL. The retention time of MT-1207 was approximately 5 minutes. The quantitation of MT-1207 samples was carried out using a calibration curve which covered a concentration range of 1 – 50 µg/mL for the phosphate buffer dissolution method and 1 – 100 µg/mL for the acetate buffer dissolution method. The HPLC method was validated in terms of linearity, limit of detection (LOD) and limit of quantitation (LOQ) as per the International Council for Harmonisation (ICH) and FDA guidelines. The LOD was 0.1 µg/mL and the LOQ was 0.4 µg/mL. The validation of the HPLC method for specificity, accuracy, intra-day and inter-day precision was carried out along with that of the dissolution method.

2.3 Flowability characterisation of the tablet blends

The flow properties of the powder mixtures are most important. The flowability directly affects the filling uniformity of the die in the tabletting machine and, therefore, the corresponding uniformity of tablet weight and drug content (210). As per the USP, the flowability was assessed in terms of bulk/tapped density, compressibility index, Hausner ratio and angle of repose.

Bulk/tapped density testing was carried out using tapped density tester (Copley®, Nottingham, United Kingdom) to determine the flow properties of the different powder mixtures as per USP <616> (211). Each time, a certain amount of powder mixture was weighed and then added inside a 100-mL graduated measuring cylinder. The initial volume (bulk volume, V_0) was recorded. Then, the mixture was tapped 10, 500 and 1250 times and the respective volumes were recorded (V_{10}, V_{500}, V_{1250}). If the difference between V_{500} and V_{1250} was not more than 2 mL then V_{1250} was considered as the final tapped volume (211). The V_0 and V_{1250} were then used to calculate the compressibility (Carr) index and Hausner ratio. These values were used to characterise the flowability of the different mixtures.

2.4 Hardness and friability of tablets

The tablets prepared were assessed in terms of their hardness using a C50 Tablet Hardness tester (Engineering Systems (Nottm)®, Nottingham, United Kingdom). The test was carried out as per USP <1217> (212). 10 tablets were tested for each formulation batch. Each time, the tablet dimensions (diameter and thickness for flat-faced cylindrical tablets; long axis diameter, short axis diameter, wall height and thickness for oval biconvex tablets) were measured. Then, the tablet was placed in the hardness tester and the hardness value was recorded in kg units. Afterwards, the tablet tensile strength was calculated as per USP (212).

The friability of the tablets was assessed as per USP <1216> (213). The tablets were weighed before being placed into the friability tester (Erweka®, Heusenstamm, Germany). The friabilator was set at a revolution rate of 25 rpm for 4 minutes. The tablets were then removed from the device, were gently wiped using a brush to remove loose materials, were weighed and the % friability calculated. As per USP, the friability should be less than 1.0 %.

2.5 Tablet weight variation

The tablet weight variation was assessed as per USP <905> (210). 10 tablets were weighed individually for each formulation. The mean tablet weight was calculated and expressed as a percentage of the target tablet weight, and the acceptance value was calculated. The tablet weight variation was considered to be within the acceptable range set in USP if the acceptance value was less than 15.

2.6 Differential scanning calorimetry (DSC) analysis of MT-1207 and tablet samples

The thermal behaviours of MT-1207 hydrochloride and pulverised tablet samples were evaluated using DSC Q2000 (TA® Instruments, Centennial Park, United Kingdom). Samples (1-5 mg) were each time weighed and sealed inside an aluminum pan with pierced aluminum lids. The analysis took place over a temperature range of 40 – 240 °C at a rate of 5

°C/min in an atmosphere of nitrogen, the flow rate of which was set at 50 mL/min. The first analysis of the MT-1207 reference standard took place over a temperature range of 40 – 300 °C to spot any potential thermal degradation at temperature values beyond 240 °C.

2.7 Fourier-Transform Infrared (FTIR) spectrophotometric studies

Fourier-Transform Infrared (FTIR) spectra were obtained for MT-1207 hydrochloride and the tablet samples using Cary 630 FTIR spectrophotometer (Agilent Technologies®, Craven Arms, United Kingdom). Each time, the solid sample was placed on the lid and scanned at the range 4000 – 650 cm^{-1}.

2.8 X-ray powder diffraction (XRPD) analysis of MT-1207 and tablet samples

The diffractograms of MT-1207 hydrochloride and pulverised tablet samples were obtained using an X'Pert Pro MPD X-ray diffractometer (Malvern Panalytical®, Malvern, United Kingdom). Cu K-alpha1 radiation was used. The samples were scanned at an angle range of 4 – 50°(2θ) with a step size of 0.01°(2θ) at 40 mV, 40 mA and a sample rotation speed of 15 rpm.

2.9 Kinetics and mechanism of drug release

Based on the results obtained from *in vitro* release testing for the optimised formulations F4, bilayer F_{HE6005} and bilayer A1, the release kinetics of MT-1207 from these formulations were studied. For this purpose, the data obtained from the *in vitro* drug release testing were plotted in various kinetic models. These models were first-order (Equation 1) as log percentage of MT-1207 remaining undissolved vs time, zero-order (Equation 2) as the cumulative amount of drug released vs time and Higuchi's models (Equation 3) as cumulative percentage of MT-1207 released vs square root of time. Finally, the data were plotted using the Hixson-Crowell cube root law to evaluate the drug release with changes in the particle/tablet surface area and diameter (Equation 4) (46).

$$LogQ_1 = LogQ_0 - k_1t/2.303 \quad [1]$$

where Q_1 is the amount of the drug in the tablet at time t, Q_0 is the total amount of the drug and k_1 is the first-order constant.

$$C = k_0t \quad [2]$$

where C is the concentration of the drug at time t and k_0 is the zero-order constant.

$$Q = k_Ht^{1/2} \quad [3]$$

where Q is the cumulative % of drug released at time t and k_H is a constant the value of which depends on the system design variables (46).

$$\sqrt[3]{Q_0} - \sqrt[3]{Q_t} = k_{HC} \times t \quad [4]$$

where Q_t is the amount of drug released in time t, Q_0 is the initial total amount of drug in the tablet and k_{HC} is the rate constant for the Hixson-Crowell equation which refers to the plot of the cube root of the drug remaining in the tablet vs time.

The mechanism of drug release from F4, F_{HE6005} and bilayer A1 tablets was determined using the Korsmeyer-Peppas model (214). The data from the *in vitro* dissolution

testing were plotted in the Korsmeyer-Peppas equation (Equation 5) as log cumulative percentage of drug released vs log time. The exponent *n* was calculated by measuring the slope of the straight line.

$$M_t/M_\infty = kt^n \quad [5]$$

where M_t is the amount of drug released at time *t*, M_∞ is the total amount of drug, *k* is a kinetic constant the value of which is characteristic of the drug/polymer system and *n* is an exponent that is used to characterise the mechanism of drug release (214). For cylinder tablets, $n = 0.45$ corresponds to drug release controlled by Fickian diffusion, $0.45 < n < 0.89$ corresponds to anomalous (non-Fickian diffusion) which refers to a combination of Fickian diffusion and polymer relaxation mechanisms, while $n > 0.89$ defines super Case-II transport where drug release is controlled by polymer relaxation (134, 215, 216).

2.10 Bioanalytical method

MT-1207 in plasma samples collected during the pharmacokinetic studies was determined by a validated UPLC-MS/MS method using verapamil hydrochloride as an internal standard. Each time 10 µL of plasma sample were pipetted in 1.5 mL Eppendorf® tube. 200 µL of verapamil hydrochloride 2 ng/mL in acetonitrile were added and vortex was carried out for 5 minutes. Centrifugation was then carried out at 15000 rpm for 5 minutes and 100 µL of supernatant were collected for UPLC-MS/MS analysis. The ion source was an electron spray ionisation (ESI) source. A positive ion scanning method was used for detection. The solvent gas (nitrogen) flow rate was 1000 L/h, the temperature of the solvent gas was 500 °C, and the capillary voltage was 3.0 kV. The scanning method was Multiple Response Monitoring (MRM). The cone voltage was set at 40 V, while the collision energy

was 20 eV. For quantitative analysis, the ion pairs used had m/z 393.26 → 274.04 (MT-1207) and m/z 455.25 → 156.06 (internal standard). The samples were applied to an ACQUITY Ultra Performance Liquid Chromatography system with Xevo TQ-XS Triple Quadrupole Mass Spectrometer with operating software MassLynx V4.2 (Waters Technology Limited Company). The column used was an ACQUITY UPLC BEH C18 liquid chromatography column (2.1 × 50 mm, 1.7 μm). The mobile phase consisted of 0.1 % formic acid in water (mobile phase A) and acetonitrile (mobile phase B). Verapamil hydrochloride was used as the internal standard for determination. The gradient elution was: 0 – 1.2 min: 20 – 45 % B, 1.2 – 1.5 min: 45 – 95 % B, 1.5 – 1.8 min: 95 % B, 1.8 – 2.5 min: 95 – 20 % B. The flow rate was set at 0.5 mL/min. The column temperature was set at 45 °C.

Quantification was carried out using a calibration curve. 10 mg MT-1027 were accurately weighed and dissolved in DMSO to prepare a stock solution of MT-1207 with a concentration of 10 mg/mL. This was gradually diluted with a 50 % acetonitrile solution to obtain standard working solution concentrations of 10, 20, 40, 100, 200, 400, 1000, 2000, 4000 ng/mL. The concentrations of the quality control samples were 30, 320, 3200 ng/mL. To prepare a quality control working solution, 10 μL were added to 190 μL Beagle dog blank plasma. Vortex mixing was carried out to obtain the standard curve with drug concentration values of 0.5, 1, 2, 5, 10, 20, 50, 100 and 200 ng/mL, and plasma with drug concentration values of 0.5, 1.5, 16 and 160 ng/mL. 20 μL of medicated plasma were transferred into a 1.5 mL Eppendorf® tube and 200 μL of 2 ng/mL verapamil hydrochloride in acetonitrile were added. Vortex was carried out for 5 minutes, followed by centrifugation at 15,000 rpm for 5 minutes. 100 μL of supernatant were collected for UPLC-MS/MS measurement. The lower limit of quantitation (LLOQ) was 0.500 ng/mL. The R^2 of the standard curve was around 0.9978. The accuracy and precision values of the quality control samples were 101.0 % and 3.2 % CV, respectively.

3 Chapter 3: Preparation, *In Vitro* Characterisation and *In Vivo* Evaluation of MT-1207 Sustained-Release HPMC Matrix Tablets

Napoleon-Nikolaos Vrettos[a*], Peng Wang[b,c*], Yan Zhou[c], Clive J. Roberts[a], Jinyi Xu[b], Hong Yao[b] and Zheying Zhu[a]

[a] School of Pharmacy, University of Nottingham, Nottingham, United Kingdom

[b] School of Pharmacy, China Pharmaceutical University, Nanjing, China

[c] Shenyang Haiwang Biotechnology Co. Ltd., Shenyang, China

* Equal first authors

This chapter has been published as the following research article:

Vrettos NN, Wang P, Zhou Y, Roberts CJ, Xu J, Yao H, Zhu Z. In vitro *and* in vivo *evaluation of a sustained-release once-a-day formulation of the novel antihypertensive drug MT-1207*. Pharmaceutical Development and Technology. 2021. 26(3): 349-361. DOI: https://doi.org/10.1080/10837450.2021.1872087

Acknowledgement of research work done by co-authors

Wang P, Zhou Y: Provided API materials, IR tablets, information on the physicochemical properties, pharmacological mechanism of action and the *in vivo* PK parameters of MT-1207 materials in Beagle dogs, ensured funding of the *in vivo* study, and critically reviewed the manuscript.

Xu J, Yao H: Conducted the *in vivo* study, and critically reviewed the manuscript.

Roberts CJ, Zhu Z: Academic supervisors to NN Vrettos. Also, supervised him during writing the manuscript. Critically reviewed the manuscript and editing.

A special thanks to Professor Xijin Chen (School of Basic Medicine and Clinical Pharmacy, China Pharmaceutical University) for his help with the *in vivo* study on the pharmacokinetics of MT-1207. Also, a special thanks to Colin Wills (School of Pharmacy Building, University of Nottingham, United Kingdom) for training and supporting NN Vrettos on the use of the tabletting machine.

Keywords: MT-1207; Sustained-release tablets; Hydrophilic matrix; Drug release; Pharmacokinetics

3.1 Introduction

As was mentioned earlier in Chapter 1 of the thesis, matrix systems are commonly used as controlled-release formulations. In dissolution-controlled matrix systems, hydrophilic polymers are used as the matrix formers and are mixed with the API(s) and excipients. The release of drugs from these systems is controlled by polymer wetting and water diffusion through the matrix, drug diffusion through the matrix, as well as matrix erosion (46, 47).

Many different hydrophilic polymers can be used to prepare controlled-release matrix systems. The most commonly used ones are cellulose ether derivatives which include HPMC (48). HPMC polymers of different viscosities have been employed as release retardants alone or in combination with HPMC of other viscosities and/or other polymers in many different applications for both hydrophilic and hydrophobic drugs (45, 46, 49, 50, 64, 67, 217-219). High viscosity grades of HPMC can be used in tablets to retard drug release from matrices at a percentage of 10 − 80% w/w (51).

3.1.1 Experimental aim

To date, immediate-release tablets of MT-1207 have been developed and are being tested in phase II clinical trials. However, these tablets are designed to be administered two times a day. Due to the challenges that come with hypertension, it is desirable to reduce the

dosing frequency as much as possible to improve patient compliance and reduce polypharmacy.

In the present study, a new sustained-release matrix tablet formulation of MT-1207 hydrochloride was developed. HPMC polymers of different viscosities were used as release retardants. They were selected as first-choice matrix formers and release retardants, due to their versatility and multiple successful sustained-release applications. Different tablet formulations were prepared using wet granulation and were characterised in terms of their physical properties and *in vitro* drug release. An optimised tablet formulation which provided a 24-hour release of MT-1207 *in vitro* was developed. A pharmacokinetic study was performed in Beagle dogs through oral administration of the optimised sustained-release and the immediate-release tablets.

3.2 Experimental Techniques

This section entails the experimental techniques that were used to collect the data in this chapter. These include procedures listed in Chapter 2 and mentioned below, as well as additional, chapter-specific techniques that are described in detail:

- HPLC-UV method for the quantitation of MT-1207 samples
- Flowability characterisation of the tablet blends
- Hardness and friability of tablets
- Tablet weight variation
- Differential scanning calorimetry (DSC) analysis of MT-1207 and tablet samples
- Fourier-Transform Infrared (FTIR) spectrophotometric studies
- X-ray powder diffraction (XRPD) analysis of MT-1207 and tablet samples

- Kinetics and mechanism of drug release

3.2.1 Validation of HPLC and dissolution methods

3.2.1.1 Linearity

The HPLC method was validated for its linearity. For this purpose, three replicates of the calibration curve were prepared in the concentration range 0.001 – 0.05 mg/mL. The standard solution of 0.05 mg/mL concentration was prepared through dilution from an initial MT-1207 stock solution 1 mg/mL in methanol. The rest of the working standard solutions were prepared by carrying out dilutions from the 0.05 mg/mL standard solution. The matrix of the standard solutions consisted of a mixture of dissolution medium and methanol at a ratio of 95:5 (% v/v). The linearity of the method was assessed based on the coefficient of determination (R^2) values of the three calibration curves prepared over three different days.

3.2.1.2 Limit of Detection and Limit of Quantitation

The HPLC method was validated for its LOD and LOQ. The standard deviation of the y-intercepts of the three linearity calibration curves was calculated. The LOD and LOQ values were then calculated using Equations 6 and 7.

$$LOD = 3.3 \times SD/S \quad [6]$$

$$LOQ = 10 \times SD/S \quad [7]$$

where SD is the standard deviation of the y-intercepts of the three linearity replicates of the calibration curve, and S is the slope of the calibration curve derived from the mean peak area values of the linearity calibration curves.

3.2.1.3 Specificity

The dissolution method was validated in terms of specificity. For this study, the excipients of the tablets were added in 900 mL 0.1 M phosphate pH 6.8 with 0.2% w/v SDS.

More specifically, 140 mg alpha-D-lactose monohydrate, 20 mg PVP K30, 70 mg HPMC K15M, 4 mg colloidal silicon dioxide and 0.5 mg magnesium stearate were added in the dissolution medium inside a dissolution vessel. The temperature was set at 37 ± 0.5 °C and the rotation speed of the paddles was set at 75 rpm. After 24 hours, a sample was collected and centrifuged (2300 g, 10 minutes). 1 mL from the supernatant was then transferred into an HPLC vial and injected into the HPLC system for analysis. The experiment was conducted in triplicate.

3.2.1.4 Accuracy and intra-day precision

The dissolution method was validated in terms of accuracy and intra-day precision. The method was validated at 20 %, 50 %, 80 %, 100 % and 120 % of the nominal concentration value of 20 mg MT-1207 in 900 mL dissolution medium. At each concentration level, the excipients of the tablets were added in 900 mL of dissolution medium as in the specificity study, followed by the addition of an appropriate volume of MT-1207 2 mg/mL solution in methanol. The rotation speed of the paddle was set at 75 rpm. After 24 hours, a sample was collected and centrifuged (2300 g, 10 minutes). 1 mL of the supernatant was then transferred into an HPLC vial and injected into the HPLC system for analysis. The experiment was carried out in triplicate and the intra-day precision was determined through % residual standard deviation (% RSD) for the three values per accuracy level.

3.2.1.5 Inter-day precision

The dissolution method was validated for inter-day precision. Two accuracy samples were prepared on two different days for each of the concentration levels mentioned in Section 2.3.4 and the experiment was carried out as per Section 2.3.4. The % RSD of these values and the mean of the values from the accuracy experiment was calculated and the inter-day precision of the method was assessed.

3.2.2 Scanning electron microscopy (SEM) analysis of MT-1207 reference standard and micronised MT-1207

The MT-1207 hydrochloride reference standard and micronised MT-1207:silicon dioxide 5:1 mixture were examined by scanning electron microscopy (Philips® XL30 SEM, Netherlands) using 10 kV accelerating voltage. Before imaging, the samples were sputtered with gold using an SC7640 Sputter Coater (Polaron®, United Kingdom). Coated samples were then observed in the SEM at 10 kV under vacuum conditions at ambient temperature.

3.2.3 Solubility measurements of MT-1207:colloidal silicon dioxide 5:1 mixture

Solubility testing was carried out for the MT-1207 reference standard and the micronised MT-1207:colloidal silicon dioxide 5:1 mixture. The aim was to determine the solubility of MT-1207 in different pH values and to define whether micronisation had an effect on the solubility of MT-1207 agent. The testing was carried out in hydrochloric acid (HCl) pH 1.2 and 0.1 M phosphate buffer pH 6.8 simulating the pH values in the fasted stomach and small intestine, respectively. Solubility studies were carried out using the shake-flask method (220). A known excess quantity of the drug was weighed each time and dispersed in 5 mL of medium. Then, the dispersions were placed in a Stuart® orbital incubator and were shaken for 24 hours at 37 °C. Afterwards, 3 mL were placed in Sarstedt® tubes and centrifuged in an Eppendorf® Centrifuge 5810 R (2700 g, 15 minutes). A two-step dilution was carried out for the supernatant. For the samples in hydrochloric acid, 500 μL of the supernatant were each time diluted to 1 mL with water:methanol 50:50 (% v/v) and, then, 100 μL of the diluted solution were further diluted to 1 mL with water:methanol 50:50 (% v/v). For the samples in 0.1 M phosphate pH 6.8, 500 μL were diluted to 1 mL with methanol and, then, 100 μL from the diluted solution were further diluted to 1 mL with 0.1 M phosphate pH 6.8:methanol 50:50 (% v/v). Each time, the final diluent was transferred into an amber HPLC vial for HPLC analysis.

3.2.4 Preparation of MT-1207 tablet formulations

The HPMC matrix tablets were prepared using a wet granulation method. The micronised MT-1207:silicon dioxide mixture was geometrically diluted with alpha-D-lactose monohydrate and then the rest of the excipients were added. Mixing was carried out for 15 minutes manually. The powder mixture was then transferred into a beaker and the required amount of isopropyl alcohol (IPA) was added as droplets under manual mixing that was conducted using a spatula. IPA has low toxicity in humans and is, therefore, classified as Class 3 solvent, as per United States Pharmacopeia (USP) <467> (221). Afterwards, there was a wet massing time of 30 seconds. The wet mass was manually pressed through a 12-mesh stainless-steel sieve. The wet granules were then left in the fume hood to dry for two hours and were then placed in the tray drier for two hours at 60 °C. The dried granules were then sieved through a 25-45-170-mesh sieve array and the few fines (particle size < 90μm) were discarded. Magnesium stearate was added as a lubricant in the granulated mixture and mixing was carried out for 5 minutes. The granules were then compressed into tablets using a Piccola rotary tablet press machine (Riva®, Argentina). 8 mm flat-faced round punches and dies were used during the compression process. The compression force applied during the preparation of the different tablet formulations was 6.5 kN. The target tablet weight was 224.5 mg for formulations F1-F4 and 226.5 mg for formulation A1. Formulation F1 contained 18% w/w HPMC K4M, while formulations F2, F3 and F4 contained 18% w/w, 22% w/w and 31% w/w HPMC K15M, respectively. The compositions of the different tablet formulations can be seen in Table 3-1. Three different batches of the optimised formulation were prepared and characterised to ensure the reproducibility of the manufacturing method. Finally, formulation A1 used in the pharmacokinetic study was prepared based on the optimised formulation containing 30 mg MT-1207, instead.

Table 3-1: *Compositions of the MT-1207 sustained-release tablets.*

Ingredients (mg)	Formulation batch				
	F1	F2	F3	F4	A1
MT-1207 Hydrochloride	20	20	20	20	30
Alpha-D-lactose monohydrate	140	140	130	110	100
Polyvinylpyrrolidone K30	20	20	20	20	20
HPMC K15M	-	40	50	70	70
HPMC K4M	40	-	-	-	-
Colloidal silicon dioxide	4	4	4	4	6
Magnesium stearate	0.5	0.5	0.5	0.5	0.5
Tablet Weight	**224.5**	**224.5**	**224.5**	**224.5**	**226.5**

3.2.5 Flowability characterisation of the powder mixtures

Apart from bulk/tapped density testing, also the angle of repose testing was used to characterise the flowability of the different granulated powder mixtures. The fixed funnel method was used, as per USP <1174> (222). Each time, an amount of powder was added inside a funnel and left to flow through it. As the tip of the powder cone reached the bottom of the funnel, the funnel was carefully moved upwards. When the diameter of the cone reached slightly more than 6 cm the diameter of the base and the height of the cone were measured using a ruler. These values were then used to calculate the angle of repose. The flowability of the mixture was characterised based on the values of Carr index, Hausner ratio and angle of repose as per USP (222).

3.2.6 In vitro release of MT-1207 from sustained-release tablets

In vitro dissolution studies were carried out using a USP II dissolution apparatus (Copley®, Nottingham, United Kingdom) equipped with paddles. The apparatus was set at a constant rotation speed of 75 rpm. Dissolution studies were carried out in 900 mL of 0.1 M phosphate buffer pH 6.8 with 0.2% w/v SDS at 37 ± 0.5 °C. Sinkers were used to prevent

floating of tablets and their adhesion to the bottom of the vessels. Sampling was carried out manually at certain time intervals (0.08, 0.25, 0.5, 1, 1.5, 2, 3, 4, 6, 8, 10, 12, 14, 16, 18, 20, 22 and 24 hours), followed by centrifugation of the samples (2300 g, 10 minutes). Then, each time, 1 mL from the supernatant was transferred into an HPLC vial and 20 μL were injected into the HPLC for analysis. The *in vitro* release study was carried out in triplicate for each formulation.

3.2.7 Swelling and erosion studies

Swelling and erosion studies were carried out for the F4 tablets in dissolution medium, 0.1 M phosphate pH 6.8 with 0.2% w/v SDS. The USP II dissolution apparatus was used. Each time, the pre-weighed tablet (initial weight, W_0) was immersed in 900 mL dissolution medium within a dissolution vessel. The temperature was maintained at 37 ± 0.5 °C. The paddle speed was set at 75 rpm. At certain time intervals (1, 2, 4, 6, 8, 12, 16, 20 and 24 hours) the tablet was taken out of the dissolution vessel and excess water was carefully blotted from its surface. The wet tablet was weighed and the wet weight value, W_t, was obtained. The % swelling index of the tablets was calculated using Equation 8:

$$\% \text{ Swelling index} = (Wt - W_0) \times 100/W_0 \quad [8]$$

The same tablets that were used to calculate the swelling index were also used to calculate the % erosion value. After weighing, the wet tablets were placed inside an oven and the temperature was set at 60 °C. The tablets were each time dried until constant weight. The dry weight value, W_f, was recorded. The % erosion of the tablets at each timepoint was calculated using Equation 9:

$$\% \ Erosion = (W_0 - W_f) \times 100/W_0 \quad [9]$$

All experiments were done in triplicate and the results were recorded as mean ± standard deviation.

3.2.8 *In vivo animal study*

An *in vivo* animal study was carried out as per the principles of the Declaration of Helsinki in Beagle dogs (body weight 10 ± 2 kg) for MT-1207 30 mg sustained-release (A1) and 10 mg immediate-release tablets. Eight healthy beagle dogs were used, half male and half female. According to gender and weight, they were randomly divided into two groups, 4 in each group (2 males and 2 females). After fasting for 12 hours (h), the two groups of animals were given MT-1207 tablets orally. In the first half of the first group (Group 1-A), the sustained-release tablets were administered once a day, one tablet at a time, and blank blood was taken before administration. After administration, at 0.25 h, 0.5 h, 1 h, 1.5 h, 2 h, 3 h, 4 h, 6 h, 8 h, 12 h, 16 h, 24 h and 32 h timepoints approximately 1.5 mL of venous blood were each time collected. In the second half of the first group (Group 1-B) immediate-release tablets were administered three times a day, one tablet at a time, with an interval of 8 hours. Blank blood was collected before administration and then at 0.25 h, 0.5 h, 1 h, 2 h, 4 h, 8 h after the first administration (second administration), 8.25 h, 8.5 h, 9 h, 11 h, 13 h, 16 h (third dose), 16.25 h, 16.5 h, 17 h, and 24 h. Approximately 1.5 mL of venous blood were collected at each timepoint. Two groups of animals were cross-administered with another formulation after 7 days of wash-out period. In the second group (Group 2), the immediate-release tablets were administered once a day, three tablets at a time, and blank blood was taken before administration, and at 0.25 h, 0.5 h, 1 h, 1.5 h, 2 h, 3 h, 4 h, 8 h, and 24 h timepoints. Approximately, 1.5 mL of venous blood was collected at each timepoint. In all the cases,

each sample was placed in a test tube containing heparin, centrifuged and the plasma was separated and stored at -20 °C. MT-1207 in plasma samples was determined using UPLC-MS/MS.

The bioanalytical method that was used for the analysis of plasma samples was the same to the one described in Chapter 2 of the thesis.

3.2.9 *In vitro and in vivo data analysis*

The similarity or difference between the *in vitro* drug release profiles of the different formulations was assessed using the difference factor (f_1) and similarity factor (f_2), as per the FDA guidelines (223).

The peak plasma concentration of MT-1207 (C_{max}), the time to reach C_{max} (T_{max}) and the area under the concentration-time curve from 0 hours to 24 hours (AUC_{0-24h}) and to infinity ($AUC_{0-\infty}$) values were calculated from the plasma concentration vs time profile using WinNonlin® version 6.4. Furthermore, the half-life ($t_{1/2}$), clearance (CL), apparent volume of distribution (V_d), and mean residence time (MRT) values of MT-1207 after administration of the tablets following the different dosing regimens were also calculated using WinNonlin® version 6.4. Finally, the bioequivalence between the sustained-release and immediate-release tablets was investigated by calculating the ratio of AUC_{0-24h} values of the sustained-release tablet dosing regimen and the two separate immediate-release tablet dosing regimens.

T-test and one-way analysis of variance (ANOVA) were carried out for the statistical analysis of results using Microsoft Excel® software. A statistically significant difference was reflected by a *P* value less than 0.05.

3.3 Results and Discussion

3.3.1 HPLC method development for the quantitation of MT-1207 agent in dissolution samples

The peak shape of MT-1207 in the medium used for dissolution testing was acceptable in terms of peak height and asymmetry factor (Figure 3-1) under the HPLC conditions stated in Section 2.2. Also, the calibration curve (Figure 3-2) gave a R^2 value of 0.9998 which demonstrated its good linearity when the standard solutions were prepared in dissolution medium.

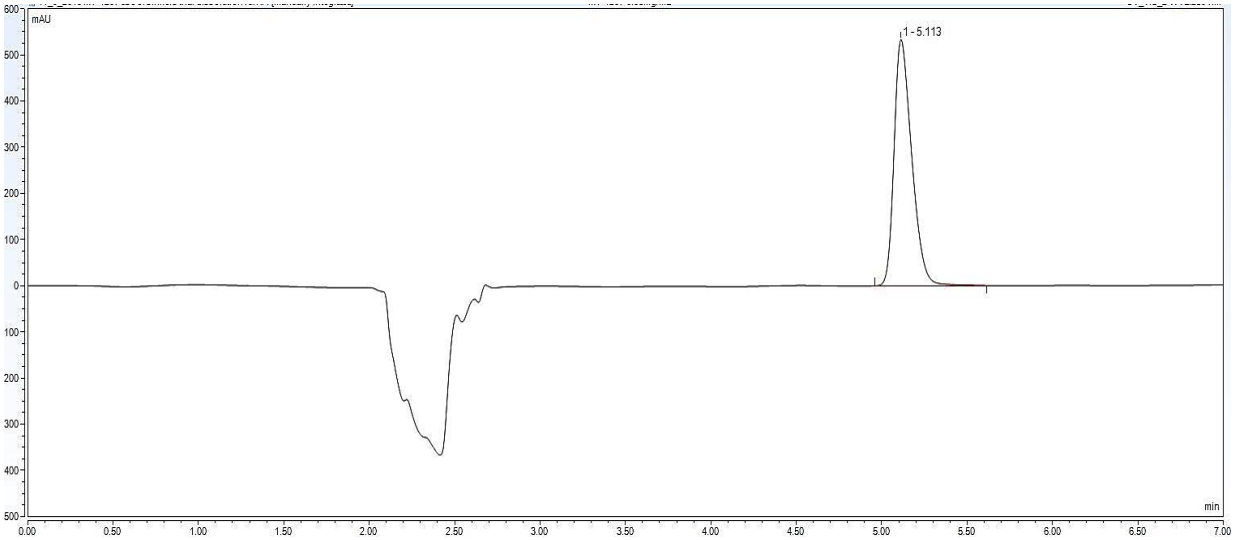


Figure 3-1: *Chromatogram of MT-1207 0.05 mg/mL standard solution in 0.1 M phosphate pH 6.8 with 0.2% w/v SDS. The MT-1207 peak was eluted at around 5.0 minutes. The solvent front was eluted at around 2.5 minutes.*

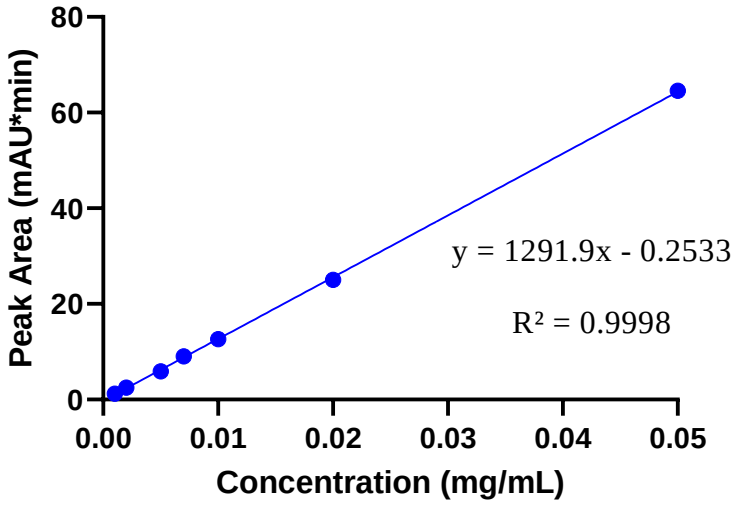


Figure 3-2: *Calibration curve of MT-1207 in 0.1 M phosphate pH 6.8 with 0.2% w/v SDS at a concentration range of 0.001 – 0.05 mg/mL.*

3.3.2 HPLC and dissolution method validation

3.3.2.1 Linearity

The HPLC method was validated for linearity in the concentration range of 0.001 − 0.05 mg/mL. Three replicates of the calibration curve in this concentration range were prepared over three different days. The R^2 should be equal to or higher than 0.99. This validation was also considered for the dissolution method since the standard matrix was used for the quantification of MT-1207 dissolution samples.

The calibration curves that were used for linearity validation and their data can be seen in Tables A-1, A-2, A-3 and Figures A-1, A-2, A-3, respectively. In all three replicates taken over three different days, the R^2 was higher than 0.999, therefore the HPLC method was considered validated in terms of linearity.

3.3.2.2 LOD and LOQ determination

The calibration curves that were used for linearity validation were also employed for the LOD and LOQ calculations. The mean of the peak areas was calculated, and a calibration

curve of the mean peak area values and the respective concentration values was plotted. Its slope was used as the S value in Equations 6 and 7. Furthermore, the standard deviation of the y-intercepts was calculated and was used as the SD value of the LOD and LOQ equations, as per the ICH guidelines (224).

The calibration curve data and plot that were used for LOD and LOQ determination can be seen in Table A-4 and Figure A-4, respectively. The slope (S) of the calibration curve was 1294. The standard deviation (SD) of the y-intercepts was 0.0576. The S and SD values were used to calculate the LOD and LOQ of the method using Equations 6 and 7.

$$LOD = 3.3 \times 0.0576/1294 = 0.0001 \text{ mg/mL} = 0.1 \text{ µg/mL}$$

$$LOQ = 10 \times 0.0576/1294 = 0.0004 \text{ mg/mL} = 0.4 \text{ µg/mL}$$

3.3.2.3 Specificity testing results

A sample chromatogram of the specificity samples can be seen in Figure A-5. As per the FDA guidance for method validation, the assay should be ensured to be free from interfering substances, including excipients and other matrix components (225). For all three replicates, no interfering peak was eluted anywhere near the retention time of MT-1207. Therefore, the dissolution method was considered validated in terms of specificity.

3.3.2.4 Accuracy, intra-day and inter-day precision results

The accuracy of the dissolution method was assessed at 20 %, 50 %, 80 %, 100 % and 120 % of the target MT-1207 concentration achieved after 100 % drug release from the tablets. Three replicates were prepared at each concentration level. As per the FDA guidelines, a method is considered accurate for each level if the mean concentration of the accuracy samples is within 85 – 115 % of the nominal concentration value (226). A method is considered precise when the % coefficient of variation (or % residual standard deviation, %

RSD) between the accuracy samples analysed within a day and three samples analysed within different days is less than or equal to 15 % (226).

Three replicates were prepared for each of the 20 %, 50 %, 80 %, 100 % and 120 % concentration levels of MT-1207 for accuracy and intra-day precision validation purposes within the same day. Also, three replicates were prepared over three different days for inter-day precision purposes. As seen in Table A-5, all accuracy values fell within 85 – 115 % of the nominal concentration, therefore, the method can be considered validated in terms of accuracy for these concentration levels. Furthermore, in Tables A-5 and A-6, the % RSD values were quite lower than 15 % for both intra-day and between-day runs. Therefore, the dissolution method was considered validated in terms of intra-day and inter-day precision.

3.3.3 Scanning electron microscopy and solubility characterisation of MT-1207

Solubility testing was carried out in hydrochloric acid pH 1.2 and phosphate buffer pH 6.8 to obtain information on the solubility of the drug at different pH values. MT-1207 was more soluble in hydrochloric acid than in phosphate buffer (Table 3-2). Since the latter was chosen as the dissolution medium in the present study, a small amount of SDS was added into phosphate buffer to ensure sink conditions during dissolution testing.

Table 3-2: *Solubility values of non-micronised MT-1207 hydrochloride reference standard and micronised MT-1207 hydrochloride:colloidal silicon dioxide 5:1 mixture in HCl pH 1.2 (n = 9) and 0.1 M phosphate buffer pH 6.8 (n = 9). Results are expressed as mean ± standard deviation.*

Sample Name	MT-1207 Solubility (mg/mL)
Non-micronised MT-1207 hydrochloride in HCl pH 1.2	1.22 ± 0.05
Micronised MT-1207 hydrochloride:colloidal silicon dioxide 5:1 mixture in HCl pH 1.2	1.34 ± 0.08
Non-micronised MT-1207 hydrochloride in 0.1 M phosphate pH 6.8	0.01
Micronised MT-1207 hydrochloride:colloidal silicon dioxide 5:1 mixture in 0.1 M phosphate pH 6.8	0.03 ± 0.01

There was no statistically significant difference between the recorded solubility values of non-micronised MT-1207 and micronised MT-1207:silicon dioxide mixture in the different media (*t*-test, $p > 0.05$) (Table 3-2). These results agree with literature findings since particle size reduction of drugs at this scale was not expected to lead to increased aqueous solubility unless it caused amorphisation of the API (227, 228). Particle size reduction could, however, enhance the dissolution rate of MT-1207, due to increased drug surface area for interaction with liquid media (229, 230). In Figure 3-3, it can be seen that the drug crystals have an elongated shape. The long-axis particle size values of the non-micronised drug and micronised drug that was used to make the tablets were 11.97 ± 7.42 µm and 4.02 ± 1.90 µm, respectively (n = 100 particles for each batch). The particle size distribution was narrower in the micronised batch than in the non-micronised drug and was used for the preparation of both immediate and sustained release tablets.

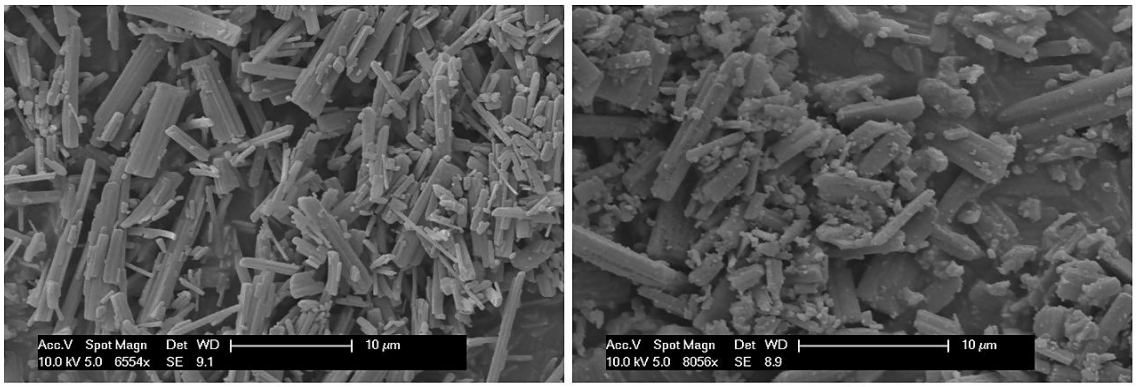


Figure 3-3: *SEM image of (A) MT-1207 reference standard and (B) micronised MT-1207:silicon dioxide 5:1 mixture.*

3.3.4 Characterisation of flowability and compressibility of the tablet powder blends

Before compression, the granulated powder blends were assessed in terms of compressibility and flowability through bulk/tapped density and angle of repose testing, as per USP.

The flowability of a powder blend is most important since it determines whether the filling of the powder in the dies of the tabletting machine is uniform, thus ensuring uniform tablet weight and dimensions and drug content uniformity (49). The flowability of a powder blend can be assessed through Carr index, Hausner ratio and/or angle of repose. Compressibility is also important since it defines the ability of a powder to compress upon application of pressure (67). Carr index is a good indicator of the powder flowability and compressibility (231). Therefore, a Carr index value between 5 % and 16 % is desirable to achieve both good flowability and compressibility (67). F1, F4 and A1 powder blends had Carr index values of 14.7, 12.2 and 13.3 %, respectively (Table 3-3), which indicated a combination of good flowability and compressibility. F3 powder blend gave a Carr index value of 15.4 % which indicated fair flowability. The F2 powder blend had a relatively high

compressibility index value of 23.5 %, but, still, its flowability was characterised as passable, which ensured its free flow in the feeder of the tabletting machine and the dies.

Table 3-3: *Flowability characterisation results.*

Tablet Formulation	Compressibility (Carr) Index (%)	Hausner Ratio	Angle of Repose (°)	Flowability (as per USP)
F1	14.7	1.17	34.2	Good
F2	23.5	1.31	33.2	Passable to Good
F3	15.4	1.18	38.7	Fair to Good
F4	12.2	1.14	42.0	Passable to Good
F4 Repeat 2	12.9	1.15	39.0	Fair to Good
F4 Repeat 3	14.0	1.16	35.6	Good
A1	13.3	1.15	36.4	Good

Hausner ratio is another measure of the flow properties of a powder blend (232). It provides information on the extent of the powder densification upon compression. Powders with a higher tendency to densify have higher Hausner ratio values. All powder blends had Hausner ratio values that indicated fair to good flowability and were in complete alignment with the respective Carr index values. For each tablet batch, both values were calculated through bulk/tapped density testing, as per USP. The Hausner ratio values ranged between 1.14 and 1.18 for the powder mixtures of formulations F1, F4 and A1 (Table 3-3) which confirmed their good flowability and compressibility, along with the respective Carr index values. The F3 powder blend gave a Hausner ratio of 1.18 which indicated a good flowability. The F2 powder blend, gave a relatively high Hausner ratio of 1.31, but, still, its flowability was characterised as fair and in alignment with the respective Carr index value.

The angle of repose can also be used to characterise the flow properties of solids. It is a characteristic related to powder cohesion or resistance to movement between particles (222). High angle of repose values correspond to high powder cohesiveness and, thus, poor flow properties. The angle of repose values for the F1, F3, F4 Repeat 3 and A1 powder mixtures were 34.2°, 33.2°, 35.6° and 36.4°, respectively (Table 3-3). These test findings were aligned with the bulk/tapped density results for the flowability of the blends. In F2 and F4 batches, there was a deviation of the angle of repose value from bulk/tapped density results. For F2 the angle of repose value (33.2°) defined a good flowability, while the rest of the results indicated a fair flowability. For F4, the angle of repose value, 42.0°, defined a passable flowability of the powder, while the bulk/tapped density results indicated a good flowability of the same blend. Finally, for the F4 Repeat 2 blend, the angle of repose value indicated fair flowability, instead of the good flowability indicated by the respective Carr index value. Such subtle variations can occur within these empirical type tests, but they remain broadly consistent.

3.3.5 Post-compression parameters of tablet formulations

The hardness of the prepared tablet formulations was assessed (Table 3-4). Increasing HPMC content and viscosity grade from formulations F1 to F4 resulted in higher hardness values. This could be due to the binding properties of HPMC, so, increasing its content probably resulted in stronger solid bridges within the tablets and, thus, higher hardness (52, 233). The hardness test was also carried out for F4 Repeats 2 and 3 (Table 3-4). There was no statistically significant difference in tablet hardness between the three F4 batches (one-way ANOVA, $p > 0.05$). Also, the hardness of A1 tablets bound to be used for animal studies was similar to that of F4 tablets (one-way ANOVA, $p > 0.05$).

Table 3-4: *Tablet hardness and friability testing results (n = 10 tablets for each formulation). Results are presented as mean ± standard deviation.*

Tablet Formulation	Diameter (mm)	Thickness (mm)	Hardness (kg)	Tensile Strength (kPa)	% Friability
F1	8.01 ± 0.03	3.51 ± 0.03	9.18 ± 0.86	2057.2 ± 186.7	0.18
F2	7.98 ± 0.04	3.49 ± 0.02	10.79 ± 0.50	2413.7 ± 114.0	0.09
F3	7.99 ± 0.03	3.52 ± 0.04	11.69 ± 0.58	2595.9 ± 134.6	0.06
F4	7.99 ± 0.03	3.50 ± 0.07	13.89 ± 1.70	3100.2 ± 336.6	0.01
F4 Repeat 2	8.00 ± 0.03	3.50 ± 0.05	14.94 ± 1.41	3332.0 ± 287.4	0.01
F4 Repeat 3	7.99 ± 0.03	3.50 ± 0.02	13.18 ± 1.51	2943.7 ± 339.6	0.14
A1	7.98 ± 0.04	3.52 ± 0.06	14.81 ± 0.40	3295.0 ± 125.2	0.04

All tablet batches gave friability values that were well within the acceptable range of 1.0 % set in USP (Table 3-4). This confirmed their good quality and their ability to withstand the expected, abovementioned mechanical shocks.

All tablet batches gave acceptable mean weight values and acceptance values, with regards to tablet weight variation (Table 3-5). Therefore, for all formulations, the tablets could probably have a uniform weight of drug substance per weight of dosage unit.

Table 3-5: *Tablet weight variation testing results (n = 10 tablets per formulation).*

Formulation	Mean Tablet Weight (% of label claim)	Standard Deviation	Acceptance Value
F1	100.4	2.8	6.7
F2	100.1	3.8	9.2
F3	99.9	0.8	2.0
F4	100.2	1.4	3.4
F4 Repeat 2	99.8	1.3	3.1
F4 Repeat 3	99.6	3.8	9.2
A1	100.0	1.2	9.2

3.3.6 DSC analysis

The thermal behaviour of an MT-1207 reference standard and that of the tablet formulations was assessed using DSC.

DSC thermograms of MT-1207 and the different formulations can be seen in Figures 3-4 and 3-5. MT-1207 hydrochloride crystal (Figure 3-4) showed a sharp endothermic peak at around 210 °C which was attributed to its melting point, while degradation seemed to take place at around 275 °C. In the thermograms of the tablet formulations (Figure 3-5) different peaks were noted. The peaks at around 150-160 °C corresponded to the dehydration of alpha-D-lactose monohydrate towards beta-lactose and melting point of PVP K30, and the peak at around 220 °C corresponded to the melting point of beta-lactose. A relatively broad endothermic peak was seen at the temperature range 178-197 °C. This was proposed to correspond to the melting point of the MT-1207 hydrochloride crystal. The reduction in the crystal melting point could potentially be due to the mixing process which, as per the Schroeder-van Laar theory, results in a lower melting point of the drug, through the reduction of the crystal solidification temperature when the drug is part of a eutectic system consisting

of a mixture of binary phase change materials. Additionally, the peak broadening and reduction in the heat of fusion that was recorded for the peak of MT-1207 could be due to the fact that, for the given molar fraction of the drug in the liquid state of the binary system, the interactions between the molecules of the drug are weaker than the interactions between the drug and the excipient molecules. Therefore, less energy is required for phase change (234).

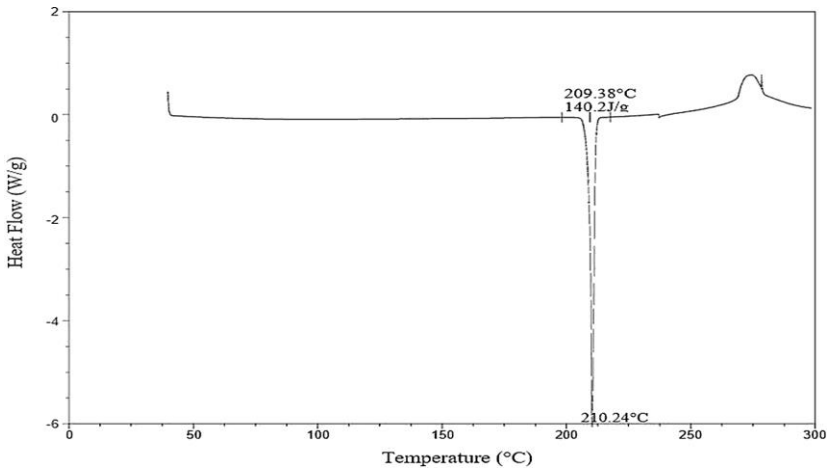


Figure 3-4: *DSC thermogram of MT-1207 hydrochloride reference standard.*

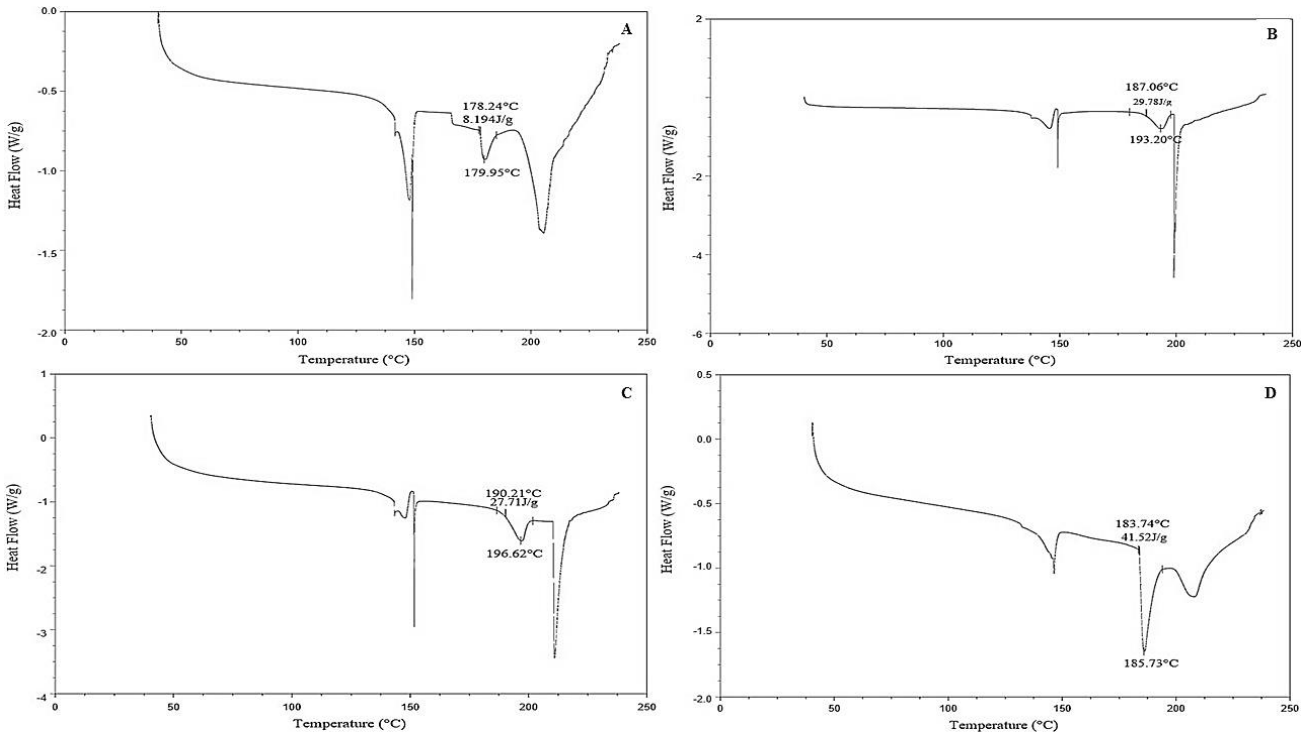


Figure 3-5: *DSC thermograms of (A) Formulation F1, (B) Formulation F2, (C) Formulation F3 and (D) Formulation F4.*

3.3.7 FTIR analysis

In Figure 3-6, the FTIR spectra of MT-1207 hydrochloride reference standard (Figure 3-6A), HPMC K15M (Figure 3-6B), colloidal silicon dioxide (Figure 3-6C) and pulverised tablets (Figure 3-6D) can be seen.

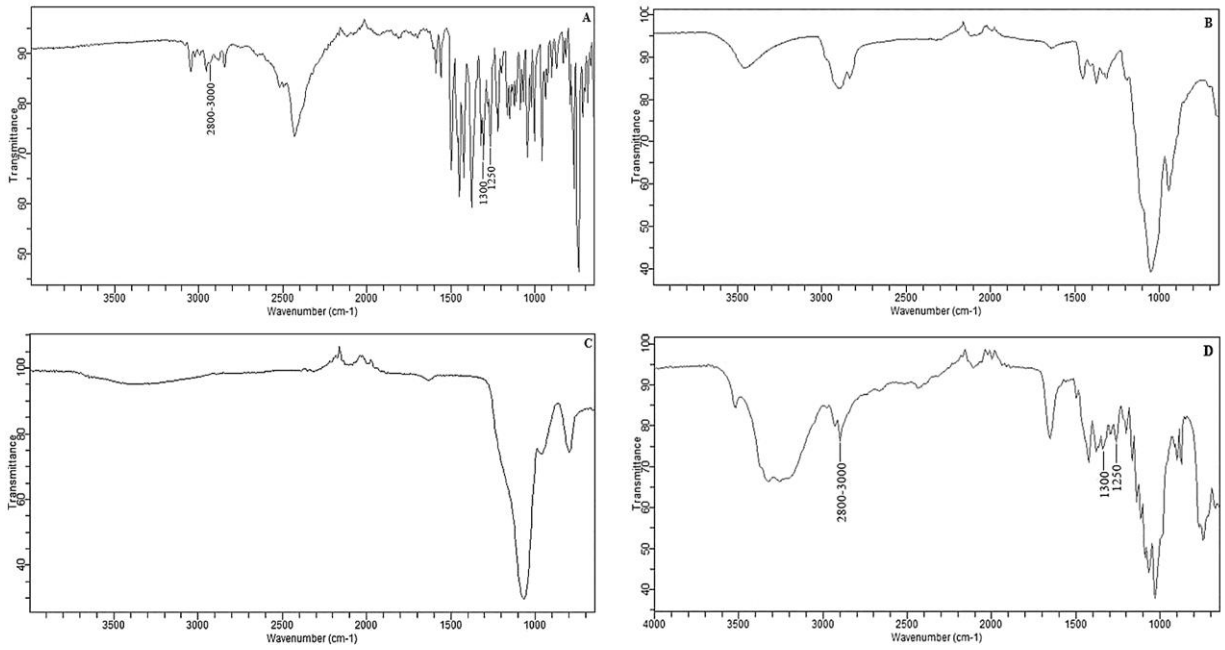


Figure 3-6: *Fourier-Transform Infrared (FTIR) spectra of (A) MT-1207 hydrochloride reference standard, (B) HPMC K15M, (C) colloidal silicon dioxide and (D) pulverised tablets [Transmittance vs Wavenumber (cm^{-1})].*

FTIR characterisation is useful in determining whether chemical reactions between the API and the excipients occur during mixing, granulation and tabletting (235). The chemical structure of MT-1207 does not contain functional groups that would readily react with the excipients. The peaks in the 2800-3000 cm^{-1} region (Figure 3-6A) that correspond to aliphatic and aromatic C-H stretch can also be seen unchanged in the pulverised tablet spectrum (Figure 3-6D). Furthermore, the peaks in the 1250-1300 cm^{-1} region that correspond to C-N stretch can be seen in the spectra of both the MT-1207 reference standard and pulverised tablets. Finally, the fingerprint region of the pulverised tablets was a simple mixture of the

fingerprint regions of MT-1207 hydrochloride (Figure 3-6A), colloidal silicon dioxide (Figure 3-6B) and HPMC K15M (Figure 3-6C) with no additional peaks observed. These results illustrated that there were no significant chemical interactions between MT-1207 and the excipients.

3.3.8 XRPD analysis

The diffractograms of MT-1207 hydrochloride reference standard and formulations F1 and F4 were acquired and can be seen in Figures 3-7A and 3-7B, respectively. The peaks of MT-1207 anhydrous crystal are assigned in Figure 3-7C. The diffractograms of the sustained-release tablet formulations were identical. In Figure 3-7C, it can be seen that the peaks of the F4 diffractogram over the angle(˚2theta) values of 11.5, 15 and 18 corresponded to the respective peaks of the MT-1207 hydrochloride reference standard, while all the other peaks of the F4 diffractogram corresponded to the peaks of alpha-D-lactose monohydrate. The reduction in peak height and broadening of the MT-1207 peaks in the F1 and F4 diffractograms (Figures 3-7B and 3-7C) could be attributed to the smaller crystal particle size of the MT-1207:colloidal silicon dioxide used in the tablets, compared to that of the reference standard. Also, it can be attributed to potential lattice strain conferred by the mixing, wet granulation and tablet compression processes during tablet preparation. All the peaks present in the diffractogram of F4 could be attributed to either MT-1207 anhydrous crystal or alpha-D-lactose monohydrate. Therefore, it can be asserted that within the sensitivity of the analysis that the drug was present in the tablets solely in the form of the anhydrous crystal.

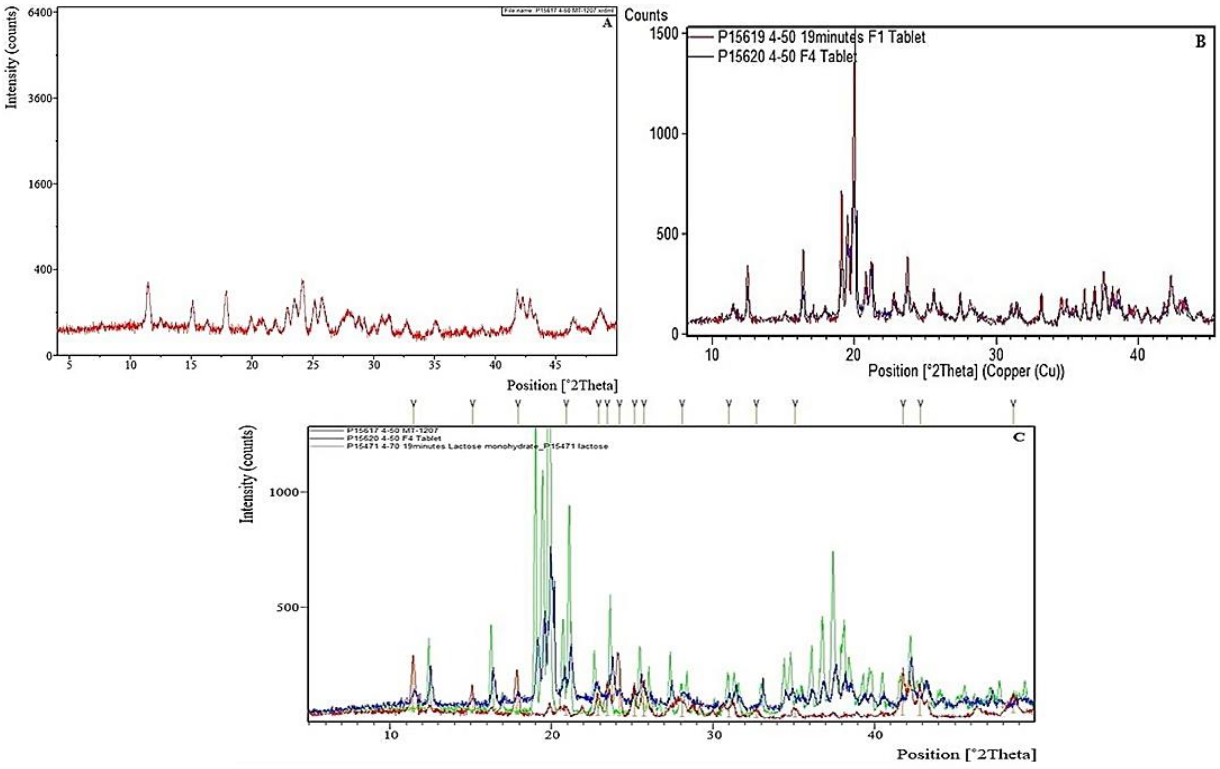


Figure 3-7: *Diffractograms of (A) MT-1207 hydrochloride reference standard, (B) formulations F1 (red) and F4 (blue) and (C) MT-1207 hydrochloride reference standard (red), F4 (blue) and alpha-D-lactose monohydrate (green) combined [Intensity (Counts) vs Position(˚2Theta)].*

3.3.9 In vitro release of MT-1207 from sustained-release tablets

The *in vitro* release profiles of the immediate-release tablets and the different sustained-release tablet batches can be seen in Figure 3-8. HPMC has been used as a release retarding polymer due to its ability to swell when in contact with water. In the present study, HPMC polymers of different molecular weight and viscosity values were used in the different formulations. HPMC K4M was the initial choice of release retarding polymer. In the literature, this viscosity grade of HPMC has been effective in retarding the *in vitro* release of different drugs from sustained-release formulations (49, 64, 236). However, when HPMC K4M was used as a sole release retardant at a percentage of 18% w/w (formulation F1) it was unable to significantly retard the release of MT-1207. For this reason, in the rest of the

batches, HPMC K4M was replaced by HPMC K15M, a polymer of higher molecular weight and viscosity.

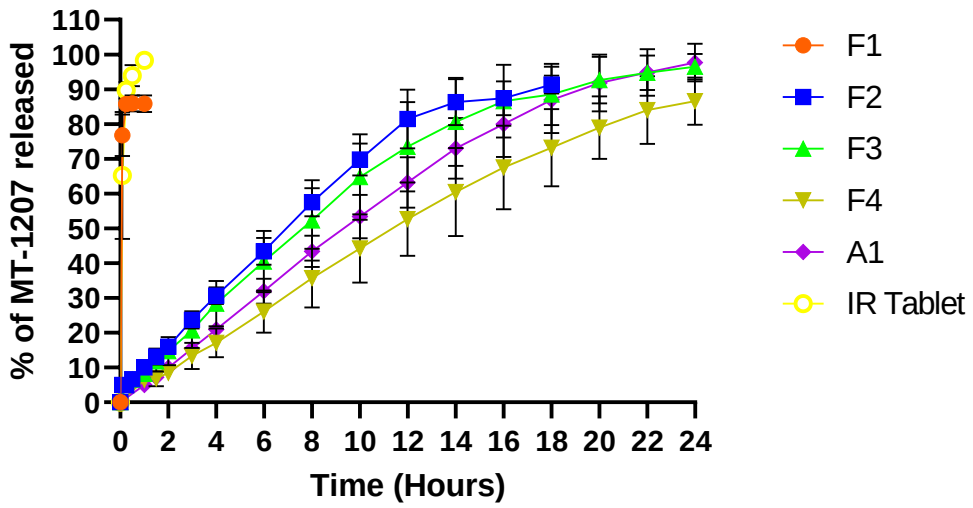


Figure 3-8: *In vitro release profiles of MT-1207 from immediate-release tablets, and formulations F1, F2, F3, F4 and A1 in 0.1 M phosphate pH 6.8 with 0.2% w/v SDS (n = 3).*

In Figure 3-8, it can be seen that a sustained release of MT-1207 was achieved from tablets with HPMC K15M. In the literature, it has been noted that drug release rate from matrix tablets decreases with increasing HPMC concentration and viscosity, due to increasing strength and thickness of the gel layer that is formed upon swelling of the polymer and the diffusion of the drug through the polymer chains being retarded (236, 237). Lactose, in contrast, promotes drug release through promoting matrix hydration, gel formation and free volume (238). Increasing the concentration of HPMC K15M from F2 to F4 resulted in a slower release of MT-1207 which was maintained linear over a longer time. The results of the present study are, therefore, fully aligned with the literature (237). There was a statistically significant release in the release profiles between F3 and F4 (f_1 = 33, f_2 = 44). The desired release profile of the drug was acquired from formulation F4 (31% w/w HPMC K15M), reaching approximately 93 % release after 24 hours of dissolution with the linearity of release

being maintained for 20 hours. This is most desirable since it could potentially ensure constant, effective levels of MT-1207 in plasma following absorption of the drug through the gastrointestinal tract (46). Therefore, formulation F4 was selected as the optimised formulation and was forwarded to the *in vivo* study. Furthermore, no statistically significant difference was noted between the release profiles from the three different F4 batches (one-way ANOVA, $p > 0.05$) ($f_1 < 15$ and $f_2 > 50$ between the *in vitro* release profiles of the three batches) (Figure 3-9). Therefore, it was concluded that the manufacturing process and the formula gave rise to tablets with reproducible properties. Finally, formulation A1 was prepared based on F4 with a change in the MT-1207 dose to 30 mg. There was no statistically significant difference in the *in vitro* release profile of MT-1207 between the F4 and A1 formulations (*t*-test, $p > 0.05$) ($f_1 = 7$, $f_2 = 75$). Therefore, the properties of F4 and A1 tablets were identical.

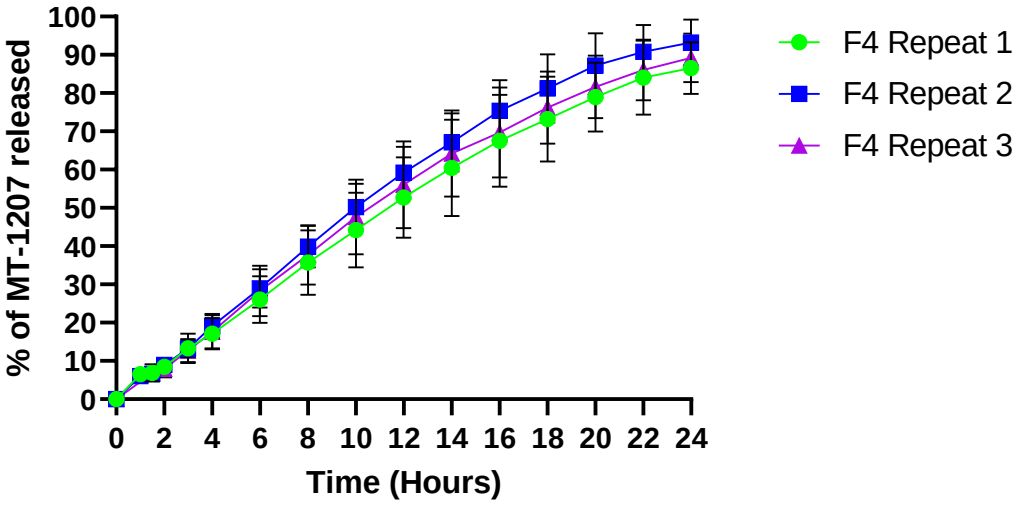


Figure 3-9: *In vitro release profiles of MT-1207 (% of MT-1207 released vs time) from the three F4 batches in 0.1 M phosphate pH 6.8 with 0.2% w/v SDS (n = 3).*

3.3.10 Swelling and erosion study

The swelling and erosion behaviour of tablets is most important since it can affect drug release kinetics. In Figure 3-10, the results from the swelling and erosion studies of F4 tablets can be seen. The tablets showed significant swelling in the dissolution medium with the tablet weight increasing by 170.6% w/w after 8 hours of dissolution. A rapid swelling phase was initially noted, since 110.3% w/w swelling took place within 2 hours of dissolution, followed by a relatively slower increase between 2 and 8 hours of dissolution. After 8 hours of dissolution, the tablet erosion reached 64.0% w/w indicating that most of the tablet mass had eroded at the time where maximum swelling of the tablets was achieved. After that timepoint, a noteworthy reduction of the erosion rate was recorded, possibly because maximum swelling was reached and, therefore, the thickness of the hydrogel and the viscosity of the surrounding viscous solution were maximised. These results, along with the *in vitro* release findings, indicate that diffusion and swelling may have contributed, to some extent, to the release of MT-1207 from the F4 tablets, but drug release was predominantly erosion-controlled.

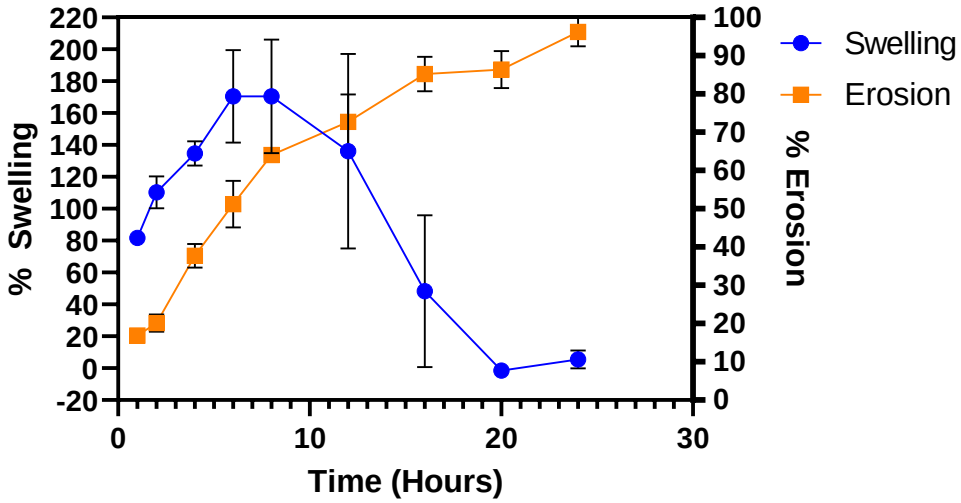


Figure 3-10: *In vitro swelling and erosion profiles of formulation F4 in 0.1 M phosphate pH 6.8 with 0.2% w/v SDS (% swelling and % erosion vs time, n = 3).*

3.3.11 Kinetics and mechanism of MT-1207 release from formulation F4

Through the selection of an appropriate molecular weight of HPMC in the matrix and the rate of matrix hydration, the rate of polymer disentanglement can be controlled. Therefore, the mechanism of drug release is dependent on the sum of drug diffusion and polymer relaxation and erosion. The release profile of F4 tablets was plotted against different models to elucidate the kinetics of drug release, while the Korsmeyer-Peppas model was used to obtain information on the mechanism of drug release. All models were used to analyse the data of up to 60 % of the release curve (215, 218).

The release data of formulation F4 were plotted in zero-order, first-order, Higuchi, Hixson-Crowell and Korsmeyer-Peppas models. The R^2 values of the different model plots can be seen in Table 3-6. The data fitted best to the zero-order model (R^2 = 0.9992). When the data were plotted against the Korsmeyer-Peppas model, the *n* value (calculated from the slope of the curve) was 0.98 (Table 3-6) which corresponded to a zero-order mechanism of release of MT-1207 from F4. Therefore, it can be assumed that both the kinetics and mechanism of the release of MT-1207 from F4 tablets were zero-order. The kinetic analysis findings were aligned with the swelling and erosion study results which, being well correlated with the *in vitro* release profiles, also indicated an erosion-controlled drug release from the F4 tablets.

Table 3-6: *Formulation F4 kinetic analysis results.*

Models	Kinetic constant	Coefficient of determination (R^2)
First-order	0.142	0.9835
Zero-order	0.001	0.9992
Higuchi	22.479	0.9849
Hixson-Crowell	0.103	0.9689
Korsmeyer-Peppas		
Kinetic constant	Coefficient of determination (R^2)	Exponent (*n*)
4.586	0.9985	0.98

3.3.12 In vivo animal study

The sustained-release and immediate-release tablets of MT-1207 were cross-administered orally in four Beagle dogs. Figure 3-11 illustrates the pharmacokinetic profiles of MT-1207 in the dog plasma after oral administration of one MT-1207 30 mg sustained-release tablet, three 10 mg immediate-release tablets with 8-hour interval between each and three 10 mg immediate-release tablets administered at one time. The pharmacokinetic parameters recorded on the respective dosing regimens in Beagle dogs can be seen in Table 3-7. As per preliminary data, the minimum effective concentration of MT-1207 in plasma has been determined to be approximately 1 ng/mL (Internal communications with Shenyang Haiwang Biotechnology Co Ltd; unreferenced). A sustained pharmacokinetic profile of MT-1207 can be seen after oral administration of the sustained-release (SR) tablet, compared to the pharmacokinetic profiles of the immediate-release (IR) tablets. There was a statistically significant decline (*t*-test, $p < 0.05$) in the C_{max} value from 62.5 ng/mL (recorded in 3 × 10 mg IR o.d.) to 37.01 ng/mL for 30 mg SR o.d. This, along with the increase recorded in T_{max} from 1 and 1.63 hours (10 mg IR t.i.d. and 3 × 10 mg IR o.d., respectively) to 4.38 hours in 30 mg SR, indicated a sustained release of the drug, along with no evidence of dose dumping after the oral administration of sustained-release tablets (44). Hence, HPMC K15M was able, as indicated in the *in vitro* data, to provide a sustained release of MT-1207 from the tablets *in vivo*. The drug level remained at similar concentration values for about 3 hours (3 − 6 hours after administration) before declining, which indicated the prevalence of drug elimination over absorption. With regards to the extent of absorption, it was noted that in all the abovementioned cases the $AUC_{0\text{-}24h}$ and $AUC_{0\text{-}\infty}$ values recorded were statistically the same (one-way ANOVA, $p > 0.05$) (Table 3-7). In addition to this, the bioequivalence between the sustained-release and immediate-release tablets was investigated by calculating the $AUC_{0\text{-}24h}$ ratio of the sustained-release tablet dosing regimen and the immediate-release tablet dosing

regimens. As per the EMA guidelines, the prerequisite for bioequivalence is that the AUC_{0-t} ratio of the test and reference products should fall within the range 80.00 − 125.00 % (239). The AUC_{0-24h} ratios of the sustained-release tablet and the t.i.d. and o.d. immediate-release tablet dosing regimens were 98.12 % and 90.05 %, respectively. Based on these findings, it can be assumed that the whole amount of drug was released from the sustained-release tablets *in vivo* and was absorbed to the same extent as when the same dose was administered in immediate-release tablets, irrespective of the dosing regimen.

Table 3-7: *Pharmacokinetic parameters of MT-1207 after oral administration of a single MT-1207 30 mg sustained-release tablet (30 mg SR o.d.), 10 mg immediate-release tablets (one tablet at a time) three times a day (10 mg IR t.i.d.) and three 10 mg immediate-release tablets administered at the same time (3 × 10 mg IR o.d.) to Beagle dogs (n = 4).*

Dosing Regimen	$t_{1/2}$ (h)	T_{max} (h)	C_{max} (ng/mL)	AUC_{0-24h} (h*ng/mL)	$AUC_{0-\infty}$ (h*ng/mL)	V_d (L/kg)	CL (L/h/kg)	MRT (h)
30 mg SR o.d.	3.44±1.49	4.38±2.14	37.01±8.29	213.6±59.8	222.1±56.4	723.3±448.1	140.9±31.1	6.40±1.09
10 mg IR t.i.d.	3.47±1.49	1.00±0.71	32.22±23.28	217.7±81.6	229.7±86.7	540.1±247.0	116.8±57.3	13.05±3.77
3 × 10 mg IR o.d.	1.69±0.20	1.63±0.25	62.50±18.65	237.2±53.8	250.8±57.8	299.7±58.8	124.1±26.5	2.84±0.27

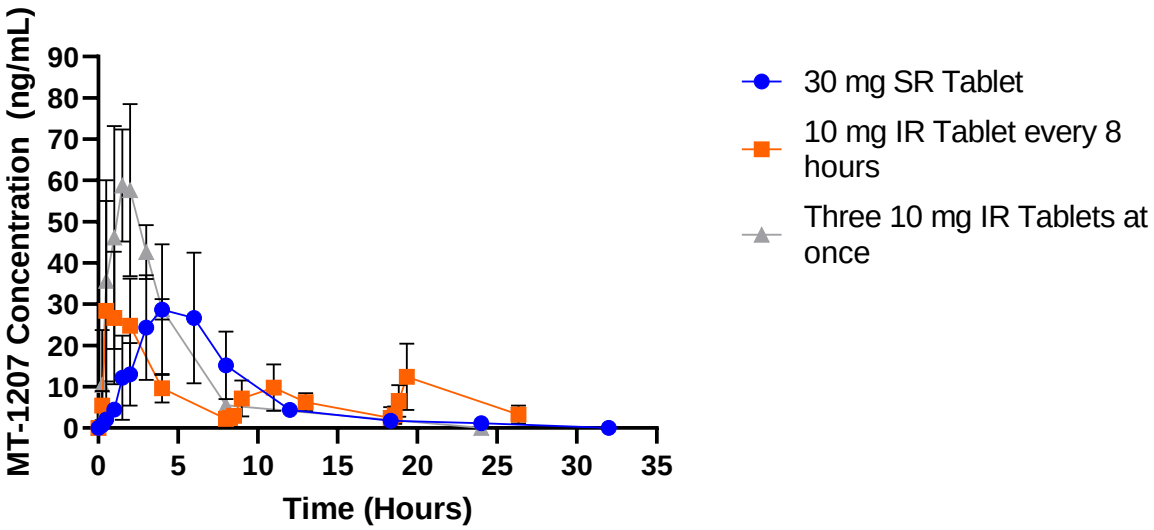


Figure 3-11: *Plasma concentration of MT-1207 in Beagle dogs after oral administration of 30 mg SR tablet o.d., 10 mg IR tablet t.i.d. and 3 × 10 mg IR tablet o.d. (n = 4).*

The distribution of MT-1207 in the body is an important parameter considered during pharmacokinetic analysis. The apparent volume of distribution, V_d, reflects the space of the body seemed to be occupied by the drug (240). V_d increases with increasing distribution of the drug to peripheral tissues. The mean residence time, MRT, reflects the average time during which the drug resides in the body. In the present case, even though the SR tablet showed the highest value for the apparent volume of distribution which was about 2.5 times higher than the IR tablet, there was no statistically significant difference (one-way ANOVA, $p > 0.05$) between the V_d values of MT-1207 recorded in SR o.d., IR t.i.d. and 3 × IR o.d (Table 3-7). Furthermore, with regards to MRT, the value obtained for 3 × IR o.d. increased more than 2 times for the same dose of MT-1207 administered as a sustained-release tablet (Table 3-7) and the difference between the two values was statistically significant (*t*-test, $p < 0.05$). This indicates that the time during which the drug resides in the body was increased significantly when MT-1207 was administered in the form of a sustained-release tablet,

compared to immediate-release tablets. There was a statistically significant difference in MRT between all three groups (one-way ANOVA, $p < 0.05$).

The half-life, $t_{1/2}$, of MT-1207 was prolonged to 3.44 hours when the sustained-release tablet was administered in the dogs, 2 to 2.5 times higher than when three immediate-release tablets administered at the same time (Table 3-7). When immediate-release tablets were administered at 8-hour intervals, the MT-1207 $t_{1/2}$ was similar to that recorded after administration of the sustained-release tablet. With regards to clearance, there was no statistically significant difference (one-way ANOVA, $p > 0.05$) between the clearance values that were recorded in Beagle dogs for the three different dosing regimens (Table 3-7).

Hepatic metabolism is generally higher in Beagle dogs than in humans (240, 241). Phase I clinical trials were carried out for MT-1207 at a certain dose range. At the 20 – 40 mg dose range, the $t_{1/2}$ value of MT-1207 was 7.28 – 7.38 hours in humans (206). Considering that formulation A1 gave a $t_{1/2}$ in Beagle dogs that was 2-2.5 times higher than that of the immediate-release tablets, the formulation could be considered as a once-a-day treatment, provided that a similar increase in $t_{1/2}$ occurs in humans.

3.4 Conclusions

In the present study, a new sustained-release tablet for the novel antihypertensive drug MT-1207 was successfully developed. To date, no once-a-day formulation has been reported for this novel drug candidate. HPMC K15M was able to provide a sustained release of MT-1207 *in vitro* and in an animal model. Amongst the different formulations, the optimised formulation (F4) containing 31% w/w HPMC K15M was chosen for a study in Beagle dogs since it provided a 24-hour *in vitro* release of MT-1207 that demonstrated a sustained release of the drug. Its MT-1207 30 mg counterpart formulation (A1) was tested in Beagle dogs. The half-life of the drug was extended, while the amount of drug absorbed was the same as that of

the immediate-release tablets. Based on the pharmacokinetic data from Beagle dogs and phase I clinical trials, this formulation can be considered for once-a-day treatment of hypertension, an advance that could have significant commercial and patient health benefits.

The results presented in this study demonstrated the promising application of A1 tablets for the once-a-day oral delivery of MT-1207. However, after further consideration, it was decided to proceed with further optimisation of the formulation. This was because the Beagle dog study indicated a much faster release of MT-1207 from the tablets *in vivo* than that recorded *in vitro*. This could be ought to the poor wet strength of the tablets which was determined to be 0.10 ± 0.02 N (n = 3 tablets) after 24 hours of *in vitro* dissolution for the tablets that did not fully disintegrate. The low tablet wet strength could have contributed towards a fast disintegration of the tablets *in vivo*, followed by a rapid release of MT-1207. Another reason why the *in vitro* release of MT-1207 from A1 tablets was more sustained *in vitro* than *in vivo* could have been the selection of the dissolution medium. 900 mL 0.1 M phosphate pH 6.8 with 0.2% w/v SDS may not have ensured sink conditions during the *in vitro* release testing, even though the USP requirements for sink conditions were met by the dissolution method.

Having considered the above, it was decided to proceed with further formulation optimisation through the incorporation of ethylcellulose into the tablet polymer matrix. Ethylcellulose is a hydrophobic polymer and its incorporation into the matrix tablet formulation could contribute to further retardation of drug release via a reduction in the hydration rate of the matrix conferred by a decline in water molecule penetration into the matrix, due to the hydrophobic nature of the polymer (242). This, in turn, could lead to a reduced erosion of the matrix, thus improving its integrity. Furthermore, in the literature, hydrophilic and hydrophobic polymers have been reported to show a synergistic effect in retarding drug release from matrix tablets (243). However, significant retardation of drug

release could result in an incomplete absorption and poor bioavailability of MT-1207 *in vivo* because of the premature evacuation of the tablets from the stomach and, thus, the upper GIT. Therefore, it was decided to incorporate a gastroretentive layer into the tablet formulation. The gastroretentive bilayer tablets should have sufficiently long GRT to achieve a complete release and absorption of MT-1207 *in vivo*. Additionally, the dissolution medium used for the tablet *in vitro* release testing purposes was switched to 0.1 M acetate pH 4.0. The solubility of MT-1207 in this medium was determined to be 6.5 mg/mL and was, therefore, sufficiently high to ensure sink conditions during the *in vitro* release studies (207).

4 Chapter 4: Preparation, Optimisation and *In Vitro* Characterisation of Non-Effervescent Gastroretentive Bilayer Tablet Formulations For Once-a-Day Delivery of MT-1207

Napoleon-Nikolaos Vrettos, Yuhan Wang, Clive J. Roberts, and Zheying Zhu

School of Pharmacy, University of Nottingham, Nottingham, United Kingdom

Acknowledgement of research work done by co-authors

Wang Y: MRes student. Provided valuable help and support during the *in vitro* release study.

Roberts CJ, Zhu Z: Academic supervisors to NN Vrettos.

A special thanks to Jason Greaves (Wolfson Building, University of Nottingham, United Kingdom) for conducting the gas pycnometry and mercury intrusion porosimetry tests.

Keywords: gastroretentive; non-effervescent; PEO; Kollidon® SR; ethylcellulose; optimisation; factorial experiment; *in vitro* buoyancy; pH effect

4.1 Introduction

As was mentioned earlier in Chapter 1 of the thesis, gastroretentive drug delivery systems are systems that are able to effectively be retained in the stomach and release drugs in the gastric fluids. They offer several advantages, including prolonged GRT of dosage forms in the stomach up to several hours, increased therapeutic efficacy of drugs by improving drug absorption, and suitability for targeted delivery in the stomach. They can enhance the controlled delivery of drugs by continuously releasing the drug for an extended period at the desired rate and to the desired absorption site until the drug is completely released from the dosage form (102-104).

GRDDS are feasible for drugs that have low absorption in the lower part of the GIT, are unstable and/or poorly soluble at alkaline intestinal pH, have a short half-life, narrow absorption window in the proximal small intestine, plasma fluctuations and/or show local activity at the upper part of the intestine for the eradication of *Helicobacter pylori* (101, 106-110, 112-114, 244).

In non-effervescent floating systems, highly swellable cellulose derivatives or gel-forming polymers are used. Non-effervescent systems include the HBS, single- and double-layer floating tablets, and microballoons/hollow microspheres. Significant advantages of non-effervescent floating systems include the non-dependence of the floating mechanism on gastric pH which is variable and can be problematic in patients with achlorhydria, and the fact that the stability of acid- or base-labile drugs is secured through the exclusion of a gas-generating agent (106).

To achieve efficient floatation for gastric retention purposes, usually, hydrophilic polymers such as HPMC, sodium alginate, PEO are used (106, 110, 142-144). To avoid long floating lag times, low-density materials should be used in the gastroretentive layer to achieve

rapid buoyancy of tablets. Additionally, rapid buoyancy could be supported by low compression force values that will allow for a higher tablet porosity which could lead to a low tablet density, more rapid polymer wetting and swelling that will further reduce the density of the dosage form (110). However, in a recent study, Kollidon® SR was used in a gastroretentive layer along with camphor. Due to the inherently low density of Kollidon® SR and the improved wet strength of the layer, due to the presence of a hydrophobic polymer, along with the reduction in the tablet density, due to camphor sublimation, a 12-hour floating was successfully reached *in vitro*, even at a rotation rate of 200 rpm (134).

Both hydrophilic and hydrophobic polymers have proved effective in achieving gastric retention, especially when combined with gas-generating or sublimating agents. However, to the best of our knowledge, the application of a combination of hydrophilic and hydrophobic polymers for gastric retention purposes in gastroretentive tablets without the use of gas-generating or sublimating agents has not been reported in the literature. The swelling properties of hydrophilic polymers, combined with a low-density hydrophobic polymer the presence of which will strengthen the forming gel, could eliminate the need for gas-generating or sublimating agents, and result in a gastroretentive formulation that would be easy to prepare and would be able to be retained in the stomach long enough to serve as a once-a-day controlled-release formulation, whilst withstanding the stomach destructive forces.

4.1.1 Experimental aim

In the previous chapter, a promising once-a-day tablet formulation of MT-1207 was developed and characterised *in vitro* and *in vivo*. However, the data from the Beagle dog study demonstrated that the plasma concentration fell rapidly after the 8-hour timepoint following the oral administration of tablets. This could mean that drug release *in vivo* was potentially much faster than *in vitro* which could impede the ability of the formulation to

ensure that the MT-1207 plasma concentration remained within therapeutic levels over 24 hours.

In the present study, MT-1207 non-effervescent bilayer tablets were prepared. The bilayer tablet development was split between two different parts: gastroretentive layer development and optimisation, and drug layer optimisation.

The two major components of the gastroretentive layer were PEO and Kollidon® SR. These materials have been used in different studies for the preparation of gastroretentive formulations (106, 109, 134, 245). The low density and swelling capability of PEO render it a good choice for the preparation of floating systems. Kollidon® SR consists of polyvinyl acetate (80 %), polyvinylpyrrolidone (19 %), sodium lauryl sulfate (0.8 %) and silica (0.2 %). The low density of Kollidon® SR could further contribute to the floatation of gastroretentive systems, while its hydrophobic nature could ensure more controlled hydration of the layer and a higher wet strength that would ensure its structural integrity *in vitro* and *in vivo*. Therefore, the combination of these two polymers in the gastroretentive layer was deemed promising. Apart from these excipients, also spray-dried lactose and HPMC K100M were used.

Different gastroretentive layer and gastroretentive bilayer tablets were prepared and characterised for their hardness, friability, tablet weight variation, *in vitro* buoyancy, and wet strength after *in vitro* buoyancy testing. The gastroretentive layer tablet study was a preliminary one to help gain an understanding of the factors affecting the tablet floatation and wet strength. This helped design a factorial experiment with the appropriate choice of factors and dependent variables that led to the optimisation of the gastroretentive layer of the bilayer tablet formulation. The optimised non-effervescent gastroretentive layer should ideally be easy to prepare, ensure an immediate and robust 24-hour tablet floatation *in vitro* and gastric

retention *in vivo*, and be able to be used in combination with different drug layers without significant alteration in the tablet buoyancy behaviour.

In the drug layer, ethylcellulose was incorporated as an additional release retardant with the aim of further sustaining the release of MT-1207 from the tablets, whilst maintaining a sufficiently high wet strength throughout 24 hours of *in vitro* release testing.

4.2 Experimental Techniques

This section entails the experimental techniques that were used to collect the data in this chapter. These include procedures listed in Chapter 2 and mentioned below, as well as additional, chapter-specific techniques that are described in detail:

- HPLC-UV method for the quantitation of MT-1207 samples
- Flowability characterisation of the tablet blends
- Hardness and friability of tablets
- Tablet weight variation
- Differential scanning calorimetry (DSC) analysis of MT-1207 and tablet samples
- Fourier-Transform Infrared (FTIR) spectrophotometric studies
- X-ray powder diffraction (XRPD) analysis of MT-1207 and tablet samples
- Kinetics and mechanism of drug release

4.2.1 Validation of HPLC and dissolution methods

4.2.1.1 Linearity

The HPLC method was validated for linearity. For this purpose, three replicates of the calibration curve were prepared in the concentration range 0.001 – 0.1 mg/mL. The 0.1 mg/mL standard solution was prepared by dissolving the appropriate amount of MT-1207

hydrochloride reference standard in 0.1 M acetate buffer pH 4.0. The rest of the working standard solutions were prepared by conducting dilutions from the 0.1 mg/mL standard solution. The matrix of the standard solutions was 0.1 M acetate buffer pH 4.0. The linearity of the method was assessed based on the R^2 values of three calibration curves prepared over three different days.

4.2.1.2 Limit of Detection (LOD) and Limit of Quantitation (LOQ)

The HPLC method was validated for the LOD and LOQ. The standard deviation of the y-intercepts of the three linearity calibration curves was calculated. The LOD and LOQ values were then calculated using Equations 6 and 7.

4.2.1.3 Specificity

The dissolution method was validated in terms of specificity. For this study, the excipients of the bilayer tablets were added in 500 mL 0.1 M acetate buffer pH 4.0. More specifically, 80 mg alpha-D-lactose monohydrate, 30 mg PVP K30, 70 mg HPMC K15M, 70 mg ethylcellulose, 500 mg PEO 8M, 300 mg Kollidon® SR, 1 mg iron (III) oxide, 50 mg spray-dried lactose, 20 mg HPMC K100M, 10 mg colloidal silicon dioxide and 2 mg magnesium stearate were added in the dissolution medium inside a vessel and the rotation speed of the paddle was set at 75 rpm. After 24 hours, a sample was collected and centrifuged (2300 g, 10 minutes). 1 mL from the supernatant was then transferred into an HPLC vial and injected into the HPLC system for analysis. The experiment was conducted in triplicate.

4.2.1.4 Accuracy and intra-day precision

The dissolution method was validated in terms of accuracy and intra-day precision. The method was validated at 20 %, 50 %, 80 %, 100 % and 120 % of the nominal concentration value of 30 mg MT-1207 in 500 mL 0.1 M acetate pH 4.0. At each concentration level, the excipients of the tablets were added in 500 mL dissolution medium as in the specificity study,

followed by the addition of the appropriate amount of MT-1207 hydrochloride reference standard. The rotation speed of the paddle was set at 75 rpm. After 24 hours, a sample was collected and centrifuged (2300 g, 10 minutes). 1 mL of the supernatant was then transferred into an HPLC vial and injected into the HPLC system for analysis. The experiment was carried out in triplicate and the intra-day precision was determined through % RSD for the three values per accuracy level.

4.2.1.5 Inter-day precision

The dissolution method was validated for inter-day precision. Two additional accuracy samples were prepared on two different days for each of the concentration levels mentioned in Section 4.2.1.4 and the experiment was carried out as per the same section. The % RSD of these values and the mean of the values from the accuracy experiment was calculated and the inter-day precision of the method was assessed.

4.2.2 Preparation of preliminary gastroretentive layer tablets and MT-1207 gastroretentive bilayer tablets

For the gastroretentive layer, the appropriate amounts of the different components (except for magnesium stearate) were each time weighed and mixed manually for 15 minutes. Then, magnesium stearate was added in the powder mixture and mixing was carried out for 5 minutes.

The preparation of the drug sustained-release layer included a wet granulation step and was the same to that used to prepare the single-layer HPMC matrix tablets in Section 3.2.4.

A Piccola rotary tablet press machine (Riva®, Argentina) was used for the compression process. For the preliminary experiments where gastroretentive layer tablets were prepared, the gastroretentive layer powder mixture was each time added into the die

manually and compressed using a compression force of either 7.5 kN or 8.5 kN. 13 mm flat-faced round (for G1 − G3) and 17 × 9 mm concave oblong (for G4 − G20) punches and dies were used during the compression process, each time depending on the tablet weight. For the factorial experiment and preparation of the optimised bilayer tablet purposes, the compression process was conducted in two steps. The gastroretentive powder mixture was first added into the die manually and a pre-compression step was applied, followed by the addition of the granulated drug layer on top of the pre-compressed gastroretentive layer. Compression was then carried out to prepare the bilayer tablets using compression force values of 5 kN, 7 kN, 7.5 kN or 10 kN. 13 mm flat-faced round and 17 × 9 mm concave oblong punches and dies were used during the compression process, each time depending on the tablet weight.

The compositions of the preliminary gastroretentive layers and the drug layers prepared can be seen in Tables 4-1 and 4-2.

Table 4-1: *Compositions of the gastroretentive layers G1 − G20.*

Gastroretentive layers	PEO 8M (mg)	Kollidon® SR (mg)	Spray-dried lactose (mg)	HPMC K100M (mg)	Colloidal silicon dioxide (mg)	Magnesium stearate (mg)	**Total weight (mg)**
G1	100	260	40	-	0.9	0.9	**401.8**
G2	260	100	40	-	0.9	0.9	**401.8**
G3	260	150	40	-	0.9	0.9	**451.8**
G4	360	200	80	-	1.5	1.5	**643.0**
G5	360	200	40	-	1.0	1.0	**602.0**
G6	410	200	40	-	1.5	1.5	**703.0**
G7	410	250	40	-	1.5	1.5	**703.0**
G8	410	250	-	-	1.5	1.5	**663.0**
G9	460	250	-	-	1.6	1.6	**713.2**
G10	460	250	40	-	1.7	1.7	**753.4**
G11	460	300	40	-	1.8	1.8	**803.6**
G12	480	300	40	-	1.8	1.8	**823.6**
G13	480	300	20	-	1.8	1.8	**803.6**
G14	480	300	40	20	1.8	1.8	**823.6**
G15	460	250	80	-	1.7	1.7	**793.4**
G16	460	250	80	20	1.8	1.8	**813.6**
G17	460	280	60	20	1.8	1.8	**823.6**
G18	460	280	60	-	1.8	1.8	**803.6**
G19	410	280	60	60	1.8	1.8	**813.6**
G20	460	280	-	20	1.8	1.8	**763.6**

Table 4-2: *Compositions of the bilayer tablet ethylcellulose-containing drug layers.*

Components (mg)	F_{HE7035}	F_{HE7030}	F_{HE6030}	F_{HE6020}	F_{HE5020}	F_{HE6015}	F_{HE6010}	F_{HE6005}	F_{HE6003}	F_{HE6001}
MT-1207 Hydrochloride	30	30	30	30	30	30	30	30	30	30
Alpha-D-lactose monohydrate	45	45	55	60	70	65	70	65	67	69
Polyvinylpyrrolidone K30	0	5	5	10	10	10	10	20	20	20
HPMC K15M	70	70	60	60	50	60	60	60	60	60
Ethylcellulose 10 cps	35	30	30	20	20	15	10	5	3	1
Iron (III) oxide	1	1	1	1	1	1	1	1	1	1
Colloidal silicon dioxide	6	6	6	6	6	6	6	6	6	6
Magnesium stearate	0.5	0.5	0.5	0.5	0.5	0.5	0.5	0.5	0.5	0.5
Total layer weight	**187.5**	**187.5**	**187.5**	**187.5**	**187.5**	**187.5**	**187.5**	**187.5**	**187.5**	**187.5**

4.2.3 Design of the factorial experiment for the gastroretentive layer

A face-centred central composite design was employed for the gastroretentive layer factorial experiment to assess the impact of the factor alterations on the *in vitro* buoyancy behaviour of the gastroretentive bilayer tablets. Based on the preliminary experiments for the gastroretentive layer, the factors that were selected for the experiment were: the amount of PEO (mg) (X_1), the % of spray-dried lactose (SDL) (X_2) and the compression force (X_3). The percentages of Kollidon® SR and HPMC K100M were maintained stable and were selected based on preliminary experiment findings. In the setup, each factor was examined over three levels (-1, 0, 1). Therefore, 27 different combinations were prepared and characterised (Table 4-3). The investigated dependent variables of the experiment were the floating lag time (the time taken for the tablets to start floating) and the total floating time (the total time during which the tablets remained buoyant and were able to re-surface after application of vertical pressure using a spatula) of the bilayer tablets.

Table 4-3: *Experimental layout of the gastroretentive layer factorial experiment.*

Formulation	PEO 8M Amount (mg)	% of SDL	Compression Force (kN)	Kollidon® SR (mg)	HPMC K100M (mg)	Drug layer (mg)	Gastroretentive layer (mg)	**Total tablet weight (mg)**
1	480	7	7.5	290	20.5	187.5	850.5	**1038**
2	480	0	7.5	256	18.2	187.5	757.8	**945.3**
3	480	7	5	290	20.5	187.5	850.5	**1038**
4	480	0	5	256	18.2	187.5	757.8	**945.3**
5	480	7	10	290	20.5	187.5	850.5	**1038**
6	480	0	10	256	18.2	187.5	757.8	**945.3**
7	320	7	7.5	193.8	13.7	187.5	570	**757.5**
8	320	0	7.5	173.4	12.2	187.5	507.8	**695.3**
9	320	7	5	193.8	13.7	187.5	570	**757.5**
10	320	0	5	173.4	12.2	187.5	507.8	**695.3**
11	320	7	10	193.8	13.7	187.5	570	**757.5**
12	320	0	10	173.4	12.2	187.5	507.8	**695.3**
13	160	7	7.5	95.2	6.7	187.5	282.7	**470.2**
14	160	0	7.5	85.7	6	187.5	252.9	**440.4**
15	160	7	5	95.2	6.7	187.5	282.7	**470.2**
16	160	0	5	85.7	6	187.5	252.9	**440.4**
17	160	7	10	95.2	6.7	187.5	282.7	**470.2**
18	160	0	10	85.7	6	187.5	252.9	**440.4**
19	480	3.5	7.5	272	19.2	187.5	802.8	**990.3**
20	320	3.5	7.5	181.3	12.8	187.5	535.2	**722.7**
21	160	3.5	5	90.7	6.4	187.5	267.7	**455.2**
22	480	3.5	5	272	19.2	187.5	802.8	**990.3**
23	320	3.5	5	181.3	12.8	187.5	535.2	**722.7**
24	480	3.5	10	272	19.2	187.5	802.8	**990.3**
25	320	3.5	10	181.3	12.8	187.5	535.2	**722.7**
26	160	3.5	7.5	90.7	6.4	187.5	267.7	**455.2**
27	160	3.5	10	90.7	6.4	187.5	267.7	**455.2**

SigmaPlot® 13 software was used to analyse the data generated from the testing of the different gastroretentive layer combinations. Polynomial models were generated for both dependent variables. The best-fitting model was selected based on the R^2 and adjusted R^2 values. Also, the selected optimised gastroretentive layer was tested for its *in vitro* buoyancy

behaviour, and its floating lag time and total floating time experimental values were compared to the ones predicted by the models to further assess the suitability of the models to accurately predict the dependent variable values for different gastroretentive layer combinations. Furthermore, the influence of factors and factor interactions on the dependent variables was evaluated by ANOVA and the significance of their effect on the variables was assessed based on the calculated *p*-values.

The following mathematical Equation 10 was employed to describe mathematically the relationship between each of the dependent variables and the different factors, and the effects of the latter on the former:

$$Y = b_0 + b_1X_1 + b_2X_2 + b_3X_3 + b_{12}X_1X_2 + b_{13}X_1X_3 + b_{23}X_2X_3 + b_{11}X_1^2 + b_{22}X_2^2 + b_{33}X_3^2 \quad [10]$$

where Y is the dependent variable, b_0 is the intercept and the other b_i values are constants describing the relationship between Y and the different factors (X_1, X_2, X_3), as well as the effects of changes occurring in two factors simultaneously. X_i^2 terms refer to the factor quadratic effect that has been included in the model for non-linear correlations. After the model equation for each of the dependent variables was generated and the effects of the factors and their interactions determined, an optimised gastroretentive layer was designed and prepared at a compression force that would ensure optimal floating lag time and total floating time values upon *in vitro* buoyancy testing.

4.2.4 In vitro buoyancy

The floating behaviour of the gastroretentive layer tablets for the preliminary gastroretentive layer experiment and that of the gastroretentive bilayer tablets for the factorial experiment and optimised gastroretentive layer selection purposes was assessed in 500 mL

fasted state simulated gastric fluid (FaSSGF) pH 1.6 in a USP II dissolution apparatus. The apparatus was set at a paddle rotation speed of 75 rpm and a temperature of 37 ± 0.5 °C. The *in vitro* buoyancy of the gastroretentive tablets was characterised by the floating lag time and total floating time parameters. Furthermore, the *in vitro* buoyancy of the optimised gastroretentive ethylcellulose-containing bilayer F_{HE6005} tablets was tested in HCl pH 1.0, phosphate buffer pH 3.0 and phosphate buffer 6.0 to assess any potential pH effects on the floating capabilities of the tablets.

4.2.5 Tablet dimension and wet strength measurements

The dimensions of the hydrated bilayer tablets after *in vitro* buoyancy testing were measured using a Vernier calliper. Then, the compression wet strength of the hydrated gastroretentive layer tablets and the bilayer tablets was measured using a TA.XT Plus texture analyser (Stable Micro Systems®, Godalming, United Kingdom). A 50-kg load cell and a 2-cm-diameter flat-tipped cylinder probe were used for the test. Peak force was recorded in Newtons (N) at 85 % strain using the force-displacement curves.

4.2.6 Tablet density and porosity determination

The true density of the optimised bilayer tablets was determined using a helium pycnometer (AccuPyc® II 1340, Micromeritics Instrument Cooperation, Norcross, GA, USA) (n = 3 tablets). The instrument was calibrated using a standard stainless-steel sphere before measurements. The tablets were then accurately weighed and placed inside the chamber. The sample solid phase volume was calculated through the pressures observed upon filling the sample chamber and then discharging into another empty chamber. The temperature inside the chamber was maintained at 21.95 °C. The measurements were repeated for five cycles. The volume and the apparent (skeletal) density of the tablets were determined.

The porosity and pore size of the optimised bilayer tablets, as well as their skeletal and bulk density, was determined via mercury intrusion porosimetry (Autopore® IV 9500, Micromeritics Instrument Cooperation, Norcross, GA, USA) (n = 3 tablets). The tablets were accurately weighed before measurements. The pressure was varied from 0 to 70 psi. A 10 s equilibration time was set for each data point.

4.2.7 SEM analysis of the optimised gastroretentive layer of the tablets in different media

Images of the optimised gastroretentive layer were collected at different timepoints of the bilayer tablet *in vitro* buoyancy runs in HCl pH 1.0, phosphate pH 3.0 and phosphate pH 6.0 using SEM (Philips® XL30 SEM, Netherlands). The timepoints selected were 12 and 22 hours for the tablets in all media, 31 hours for the tablets in phosphate pH 3.0 and phosphate pH 6.0 and an additional 43.5-hour timepoint for the tablets in phosphate pH 6.0. Before imaging, the tablet samples were dried at 40 °C until constant weight and then sputtered with gold using an SC7640 Sputter Coater (Polaron®, United Kingdom). Coated samples were then observed in the SEM at an accelerating voltage of 10 kV under vacuum conditions at ambient temperature.

4.2.8 Viscosity study

Viscosity measurements were conducted using an Anton Paar® MCR 302 rheometer (Anton Paar, United Kingdom) set at a rotation speed of 2 s^{-1} and a temperature of 37 °C. The cone-and-plate setting was used. *In vitro* buoyancy runs of the optimised ethylcellulose-containing bilayer tablets were conducted in HCl pH 1.0, phosphate pH 3.0 and phosphate pH 6.0. Approximately 7 mL of sample were collected manually at certain timepoints (1, 4, 8, 12, 22 h in all media, 31 h in phosphate pH 3.0 and phosphate pH 6.0, and 43.5 h in phosphate pH 6.0). Each time, after the viscosity measurement, the sample was transferred back to the dissolution vessel. The runs and viscosity measurements were conducted in triplicate in each medium.

4.2.9 In vitro release of MT-1207 from gastroretentive bilayer tablets

In vitro release testing was carried out using a USP II dissolution apparatus (Copley®, United Kingdom). The apparatus was set at a constant paddle rotation speed of 75 rpm. *In vitro* release testing was conducted in 500 mL 0.1 M acetate buffer pH 4.0 at 37 ± 0.5 °C. Stainless-steel sinkers were used to maintain the tablets at the bottom of the dissolution vessels to eliminate the effect of tablet floating (location of tablets within the vessels) on drug release (107, 246). Sampling was carried out manually at predetermined time intervals (1, 2, 4, 6, 8, 12, 16 and 24 hours), followed by centrifugation of the samples (2300 g, 10 minutes). Then, each time, 1 mL from the supernatant was transferred into an HPLC vial and 20 µL were injected into the HPLC for analysis. The *in vitro* release study was conducted in triplicate for each formulation. Additionally, an *in vitro* release experiment was conducted at a paddle rotation speed of 200 rpm for the bilayer tablets containing the optimised ethylcellulose-containing drug layer (F_{HE6005}) and the bilayer A1 tablets.

4.2.10 Data analysis

The *t*-test and one-way ANOVA statistical analyses of the data collected from the factorial experiment, the *in vitro* buoyancy study at media of different pH values and the viscosity analysis were conducted using SigmaPlot® 13. A statistically significant difference was reflected by a *P* value less than 0.05. Except for the factorial experiment, in the cases where one-way ANOVA analysis gave a *p*-value less than 0.05, *post hoc* Bonferroni *t*-tests were conducted for pairwise comparisons. The similarity or difference between the *in vitro* drug release profiles of the different formulations was assessed using the f_1 and f_2 factors, as per the FDA guidelines (223). Values of f_1 up to 15 (0 − 15) and f_2 values greater than 50 (50 − 100) ensured sameness or equivalence of MT-1207 *in vitro* release profiles of different formulations.

4.3 Results and Discussion

4.3.1 Flowability testing of gastroretentive and drug layer powder mixtures

Bulk/Tapped density testing was performed for the gastroretentive and drug layer powder mixtures to assess their flowability and compressibility. The assessment was based on the Carr index and Hausner ratio values calculated for each powder. A Carr index value between 5 % and 16 % is desirable to achieve both good flowability and compressibility (67).

All gastroretentive and drug layer powder mixtures gave Carr index and Hausner ratio values that indicated a passable to good flowability (Tables 4-4, 4-5 and 4-6), as per USP (222), along with potentially good compressibility since the Carr index values were higher than 10 %. Therefore, the gastroretentive and drug layer powder mixtures were forwarded to tabletting.

Table 4-4: *Bulk/Tapped density testing results for the gastroretentive layer powder mixtures of the preliminary gastroretentive layer experiments (G1 − G20).*

Gastroretentive layer	Carr Index (%)	Hausner Ratio	Flowability (USP)
G1	16.0	1.19	Fair
G2	11.8	1.13	Good
G3	13.2	1.15	Good
G4	13.8	1.16	Good
G5	14.9	1.18	Good
G6	14.3	1.17	Good
G7	13.1	1.15	Good
G8	14.8	1.17	Good
G9	14.9	1.18	Good
G10	15.2	1.18	Good
G11	14.7	1.17	Good
G12	15.5	1.18	Fair to Good
G13	13.1	1.15	Good
G14	14.3	1.17	Good
G15	15.3	1.18	Good
G16	15.1	1.18	Good
G17	15.2	1.18	Good
G18	12.6	1.14	Good
G19	16.3	1.19	Fair
G20	21.6	1.26	Passable

Table 4-5: *Flowability characterisation results of the different gastroretentive layer powder mixtures of the factorial experiment.*

Gastroretentive layer powder mixtures	Bulk Density (g/mL)	Carr Index (%)	Hausner Ratio	Flowability (as per USP)
1, 3, 5	0.3635	17.3	1.21	Fair
2, 4, 6	0.3599	13.2	1.15	Good
7, 9, 11	0.4040	10.0	1.11	Good
8, 10, 12	0.3941	11.4	1.13	Good
13, 15, 17	0.3670	12.0	1.14	Good
14, 16, 18	0.3501	14.7	1.17	Good
19, 22, 24	0.3733	13.5	1.16	Good
20, 23, 25	0.3870	13.6	1.16	Good
21, 26, 27	0.3493	14.8	1.17	Good
Optimised	0.3711	12.8	1.15	Good

Table 4-6: *Flowability characterisation results of the different drug layer powder mixtures.*

Drug layer powder mixtures	Bulk Density (g/mL)	Carr Index (%)	Hausner ratio	Flowability (as per USP)
F_{HE7035}	0.2801	22.4	1.29	Passable
F_{HE7030}	0.2850	15.7	1.19	Fair
F_{HE6030}	0.3045	17.8	1.18	Fair to Good
F_{HE6020}	0.2842	14.4	1.20	Fair to Good
F_{HE5020}	0.2863	18.1	1.22	Fair
F_{HE6015}	0.2902	13.6	1.16	Good
F_{HE6010}	0.2766	19.1	1.24	Fair
F_{HE6005}	0.2794	15.8	1.17	Fair to Good
F_{HE6003}	0.2940	15.5	1.18	Fair to Good
F_{HE6001}	0.2711	22.2	1.28	Passable

4.3.2 In vitro buoyancy and wet strength testing of the gastroretentive layer tablets

As part of the *in vitro* buoyancy assessment during the preliminary gastroretentive layer experiments, the floating lag time and total floating time values of the gastroretentive layer tablets were recorded. It was desired for the floating lag time to be as little as possible since low values could prevent a premature evacuation of the tablet from the stomach (106). The total floating time refers to the amount of time the tablets can remain buoyant. A 24-hour

floatation of the tablets was desired to ensure their gastric retention for a day. Each time, after the *in vitro* buoyancy test was completed, the wet strength of the tablets was measured. It was generally desirable for the tablet wet strength to be higher than 3.2 N which is the estimated gastric destructive force of Beagle dogs (247). This could potentially help ensure the integrity of the tablets in Beagle dogs and in humans the maximum gastric destructive force of whom has been estimated to be 1.89 N (248). Two compression force values (7.5 kN, 8.5 kN) were applied in the preparation of gastroretentive layer tablets.

As can be seen in Tables 4-7 and 4-8, increasing amounts of PEO led to the formation of tablets with longer total floating time values. This indicated the potential significance of PEO as a factor that may influence the total floating time of the gastroretentive tablets. Being a hydrophilic polymer, PEO hydrates and swells upon contact with the dissolution medium which results in a reduction of the tablet density, due to an increase of the tablet volume and internal porosity (106). As a result of this, the tablets can float and remain buoyant. On the other hand, Kollidon® SR did not seem to have a clear effect on the floating lag time or total floating time of tablets. However, higher percentages of Kollidon® SR led to higher wet strength of the tablets measured after completion of the *in vitro* buoyancy runs. Furthermore, the presence of lactose in the gastroretentive layer was probably important in achieving a robust floatation of the tablets. G20 did not give a clear total floating time since, after seemingly floating, they immediately sank to the bottom of the dissolution vessels upon application of vertical force using a spatula. Finally, the compression force influenced the floating lag time of some of the gastroretentive layer formulations. This could be due to the reduced porosity and, thus, increased density of the tablets prepared using a high compression force (110).

Table 4-7: *In vitro buoyancy, wet strength and swollen dimension measurement data of the gastroretentive layer tablets (G1 − G20) compressed using a force of 7.5 kN (n = 3 tablets). Results are presented as mean ± standard deviation.*

Gastroretentive layer	Floating Lag Time (Seconds)	Total Floating Time (Hours)	Wet Strength (N)	Swollen Long Axis Diameter (mm)	Swollen Short Axis Diameter (mm)	Swollen Thickness (mm)
G1	1.7 ± 2.9	4.5 ± 0.1	N/A	N/A	N/A	N/A
G2	0	12.7 ± 0.3	N/A	N/A	N/A	N/A
G3	150.3 ± 25.2	13.0 ± 0.3	N/A	N/A	N/A	N/A
G4	4.7 ± 4.2	18.8 ± 0.3	7.3 ± 1.9	28.2 ± 0.2	15.9 ± 0.3	11.3 ± 0.2
G5	4.7 ± 4.2	18.8 ± 0.3	9.4 ± 1.1	28.1 ± 0.1	16.1 ± 0.1	11.1 ± 0.1
G6	0	19.2 ± 0.7	9.3 ± 0.6	26.7 ± 0.3	14.1 ± 0.1	10.2 ± 0.3
G7	0	20.0 ± 2.2	15.5 ± 4.0	27.3 ±0.8	14.6 ± 0.4	11.3 ± 0.6
G8	0	20.8 ± 0.3	11.1 ± 1.3	26.2 ± 1.3	13.8 ± 1.0	11.5 ± 0.4
G9	0	18.7 ± 0.3	9.7 ± 3.4	27.1 ± 0.8	15.1 ± 0.8	12.4 ± 0.3
G10	0	23.9 ± 0.1	9.5 ± 1.1	26.5 ± 0.7	14.0 ± 0.1	12.4 ± 0.5
G11	0	23.7 ± 0.6	10.6 ± 4.1	27.5 ± 0.5	14.1 ± 1.0	12.2 ± 1.1
G12	0	22.8 ± 2.0	12.8 ± 2.0	26.0 ± 1.0	14.2 ± 0.3	12.7 ± 0.5
G13	0	< 20	12.8 ± 3.8	25.2 ± 0.8	13.7 ± 1.2	11.7 ± 0.6
G14	0	22.3 ± 2.9	16.3 ± 2.4	26.0 ± 1.7	12.8 ± 0.8	12.9 ± 0.7
G15	0	24.3 ± 0.4	5.7 ± 1.4	27.7 ± 0.3	13.9 ± 0.7	12.3 ± 0.6
G16	0	24.8 ± 0.3	7.1 ± 1.4	27.3 ± 0.6	14.2 ± 0.3	12.5 ± 0.9
G17	0	25.3 ± 0.4	9.9 ± 1.5	25.7 ± 1.2	13.6 ± 0.5	13.6 ± 0.8
G18	0	23.7 ± 3.1	12.1 ± 5.5	25.3 ± 1.5	12.8 ± 1.3	11.9 ± 1.8
G19	0	24.1 ± 0.7	8.9 ± 1.1	25.5 ± 0.7	13.9 ± 0.1	13.6 ± 0.6
G20	0	< 16	10.8 ± 0.3	25.8 ± 0.2	13.2 ± 1.0	12.6 ± 1.5

Table 4-8: *In vitro buoyancy, wet strength and swollen dimension measurement data of the gastroretentive layer tablets compressed using a force of 8.5 kN (G10 – G12 and G14 – G18) (n = 3 tablets). Results are expressed as mean ± standard deviation.*

Gastroretentive layer	Floating Lag Time (Seconds)	Total Floating Time (Hours)	Wet Strength (N)	Swollen Long Axis Diameter (mm)	Swollen Short Axis Diameter (mm)	Swollen Thickness (mm)
G10	11.3 ± 3.2	23.2 ± 1.4	11.6 ± 5.2	25.8 ± 0.4	13.5 ± 0.7	10.8 ± 0.4
G11	16.0 ± 8.7	23.7 ± 0.6	11.2 ± 3.3	26.3 ± 2.9	13.8 ± 0.8	12.7 ± 0.6
G12	0	23.3 ± 1.2	11.5 ± 2.2	26.7 ± 1.5	13.6 ± 0.5	12.5 ± 0.5
G14	19.7 ± 9.5	23.8 ± 1.3	13.0 ± 3.8	26.9 ± 2.5	13.7 ± 1.0	13.8 ± 1.0
G15	43.7 ± 18.8	24.8 ± 0.6	7.4 ± 1.1	27.3 ± 1.2	14.0 ± 0.2	12.0 ± 0.5
G16	48.0 ± 13.0	> 26.0	7.0 ± 0.5	27.5 ± 0.9	14.3 ± 0.3	12.1 ± 0.7
G17	0	25.3 ± 2.9	8.8 ± 2.1	25.3 ± 2.5	13.8 ± 0.3	12.2 ± 1.0
G18	0	24.1 ± 0.7	10.9 ± 1.6	25.3 ± 1.0	13.6 ± 0.4	13.0 ± 1.0

There was no statistically significant difference (one-way ANOVA, $p > 0.05$) in the swollen tablet dimensions between the different oval biconvex gastroretentive layer formulations (G4 − G19) after completion of the *in vitro* buoyancy testing. The dimensions of the swollen tablets were close to or higher than 12.8 mm in all axes (long axis, short axis, thickness) which is the estimated mean diameter of the resting human pyloric sphincter (249). These results showed that, apart from floating, the gastroretentive layers also showed expandable system properties that could potentially contribute to the gastric retention of the dosage form.

This preliminary study provided information on the gastroretentive layer floating performance using different formulation compositions and compression forces. The study was crucial in designing the factorial experiment that was used to determine the optimised formula for the gastroretentive layer of the bilayer tablets.

4.3.3 Factorial experiment

The three different factors (amount of PEO, % of spray-dried lactose and compression force) potentially affecting the floating lag time and total floating time of the non-effervescent bilayer tablets were selected based on the gastroretentive layer preliminary study. The two dependent variables (floating lag time and total floating time) were selected to assess the *in vitro* buoyancy behaviour of the gastroretentive tablets. The results of the factorial experiment run for the different formulations can be seen in Table 4-9.

Table 4-9: *Factorial experiment results for the different formulations, regarding their floating lag time and total floating time (n = 3 tablets). Results are expressed as mean ± standard deviation.*

Formulation	Floating Lag Time (seconds)	Total Floating Time (Minutes)
1	0.9 ± 0.0	1783.7 ± 45.0
2	1.1 ± 0.2	1286.3 ± 41.7
3	0.0 ± 0.0	2050.0 ± 7.5
4	0.0 ± 0.0	1617.3 ± 84.2
5	9096.4 ± 67.6	603.0 ± 1.4
6	9069.5 ± 50.3	594.3 ± 41.5
7	12.8 ± 2.0	1508.3 ± 100.4
8	1.9 ± 0.2	1300.0 ± 11.5
9	0.7 ± 0.0	1719.7 ± 6.4
10	0.1 ± 0.1	1379.0 ± 27.5
11	3682.5 ± 90.7	867.0 ± 34.4
12	12579.4 ± 207.8	686.7 ± 49.4
13	216.7 ± 206.7	850.0 ± 130.1
14	267.6 ± 34.0	588.3 ± 29.9
15	0.0 ± 0.0	1120.3 ± 113.9
16	231.5 ± 1.7	922.7 ± 165.4
17	11950.9 ± 740.4	684.0 ± 177.4
18	22981.0 ± 10356.2	556.0 ± 110.9
19	1.8 ± 0.3	1479.5 ± 62.9
20	254.0 ± 64.1	1341.3 ± 187.9
21	0.0 ± 0.0	1207.0 ± 8.5
22	0.0 ± 0.0	1624.7 ± 28.6
23	0.0 ± 0.0	1613.0 ± 188.4
24	1585.8 ± 183.2	848.7 ± 55.4
25	1717.8 ± 190.4	988.0 ± 19.0
26	244.5 ± 3.3	892.0 ± 215.2
27	10676.0 ± 408.2	653.3 ± 37.1
Optimised	1.5 ± 0.8	1498.0 ± 75.4

The quadratic model was the best-fitting model for floating lag time ($p < 0.001$) and the relationship between the variable and the different factors was depicted in Equation 11. The compression force was the main factor significantly affecting the tablet floating lag time in both a linear and a non-linear positive manner (one-way ANOVA, $p < 0.05$ for the linear term and $p < 0.01$ for the non-linear term). Increasing the compression force led to significantly longer floating lag time values. This could be attributed to an increase in the tablet density

that was probably linked to a reduced tablet porosity in higher compression forces (109, 250). Additionally, the ANOVA analysis demonstrated a potential interaction between the amount of PEO 8M and the compression force with a significant negative effect on the variable ($p < 0.05$). This trend was particularly noticed at a compression force of 7.5 kN, where larger amounts of PEO 8M contributed to shorter floating lag times. This finding was in contrast to a previous report where increasing amounts of PEO resulted in longer floating lag times (109). The material used in the present study had a lower bulk density of 0.3811 g/cm^3 and a larger mean particle size of 247.7 μm, compared to previous work (134). The low density and relatively large particle size of PEO may have contributed towards lower tablet density and higher tablet porosity values with increasing amounts of the material in the gastroretentive layer, thus leading to shorter floating lag time values.

$$FLT = 21589.495 - (16.601 \times X_1) - (760.991 \times X_2) - (6665.087 \times X_3) + (1.687 \times X_1X_2) - (5.338 \times X_1X_3) - (187.326 \times X_2X_3) + (0.0647 \times X_1^2) + (186.544 \times X_2^2) + (725.058 \times X_3^2) \quad [11]$$

The model did not fit as well to the experimental data as might have been desired, since the R^2 value was 0.829 and the adjusted R^2 value was 0.738. Despite this, it was still able to demonstrate which factor and factor interaction had a significant impact on the floating lag time of the gastroretentive tablets. However, given the model fit, it was only used in an informative way to demonstrate which factors had an impact on floating lag time rather than to a predictive capacity. Based on the experimental data, a compression force value between 5 and 7.5 kN would be a good choice to ensure a minimal floating lag time which is the target for gastroretentive floating systems (109). When considering the choice of the optimal compression force, though, apart from the floating lag time, the tablet hardness and the wet strength of the tablets after the *in vitro* buoyancy test also need to be considered. In Table

4-10, it can be seen that increasing compression force values had a statistically significant positive effect on the tablet hardness and wet strength, especially for high-weight tablets containing 320 mg and 480 mg PEO (one-way ANOVA, $p < 0.001$ and *post hoc* Bonferroni, $p < 0.05$ for pairwise comparisons regarding tablet hardness, one-way ANOVA, $p < 0.01$ and *post hoc* Bonferroni, $p < 0.05$ for pairwise comparisons regarding wet strength). The tablet hardness should be high enough to ensure the mechanical integrity of tablets during handling, while the wet strength of the tablets should be higher than 3.2 N which is the estimated gastric destructive force experienced in the stomachs of Beagle dogs (247). Therefore, based on the experimental data, a compression force value close to 7.5 kN should be chosen as the optimal one since it would help ensure a short floating lag time of the tablets, alongside sufficient hardness and wet strength.

Table 4-10: *Post-compression parameters of the factorial experiment bilayer tablets and wet strength characterisation results after the in vitro buoyancy run (n = 3 tablets). Results are reported as mean ± standard deviation.*

Formulation	Tablet Shape	Long Diameter (mm)	Short Diameter (mm)	Tablet Thickness (mm)	Hardness (kg)	Tensile Strength (kPa)	Wet Strength After *In Vitro* Buoyancy (N)
1	Oval biconvex	17	9	8.64 ± 0.00	19.32 ± 0.06	1014.2 ± 3.3	12.6 ± 4.3
2	Oval biconvex	17	9	7.61 ± 0.02	16.97 ± 0.74	1036.8 ± 42.1	13.8 ± 1.0
3	Oval biconvex	17	9	9.29 ± 0.01	11.09 ± 0.14	534.8 ± 7.2	4.2 ± 0.3
4	Oval biconvex	17	9	8.21 ± 0.01	12.27 ± 0.17	684.7 ± 8.2	7.5 ± 2.5
5	Oval biconvex	17	9	8.02 ± 0.02	25.79 ± 0.72	1480.8 ± 44.6	22.0 ± 0.9
6	Oval biconvex	17	9	7.11 ± 0.01	27.86 ± 1.38	1853.2 ± 94.5	23.5 ± 2.6
7	Oval biconvex	17	9	6.49 ± 0.01	14.25 ± 0.65	1061.9 ± 50.3	7.7 ± 1.9
8	Oval biconvex	17	9	6.10 ± 0.00	13.39 ± 0.52	1081.5 ± 42.1	9.6 ± 2.2
9	Oval biconvex	17	9	6.41 ± 0.02	7.69 ± 0.57	582.6 ± 45.5	5.5 ± 0.9
10	Oval biconvex	17	9	6.60 ± 0.01	8.09 ± 0.49	590.6 ± 35.6	7.9 ± 1.5
11	Oval biconvex	17	9	6.23 ± 0.02	19.61 ± 1.78	1541.7 ± 137.0	14.6 ± 2.6
12	Oval biconvex	17	9	5.81 ± 0.01	17.62 ± 0.12	1516.6 ± 7.4	16.2 ± 1.4
13	Round	13	13	3.41 ± 0.01	8.39 ± 0.06	1180.6 ± 4.4	4.6 ± 2.3
14	Round	13	13	3.27 ± 0.03	7.42 ± 0.14	1091.6 ± 29.9	6.3 ± 0.3
15	Round	13	13	3.73 ± 0.01	4.70 ± 0.38	604.5 ± 49.8	7.2 ± 2.8
16	Round	13	13	3.54 ± 0.00	4.32 ± 0.35	586.4 ± 48.0	1.8 ± 0.1
17	Round	13	13	3.28 ± 0.00	10.70 ± 0.40	1568.0 ± 59.2	6.8 ± 2.3
18	Round	13	13	3.09 ± 0.01	10.55 ± 0.25	1642.8 ± 33.6	4.2 ± 1.7
19	Oval biconvex	17	9	8.35 ± 0.01	19.71 ± 0.27	981.3 ± 15.0	13.3 ± 2.8
20	Oval biconvex	17	9	6.21 ± 0.01	12.99 ± 0.59	938.4 ± 40.4	10.0 ± 3.5
21	Round	13	13	3.68 ± 0.05	4.61 ± 0.53	602.9 ± 76.0	3.1 ± 0.6
22	Oval biconvex	17	9	8.49 ± 0.01	10.82 ± 0.15	527.9 ± 7.6	3.5 ± 0.9
23	Oval biconvex	17	9	6.71 ± 0.01	8.13 ± 0.08	530.7 ± 5.7	6.6 ± 2.0
24	Oval biconvex	17	9	7.97 ± 0.03	26.71 ± 0.83	1408.4 ± 49.9	9.2 ± 0.8
25	Oval biconvex	17	9	6.09 ± 0.01	16.42 ± 0.64	1214.8 ± 44.8	14.7 ± 4.4
26	Round	13	13	3.35 ± 0.01	8.15 ± 0.26	1167.7 ± 33.8	5.6 ± 3.1
27	Round	13	13	3.17 ± 0.02	11.28 ± 0.53	1708.4 ± 92.1	7.9 ± 5.1
Optimised	Oval biconvex	17	9	7.44 ± 0.01	16.91 ± 0.35	1594.1 ± 31.9	8.7 ± 1.6

With regards to the total floating time, a quadratic model was again the best fit. The relationship between the variable and the factors and factor interactions can be seen in Equation 12.

$$TFT = -1014.457 + (8.808 \times X_1) + (107.952 \times X_2) + (280.496 \times X_3) + (0.0523 \times X_1X_2) - (0.394 \times X_1X_3) - (6.229 \times X_2X_3) - (0.00704 \times X_1^2) - (5.797 \times X_2^2) - (18.883 \times X_3^2) \quad [12]$$

The amount of PEO in the gastroretentive layer was the main factor affecting the total floating time of the tablets in both a linear and a non-linear trend (one-way ANOVA, $p < 0.001$ for the linear term and $p < 0.01$ for the non-linear term). The buoyancy of gastroretentive formulations has been reported to be strongly dependent on the swelling of the hydrocolloid particles that come in contact with the gastric fluids (251). This is because, upon hydration, PEO swells, thus increasing tablet volume and reducing the density. At some point, the hydration volume is maximised, and polymer disentanglement and erosion become dominant, thus leading to volume reduction. Higher proportions of PEO can increase the tablet volume attained upon hydration and the time required for the hydration volume to become maximum, thus resulting in prolonged floating times (110). Furthermore, increased amounts of PEO may result in the formation of a stronger gel (109) which could slow the gel erosion process and can be a limiting factor for the magnitude and maintenance of the hydrated tablet size (134). The tablet size is linked to hydrated tablet density and, thus, floatability. Hence, these factors may have contributed to the increasing tablet total floating time values recorded with increasing amounts of PEO in the gastroretentive layer.

Apart from the amount of PEO, the compression force was also a significant factor affecting the total floating time in a non-linear manner (one-way ANOVA, $p < 0.05$). Higher compression forces can lead to a reduced internal porosity of the tablets. In hydrophilic matrix tablets, it has been demonstrated that the reduced tablet porosity could lead to a reduced water transport rate through the matrix during contact with aqueous media (252). This could result in longer times to achieve maximum hydration volume, as well as lower levels of maximum hydration volume, compared to tablets compressed using lower forces (110). Furthermore, visual observation of the tablet floating behaviour upon application of

vertical pressure showed that tablets compressed using lower compression forces had a higher tendency to re-surface on the medium. This trend was also noted in a study by Goole et al. (253) and may have contributed towards a more efficient and robust floatation leading to longer total floating times in lower compression force values.

A significant negative effect on the total floating time was conferred by the interaction between the amount of PEO and the compression force (one-way ANOVA, $p < 0.001$). As discussed, these two factors had opposite effects on the dependent variable. The prevailing negative effect of the combined factors on the total floating time was because the negative effect of the compression force on the variable was dominant for higher tablet weights and, therefore, higher amounts of PEO, especially for the tablets that contained 320 mg and 480 mg PEO (one-way ANOVA, $p < 0.001$, and *post hoc* Bonferroni $p < 0.01$ for pairwise comparisons). Clear differences were recorded in the total floating time for the same tablet formulas under different compression force values (Table 4-9). Finally, the percentage of spray-dried lactose in the gastroretentive layer had a minor positive effect on the total floating time of the tablets, but it was not statistically significant (one-way ANOVA, $p > 0.05$).

The total floating time quadratic model fitted the experimental data well, indicated by an R^2 value of 0.923 and an adjusted R^2 value of 0.883. However, it was realised that, if the non-significant linear term of compression force was eliminated from the equation, the model fit to the data would improve. Therefore, Equation 13 was generated with an R^2 value of 0.921 and an adjusted R^2 value of 0.887.

$$TFT = 41.919 + (8.470 \times X_1) + (100.213 \times X_2) + (0.0523 \times X_1X_2) - (0.348 \times X_1X_3) - (5.197 \times X_2X_3) - (0.00704 \times X_1^2) - (5.797 \times X_2^2) - (1.548 \times X_3^2) \quad [13]$$

Kollidon® SR was a major component of the gastroretentive layer. The preliminary gastroretentive layer study demonstrated that it did not have a significant effect on the

floating lag time and total floating time of tablets. However, high percentages of Kollidon® SR did lead to higher tensile strength and higher wet strength values of the tablets. Based on these results, the percentage of Kollidon® SR selected for all the factorial experiment runs (34.0 %) was deemed crucial in ensuring an adequately high wet strength of the tablets, apart from a sufficiently high compression force.

Based on Equation 13, as well as floating lag time, tablet hardness and tablet wet strength considerations, a candidate optimised gastroretentive layer was designed and a compression force of 7 kN was selected for the tablet preparation. The gastroretentive tablets were prepared using a simple direct compression process. The composition of the optimised layer is in Table 4-14. The bilayer tablets containing this layer were characterised in terms of their *in vitro* buoyancy properties. As can be seen in Table 4-9, the tablets demonstrated a negligible floating lag time and a total floating time that was longer than 24 hours and close to the theoretical value calculated via Equation 13. This further confirmed the suitability of the model to predict the total floating time values of formulation combinations. Also, the hardness and tensile strength values of the tablets were sufficiently high to ensure their mechanical integrity (Table 4-10), while their wet strength value of 8.7 ± 1.6 N after the *in vitro* buoyancy test could contribute to their integrity *in vivo*. Finally, in terms of the swollen tablet dimensions, after sinking, the tablets had a long axis diameter of 25.8 ± 0.8 mm, a short axis diameter of 13.7 ± 0.6 mm and a thickness of 13.2 ± 1.1 mm (n = 3 tablets). These dimensions were larger on average than the estimated average pyloric sphincter diameter of 12.8 mm (194, 254). This could further contribute towards extended gastric retention of the tablets, alongside their prolonged buoyancy. Therefore, this gastroretentive layer was selected as the optimal.

The *in vitro* buoyancy of bilayer A1 tablets in FaSSGF pH 1.6 was characterised since they were also considered promising as a once-a-day oral formulation for MT-1207. Their

floating lag time was 1.8 ± 0.5 seconds and their total floating time was 1599.7 ± 130.0 minutes. Additionally, after the *in vitro* buoyancy run, their wet strength was sufficiently high (6.9 ± 1.4 N), and, in terms of their swollen dimensions, their long axis diameter was 26.1 ± 0.7 mm, their short axis diameter was 13.5 ± 0.5 mm and their thickness was 12.9 ± 0.5 mm (n = 3 tablets). The negligible floating lag time and total floating time longer than 24 hours confirmed the promising gastroretentive application of the bilayer A1 tablets. Furthermore, there was no statistically significant difference in the floating lag time and total floating time values between the bilayer A1, F_{HE6005} and F_{HE7035} (floating lag time of 1.0 ± 0.9 s, total floating time of 1557.3 ± 126.9 minutes) tablets (one-way ANOVA, $p > 0.05$). These findings indicate that the *in vitro* buoyancy behaviour of the bilayer tablets was mainly dependent on the gastroretentive layer with no significant effect from the drug layer. Therefore, the versatility of the selected optimised gastroretentive layer and its ability to be combined with different drug layers for gastroretentive formulation development purposes was confirmed.

4.3.4 Post-compression characterisation of tablets

The hardness values of the prepared tablet formulations containing the different drug layers can be seen in Table 4-11. There was no trend in the tensile strength between different formulations. Therefore, the content of ethylcellulose did not seem to have a significant effect on tablet tensile strength, despite the fact that it has binder properties (51). The reason for this could be that, in many of these formulations, PVP K30 was also included as a binder which could have affected the tensile strength of the tablets. All formulations demonstrated sufficiently high tablet hardness and tensile strength values to ensure their mechanical integrity during transportation or other stresses.

Table 4-11: *Hardness and friability testing results for the bilayer tablets containing different drug layers (n = 10 tablets). The thickness, hardness and tensile strength results are presented as mean ± standard deviation.*

Formulation	Long Axis Diameter (mm)	Short Axis Diameter (mm)	Thickness (mm)	Hardness (kg)	Tensile Strength (kPa)	Friability (%)
F_{HE7035}	17	9	7.47 ± 0.05	20.26 ± 0.36	1191.8 ± 34.1	0.02
F_{HE7030}	17	9	7.48 ± 0.04	17.12 ± 0.81	972.6 ± 9.9	0.01
F_{HE6030}	17	9	7.45 ± 0.01	15.18 ± 0.42	954.0 ± 26.4	0.01
F_{HE6020}	17	9	7.43 ± 0.02	14.36 ± 0.32	903.2 ± 21.1	0.01
F_{HE5020}	17	9	7.42 ± 0.02	15.11 ± 0.35	952.4 ± 21.9	0.01
F_{HE6015}	17	9	7.41 ± 0.02	14.64 ± 0.41	923.4 ± 26.2	0.01
F_{HE6010}	17	9	7.44 ± 0.01	12.96 ± 0.14	814.6 ± 8.5	0.01
F_{HE6005}	17	9	7.34 ± 0.01	16.91 ± 0.35	1062.7 ± 21.2	0.02
F_{HE6003}	17	9	7.34 ± 0.02	16.03 ± 0.14	1023.9 ± 9.3	0.02
F_{HE6001}	17	9	7.34 ± 0.02	15.64 ± 0.22	999.7 ± 12.9	0.02
Bilayer A1	17	9	7.68 ± 0.01	14.95 ± 0.18	923.7 ± 11.1	0.02

The thickness of the tablets containing the optimised gastroretentive layer ranged between 7.3 and 7.7 mm and the diameter of the semicircle on each side of the oval biconvex tablets was 1 mm.

The friability of all bilayer tablets was less than 1.0 % (Table 4-11). This test provided another confirmation of the ability of the tablets to withstand the expected mechanical shocks during handling and transportation, as per USP (213).

All tablet batches gave acceptable mean weight values and acceptance values below 15.0, with regards to tablet weight variation (Table 4-12). Therefore, for all formulations, the tablets were considered uniform in weight, as per USP (210).

Table 4-12: *Tablet weight variation testing results for the bilayer tablets containing different drug layers (n = 10 tablets).*

Formulation	Mean Tablet Weight (% of label claim)	Standard Deviation	Acceptance Value
F_{HE7035}	99.9	2.8	6.7
F_{HE7030}	100.0	1.2	2.9
F_{HE6030}	100.1	1.3	3.2
F_{HE6020}	100.1	1.1	2.7
F_{HE5020}	100.2	2.0	4.7
F_{HE6015}	100.2	1.9	4.5
F_{HE6010}	100.1	1.5	3.6
F_{HE6005}	100.1	1.8	4.3
F_{HE6003}	100.2	1.5	3.6
F_{HE6001}	100.3	1.3	3.0
Bilayer A1	100.2	1.4	3.4

4.3.5 Physicochemical characterisation of MT-1207 and the optimised tablets

Physicochemical characterisation of MT-1207 and the drug layer of the optimised bilayer F_{HE6005} tablets was conducted to assess any physical and chemical interactions that may have taken place between the API and the different excipients in the tablets. DSC and XRPD analyses were conducted to examine the presence of physical interactions, as well as the impact that the whole tablet preparation process may have had on the integrity of the MT-1207 anhydrous crystal. ATR-FTIR analysis was conducted to conclude whether any significant chemical interactions may either have taken place between the API and the excipient(s) during the tablet preparation process or have existed within the tablet.

The thermal behaviour of the MT-1207 reference standard and that of the F_{HE6005} drug layer was assessed using DSC (Figure 4-1). In Figure 4-1A, the sharp endothermic peak at around 210 °C potentially corresponded to the melting point of the MT-1207 hydrochloride anhydrous crystal. On the other hand, different peaks were recorded in the thermogram of the drug layer of the optimised bilayer F_{HE6005} tablets (Figure 4-1B). The peaks at around 150 −

160 °C were potentially linked to the dehydration of alpha-D-lactose monohydrate towards beta-lactose and the melting point of PVP K30, while the peak at around 200 °C corresponded to the melting point of beta-lactose. Additionally, a broad small endothermic peak was seen at 183.69 °C. This was proposed to correspond to the melting point of the MT-1207 hydrochloride crystal that was present in the tablets. The peak, however, was much broader than that of the reference standard and the heat of fusion was much lower. As mentioned in Chapter 3, the reduction in the crystal melting point could potentially be due to the mixing process which, as per the Schroeder-van Laar theory, results in a lower melting point of the drug crystal, through the reduction of the crystal solidification temperature when the drug is part of a mixture of binary phase change materials. Additionally, the peak broadening and reduction in the heat of fusion that was recorded for the peak of MT-1207 could be due to the fact that, for the given molar fraction of the drug in the liquid state of the binary system, the interactions between the molecules of the drug are weaker than the interactions between the drug and the excipient molecules. Therefore, less energy is required for phase change (234).

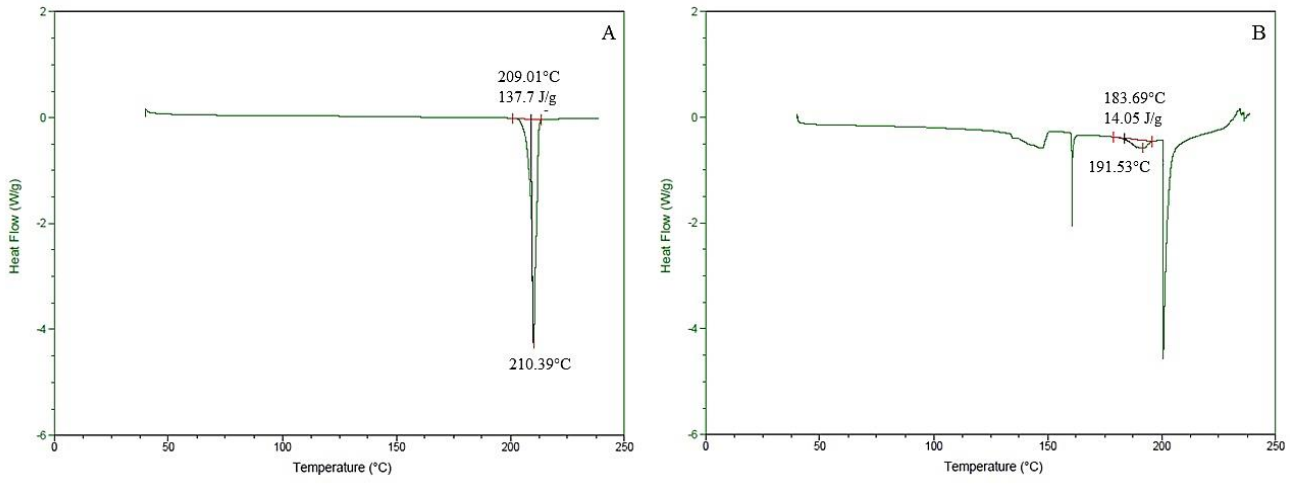


Figure 4-1: *DSC thermograms of (A) MT-1207 hydrochloride reference standard and (B) optimised drug layer of the bilayer tablets.*

While DSC was able to indicate the presence of a drug crystal in the tablets, it was unable to provide information on the crystal structure. Towards that end, XRPD analysis was conducted for the MT-1207 hydrochloride reference standard, the drug layer of the optimised bilayer F_{HE6005} tablets and alpha-D-lactose monohydrate which was the only crystalline excipient used. The diffractograms of the different powders can be seen in Figure 4-2. In the drug layer diffractogram, the peaks over the angle(°2theta) values of 11.5, 15 and 18 were linked to the respective peaks of the MT-1207 hydrochloride reference standard, while all the other peaks were linked to the peaks of alpha-D-lactose monohydrate and the brass specimen holder. The peaks in the drug layer diffractogram were broader and shorter than those of its single-material counterparts. This could be attributed to the smaller crystal particle size of the MT-1207:colloidal silicon dioxide used in the tablets, compared to that of the reference standard. Also, it can be attributed to potential lattice strain conferred by the mixing, wet granulation and tablet compression processes during tablet preparation. No additional peaks were recorded in the drug layer diffractogram, apart from those corresponding to the MT-1207 anhydrous crystal, the alpha-D-lactose monohydrate crystal and the brass specimen holder. Therefore, it can be asserted that, within the sensitivity of the analysis, the drug was present in the tablets solely in the form of its anhydrous crystal.

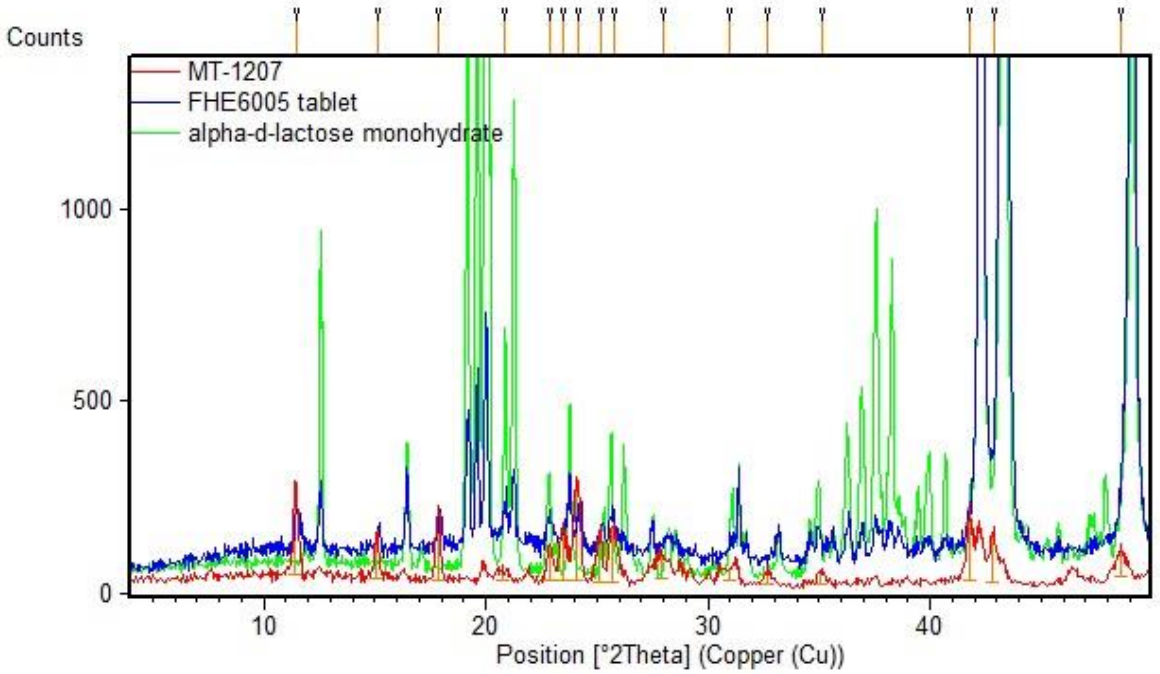


Figure 4-2: *Diffractograms of MT-1207 hydrochloride reference standard (red), alpha-D-lactose monohydrate (green) and the drug layer of the optimised bilayer* F_{HE6005} *tablets (blue).*

FTIR characterisation can be useful in indicating whether chemical interactions between the API and the excipients may have occurred during mixing, granulation and tabletting (235). The peaks in the 2800-3000 cm^{-1} region in the FTIR spectrum of MT-1207 (Figure 4-3) corresponded to the aliphatic and aromatic C-H stretching bonds and were also seen unchanged in the optimised drug layer spectrum. Furthermore, the peaks in the 1250-1300 cm^{-1} region corresponding to the C-N stretch can be seen in the spectra of both MT-1207 reference standard and optimised drug layer. Finally, the fingerprint region of the drug layer was a simple mixture of the fingerprint regions of MT-1207 hydrochloride and the rest of the excipients the FTIR spectra of which were recorded in our previous study (255). No additional peaks were recorded. These results illustrated that there were no significant chemical interactions between MT-1207 and the excipients.

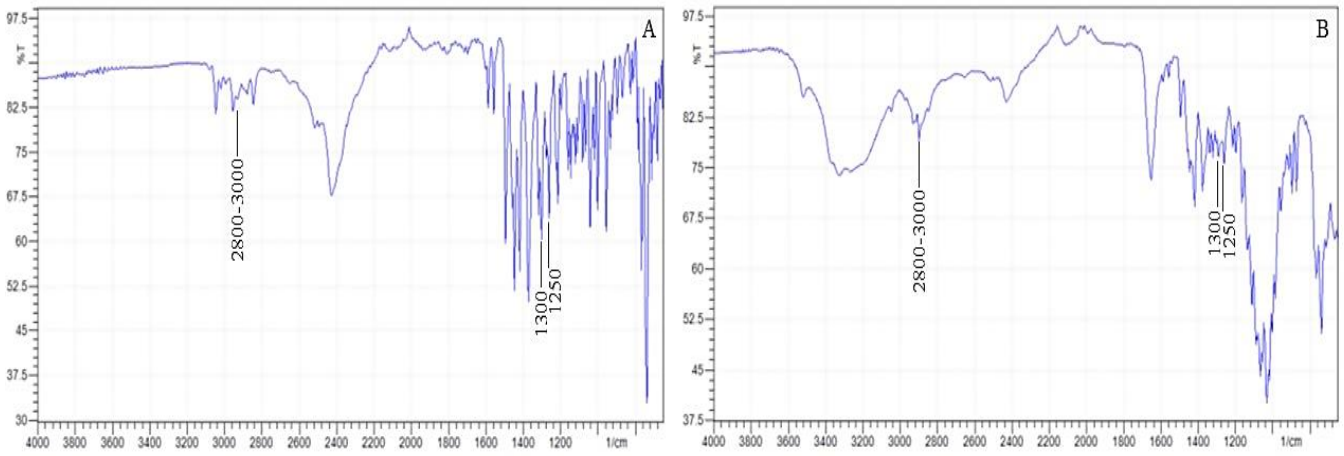


Figure 4-3: *FTIR spectra of (A) MT-1207 hydrochloride reference standard and (B) drug layer of the optimised bilayer F_{HE6005} tablets.*

4.3.6 Tablet density and porosity characterisation

Information on the density and porosity of the optimised bilayer F_{HE6005} tablets was provided through helium pycnometry and mercury intrusion porosimetry analyses. The tablet volume was 2.0119 ± 0.0033 cm^3. The total mercury intrusion volume was 0.2381 ± 0.0050 mL/g, the volume pore diameter was 1.40 ± 0.14 μm and the tablet porosity was 23.7 ± 0.5 %. As per a previous report, this level of tablet porosity can be considered to be relatively high, with tablet porosity values higher than 20 % linked to low tensile strength (109). However, this was not the case in the present study since the optimised bilayer F_{HE6005} tablets were characterised to have sufficiently high hardness and tensile strength values (Table 4-11).

Both helium pycnometry and mercury intrusion porosimetry methods provided tablet skeletal density information. The values reported using the different methods were consistent. The tablet skeletal density was estimated to be 1.2875 ± 0.0015 g/cm^3 using helium pycnometry and 1.3051 ± 0.0497 g/cm^3 using mercury intrusion porosimetry. However, the tablet bulk density determined using mercury intrusion porosimetry was 0.9957 ± 0.0326 g/cm^3. The bulk density calculation takes the air-filled pore spaces within the tablets into

account, in contrast to the skeletal density measurements. Therefore, since the tablet density on average was lower than 1.004 g/cm^3, it was inferred that this was most likely the reason for the nearly immediate floatation of the optimised bilayer tablets in aqueous media.

4.3.7 In vitro buoyancy in media of different pH values

The buoyancy capability of floating gastroretentive tablets is critical in ensuring robust gastric retention *in vivo*. Non-effervescent gastroretentive formulation applications benefit from the fact that their floating lag time is not affected by the gastric pH, thereby enabling their suitability for patients with achlorhydria (106). Furthermore, other factors, such as sugar and salt stomach contents during fed state, have been reported to affect the swelling properties of polymers such as HPMC, and, thus, the floatation of gastroretentive formulations (106). However, to the best of our knowledge, no study has investigated the effect of pH on the total floating time of non-effervescent gastroretentive formulations.

In the present study, the *in vitro* buoyancy of the optimised gastroretentive bilayer F_{HE6005} tablets was assessed in media of different pH values, namely, HCl pH 1.0, phosphate buffer pH 3.0, and phosphate buffer pH 6.0. The media were selected to cover a pH range 1.0 − 6.0 where human gastric pH usually falls in during fasted and fed states, although sometimes it can assume higher values (256). The floating lag time and total floating time values recorded in each of the different media can be seen in Table 4-13.

Table 4-13: *In vitro buoyancy testing results for the optimised gastroretentive bilayer F_{HE6005} tablets in HCl pH 1.0, phosphate pH 3.0, and phosphate pH 6.0. Results are presented as mean ± standard deviation.*

Medium	Floating Lag Time (Seconds)	Total Floating Time (Minutes)
HCl pH 1.0	1.00 ± 0.88	1335.7 ± 149.3
Phosphate pH 3.0	1.70 ± 0.44	1854.0 ± 152.0
Phosphate pH 6.0	1.72 ± 0.15	2232.3 ± 88.2

There was no statistically significant difference between the tablet floating lag time values recorded in the different media (one-way ANOVA, $p > 0.05$). This was expected since the immediate buoyancy of the tablets was most likely achieved due to their bulk density, that being lower than 1.004 g/cm^3, as demonstrated during the gas pycnometry study. However, there was a statistically significant difference in the total floating time values of the tablets in the different media (one-way ANOVA, $p < 0.001$). The pairwise comparisons conducted as part of the *post hoc* Bonferroni *t*-test demonstrated significant differences between the tablet total floating time values recorded in HCl pH 1.0 and phosphate pH 3.0 ($p < 0.01$), HCl pH 1.0 and phosphate pH 6.0 ($p < 0.001$), and phosphate pH 3.0 and phosphate pH 6.0 ($p < 0.01$).

To the best of our knowledge, a significant pH effect on the total floating time of non-effervescent gastroretentive formulations has not been reported in the literature. Apart from MT-1207, the rest of the tablet components were non-ionic and, thus, their dissolution and/or swelling behaviour could not have been affected by the medium pH. Therefore, the reason for the recorded differences could lie with other physicochemical attributes of the excipients.

From the factorial experiment for the gastroretentive layer, it was concluded that the major factors affecting the total floating time were the amount of PEO, the compression force and the interaction between these two factors. Previous studies have demonstrated that PEO

most likely undergoes degradation in strongly acidic pH. McGary first reported relevant findings where it was concluded that PEO degradation was accelerated in aqueous solutions in the presence of strong acids, as determined by a reduction in solution viscosity (257). The reason for this was probably not only acid hydrolysis of the polymer taking place, but also an additional free-radical mechanism. It was believed that hydroperoxides that are present in the polymer could undergo ionic rearrangement within the polymer structure that may result in chain scission (257). Additionally, the results of a study conducted by Crowley et al. showed that small quantities of ascorbic acid could significantly reduce the molecular weight of PEO through an acid catalysed chain scission reaction (258). Finally, Yang et al. reported that the acid effect on PEO could be enhanced at higher temperatures. FTIR spectra of Pluronic P123 aqueous solutions in the presence of 2 M HCl showed two additional peaks at temperatures equal to or higher than 36 °C, compared to the spectra of the same solutions analysed at lower temperatures. The presence of these peaks could be attributed to the C-O-C stretch mode of small PEO segments derived from ether bond cleavage. Therefore, it seemed that temperature values equal to or higher than 36 °C could contribute to the PEO acid-induced degradation (259).

PEO was a major component of the gastroretentive layer of the bilayer tablets and a significant factor affecting their floatation. Based on the abovementioned information from previous studies, it was hypothesized that the statistically significant differences between the tablet total floating time values recorded in the different media could be attributed to differences in the rate and extent of PEO degradation in the media. To investigate this hypothesis, an SEM analysis of the gastroretentive layer of the tablets was performed at selected timepoints during *in vitro* buoyancy testing to visualise the layer and how it may have changed over time, alongside a viscosity analysis of the solutions at different timepoints to provide quantitative information on their PEO content at certain timepoints.

Figure 4-4 illustrates SEM images of the optimised gastroretentive layer of the bilayer tablets in their dry state. The surface of the gastroretentive layer appeared to be quite porous with most of it covered by irregular, porous particles, proposed to be PEO, that were well mixed with spherical Kollidon® SR particles.

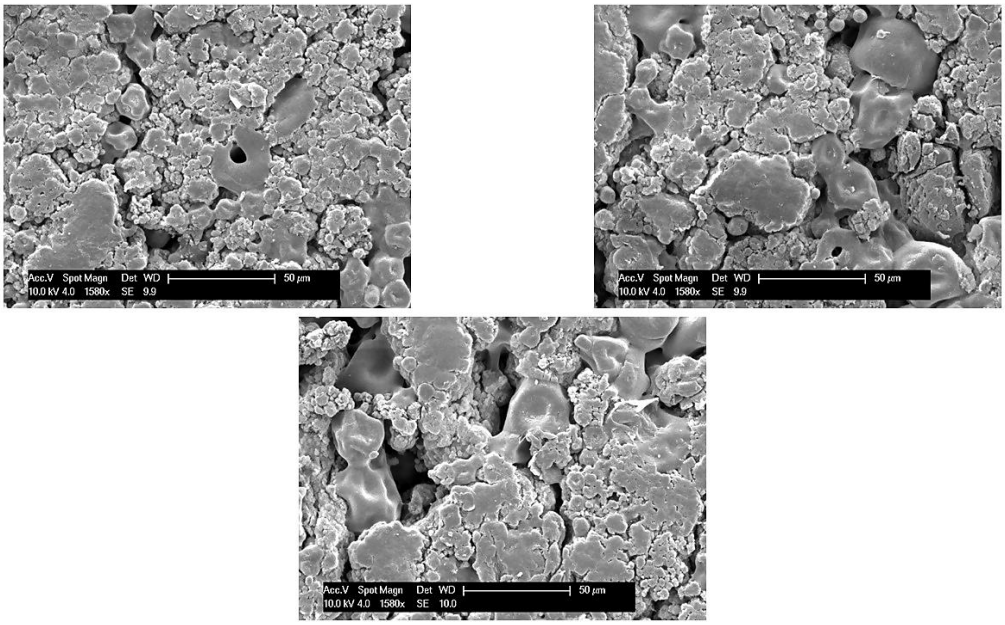


Figure 4-4: *SEM images of the optimised gastroretentive layer of the dry bilayer tablets.*

Figure 4-5 illustrates SEM images of the gastroretentive layer of the bilayer tablets during *in vitro* buoyancy in the different media at the 12-hour timepoint. The surface of the gastroretentive layer appeared fibrous in all media. These fibres probably contained amorphous PEO polymer that occurred from drying of the swollen PEO gel that had formed during the *in vitro* buoyancy test. The spherical particles present in the different images corresponded to Kollidon® SR particles. The small, irregular particles probably corresponded to PEO that crystallised during the drying process (260). Based on the above, it could be assumed that at the 12-hour timepoint of the *in vitro* buoyancy test there was a strong presence of PEO in the gastroretentive layer of the tablets in the different media.

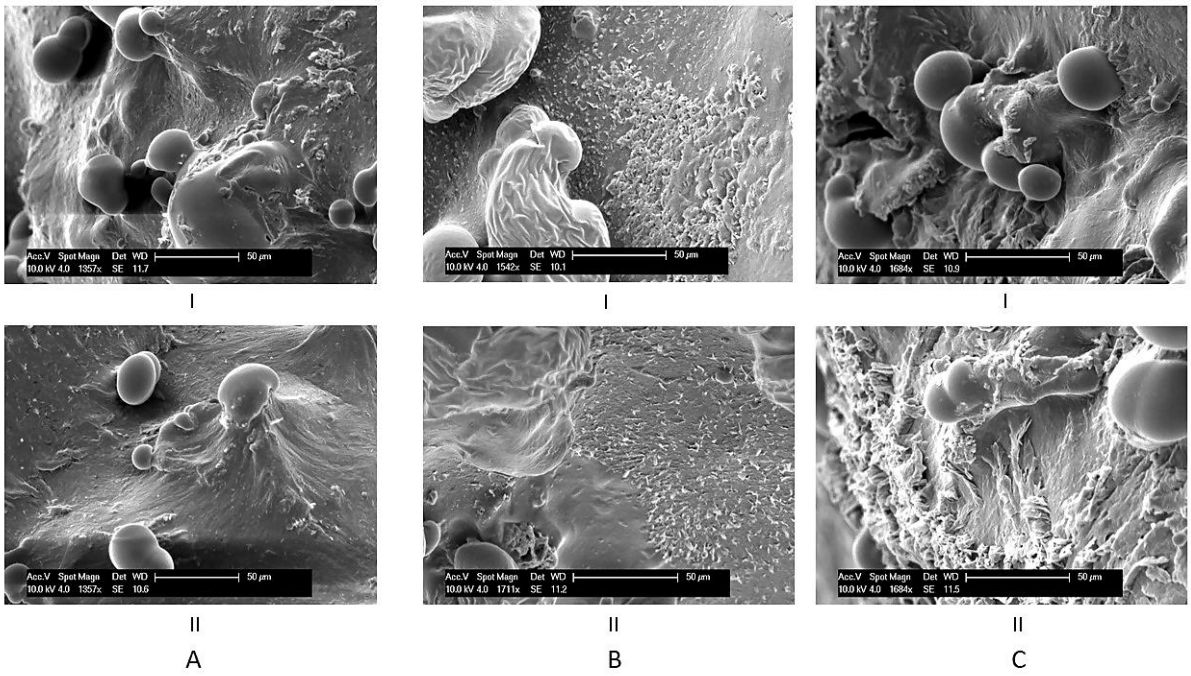


Figure 4-5: *SEM images of the optimised gastroretentive layer of the bilayer tablets after 12 hours of in vitro buoyancy testing in (A) HCl pH 1.0, (B) phosphate pH 3.0, and (C) phosphate pH 6.0.*

Figure 4-6 illustrates the SEM images of the gastroretentive layer of the bilayer tablets during *in vitro* buoyancy in the different media at the 22-hour timepoint which was the average sinking time of the tablets in HCl pH 1.0. It seemed that the presence of fibres in the gastroretentive layer of the tablets was much weaker after 22 hours of *in vitro* buoyancy testing in HCl pH 1.0, compared to the 12-hour timepoint in the same medium and the 22-hour timepoint in the other media. As seen in Figure 4-6B and Figure 4-6C, the surface of the tablet gastroretentive layer was characterised by a strong presence of fibres and small irregular particles that were believed to correspond to amorphous and crystallised PEO, respectively. The presence of fibres was more evident in the gastroretentive layer of the tablets tested in phosphate pH 6.0. Therefore, it could be assumed that the presence of PEO in the gastroretentive layers of the tablets tested in phosphate pH 3.0 and phosphate pH 6.0 was still strong at the 22-hour timepoint of the *in vitro* buoyancy experiment.

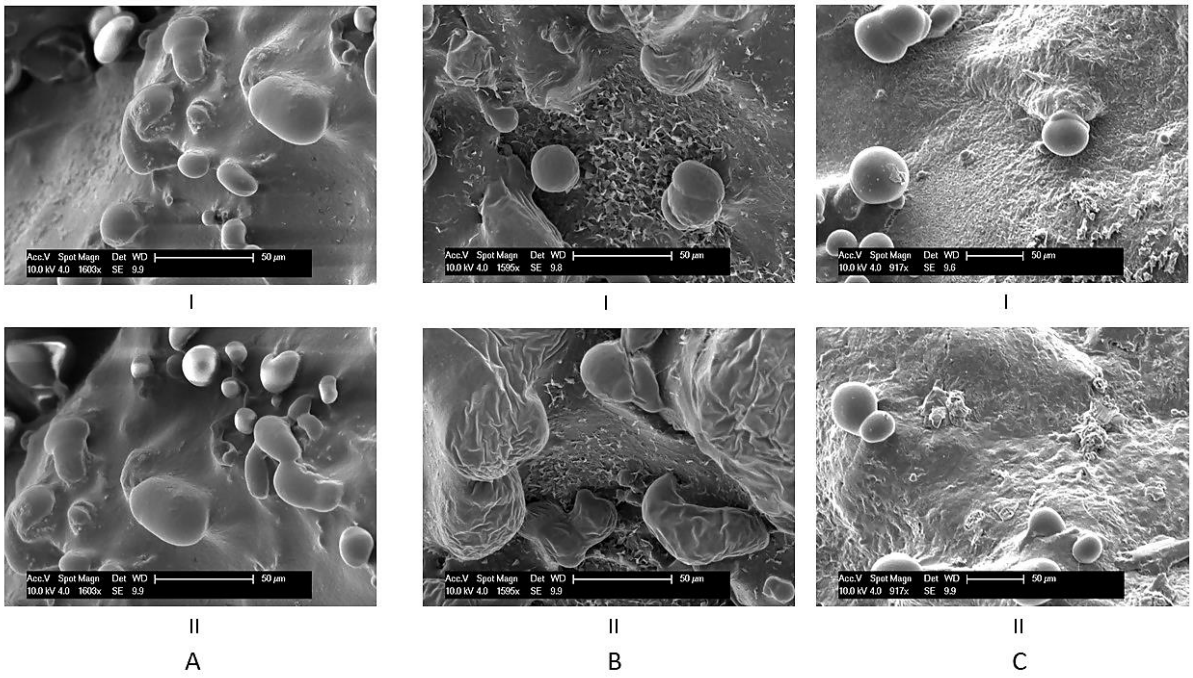


Figure 4-6: *SEM images of the optimised gastroretentive layer of the bilayer tablets after 22 hours of in vitro buoyancy testing in (A) HCl pH 1.0, (B) phosphate pH 3.0, and (C) phosphate pH 6.0.*

Figure 4-7 illustrates the SEM images of the gastroretentive layer of the bilayer tablets during *in vitro* buoyancy in phosphate pH 3.0 and phosphate pH 6.0 at the 31-hour timepoint which was the average sinking time of the tablets in the former. As seen in Figure 4-7A, the presence of PEO in the form of fibres and irregular particles was still noticeable in the gastroretentive layer of the tablets after 31 hours of *in vitro* buoyancy test in phosphate buffer pH 3.0. However, the presence of PEO was much weaker, compared to the 22-hour timepoint of the tablet *in vitro* buoyancy test in phosphate buffer pH 3.0, and the 31-hour timepoint of the tablet *in vitro* buoyancy test in phosphate buffer pH 6.0 (Figure 4-7B).

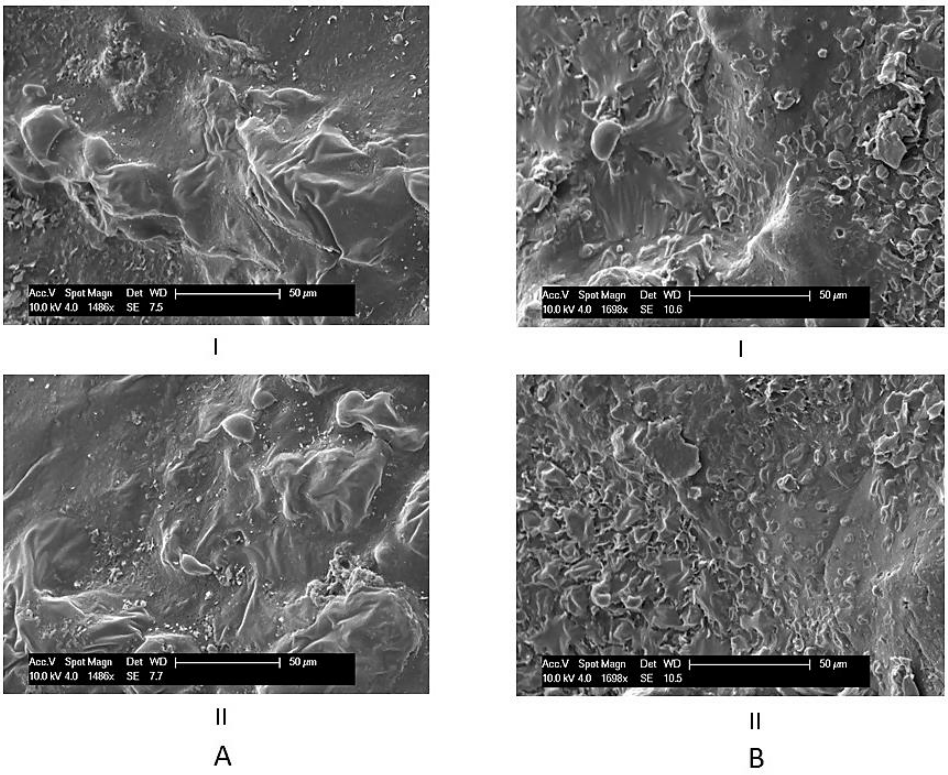


Figure 4-7: *SEM images of the optimised gastroretentive layer of the bilayer tablets after 31 hours of in vitro buoyancy testing in (A) phosphate pH 3.0, and (B) phosphate pH 6.0.*

Figure 4-8 shows SEM images of the gastroretentive layer of the bilayer tablets during *in vitro* buoyancy in phosphate pH 6.0 at the 43.5-hour timepoint which was the average sinking time of the tablets in the medium. The presence of PEO in the form of fibres was still clear, even after 43.5 hours of *in vitro* buoyancy testing. However, the surface of the layer had become quite porous which indicated that erosion may have taken place during the *in vitro* buoyancy testing between the 31- and 43.5-hour timepoints.

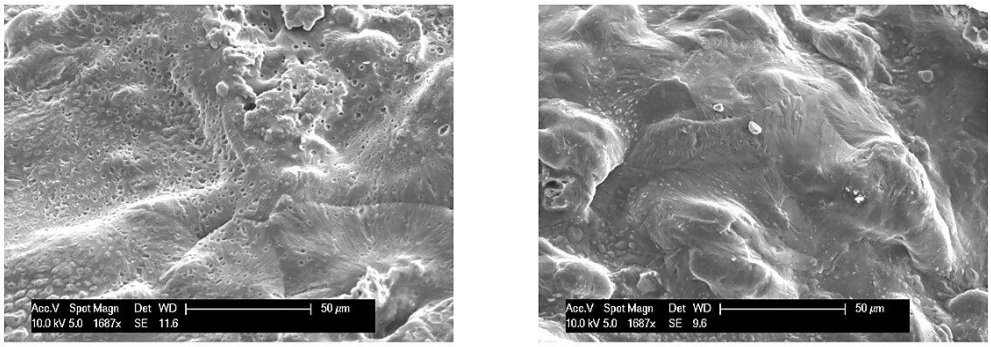


Figure 4-8: *SEM images of the optimised gastroretentive layer of the bilayer tablets after 43.5 hours of in vitro buoyancy testing in phosphate pH 6.0.*

The SEM imaging indicated potential differences in the presence of PEO in the gastroretentive layer of the tablets between the different media in which *in vitro* buoyancy testing was performed, as well as between different timepoints of the test within the same medium. Therefore, the statistically significant differences in the tablet total floating time values between the different media could be linked to differences in the rate and extent of PEO degradation in the different aqueous solutions. However, the SEM imaging only provided qualitative information and data for testing this hypothesis. To obtain more solid information on the trueness of the hypothesis, the acquisition of quantitative data was deemed crucial.

Viscosity analysis of the different media in different timepoints during the tablet *in vitro* buoyancy testing was performed to obtain quantitative information on potential changes and/or differences in the PEO content over time during the buoyancy test and between the different media, respectively (Figure 4-9).

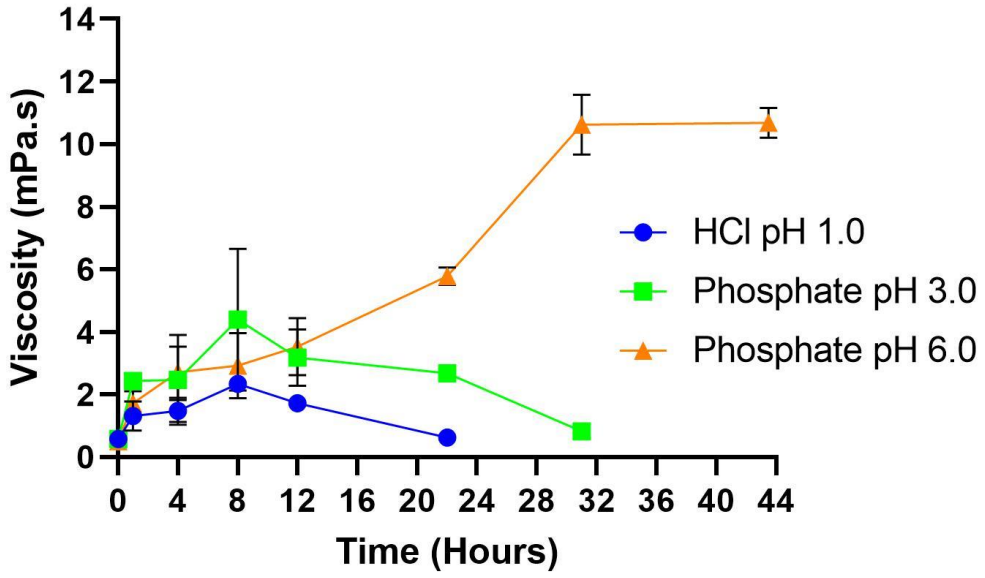


Figure 4-9: *Viscosity of HCl pH 1.0, phosphate pH 3.0 and phosphate pH 6.0 media during in vitro buoyancy testing of the optimised gastroretentive bilayer tablets (n = 3). Results are presented as mean ± standard deviation.*

Up to 12 hours, there was no statistically significant difference between the different media in terms of the recorded viscosity values (one-way ANOVA, $p > 0.05$). This was in alignment with the SEM images at the same timepoint (Figure 4-5) where the tablets seemed to have a strong presence of PEO in the gastroretentive layer in the different media.

At the 22-hour timepoint, which was the approximate average sinking time of the bilayer tablets in HCl pH 1.0, statistically significant differences were recorded in the viscosity values between all different media (one-way ANOVA, $p < 0.001$, *post hoc* Bonferroni, $p < 0.001$). These findings, too, were aligned with the SEM images for the same timepoint (Figure 4-6) which indicated differences in the PEO content of the gastroretentive layer of the tablets in the different media. The SEM images for tablets in HCl pH 1.0 at the 22-hour timepoint showed the weak presence of PEO in the gastroretentive layer at this average sinking time of the tablets in the medium. Additionally, at the 31-hour timepoint,

which was the approximate average sinking time of the bilayer tablets in phosphate pH 3.0, there was a statistically significant difference between the viscosity values recorded in phosphate pH 3.0 and phosphate pH 6.0 (*t*-test, $p < 0.01$). These findings were again in alignment with the respective SEM images (Figure 4-7) which indicated potential differences in the PEO content of the gastroretentive layer of the tablets in the different media. Therefore, it can be asserted that the differences in the *in vitro* buoyancy behaviour of the bilayer tablets in the different media could be attributed to differences in the rate and extent of PEO degradation in the different media depending on their acidity. This potential acid-induced degradation could further be conferred by the temperature since 37 °C is considered high enough to induce chain scission within the polymer, based on previous, abovementioned findings (259).

A final viscosity measurement was conducted in phosphate pH 6.0 after 43.5 hours of *in vitro* buoyancy testing which was the approximate average sinking time of the tablets in that medium. There was no statistically significant difference between the viscosity values recorded at 31 hours and 43.5 hours (*t*-test, $p > 0.05$). This indicated that polymer degradation in this nearly neutral medium was probably very slow and that polymer swelling had probably peaked by 31 hours, thus resulting in similar medium viscosity values at the two timepoints. This result was in agreement with the SEM images of the gastroretentive layer collected at the same timepoint (Figure 4-8) since the presence of PEO in the layer had been estimated to be still significant. Therefore, in this case, the tablets probably sank due to their extensive hydration which has also been reported to affect the duration of the buoyancy of floating systems (157).

These findings demonstrate the potential of pH effect on the buoyancy behaviour of non-effervescent gastroretentive formulations. These results further stress the importance of taking the physicochemical and stability properties of formulation components into account

during the development of gastroretentive formulations. The results of the present study demonstrate that PEO-based floating systems should potentially be administered after a meal, not only because of the lower gastric emptying rates and the disruption of the migrating myoelectric complex (MMC) during the stomach fed state, but also because of the elevated gastric pH during that state. The weakly acidic to neutral pH conditions of the human stomach during the fed state could potentially promote the buoyancy of PEO-based formulations, due to a much slower degradation of the polymer, compared to the strongly acidic conditions prevailing during the fasted state. However, potential effects of other factors, such as sugar and/or salt stomach contents, on the buoyancy of PEO-based formulations should also be investigated.

4.3.8 In vitro release study

4.3.8.1 Validation of the HPLC and dissolution methods

4.3.8.1.1 Linearity

The HPLC method was validated for linearity in the concentration range of 0.001 − 0.1 mg/mL. Three replicates of the calibration curve in this concentration range were prepared over three different days. The R^2 should be equal to or higher than 0.99 for all three replicates for the method to be considered validated for linearity (261). This validation was also considered for the dissolution method since the standard solution matrix was the same as that of MT-1207 dissolution samples.

The calibration curves that were used for linearity validation and their data can be seen in Tables A-7, A-8 and A-9, and Figures A-6, A-7 and A-8, respectively. In all three replicates taken over three different days, the R^2 was higher than 0.999. Therefore, the HPLC method was considered validated in terms of linearity.

4.3.8.1.2 LOD and LOQ determination

The calibration curves that were used for linearity validation were also employed for the calculation of the method LOD and LOQ values. The mean of the peak areas was calculated, and a calibration curve of the mean peak area values and the respective concentration values was plotted. Its slope was used as the S value in Equations 6 and 7. Furthermore, the standard deviation of the y-intercepts was calculated and was used as the SD value of the LOD and LOQ equations, as per ICH guidelines (224).

The calibration curve data and plot that were used for the LOD and LOQ determination can be seen in Table A-10 and Figure A-9, respectively. The S of the calibration curve was 1344.5. The SD of the y-intercepts was 0.0434. The S and SD values were used to calculate the LOD and LOQ of the method using Equations 6 and 7.

$$LOD = 3.3 \times 0.0434/1344.5 = 0.000107 \text{ mg/mL} = 0.1 \text{ µg/mL}$$

$$LOQ = 10 \times 0.0434/1344.5 = 0.000323 \text{ mg/mL} = 0.3 \text{ µg/mL}$$

4.3.8.1.3 Specificity results

A sample chromatogram of the specificity samples can be seen in Figure A-10. As per the FDA guidance for method validation, the assay should be ensured to be free from interfering substances including excipients and other matrix components (226). For all three replicates, the chromatogram was the same as the one in Figure A-10 where no interfering peak was eluted anywhere near the retention time of MT-1207. Therefore, the dissolution method was considered validated in terms of specificity.

4.3.8.1.4 Accuracy, intra-day and inter-day precision results

The accuracy of the dissolution method was assessed at 20 %, 50 %, 80 %, 100 % and 120 % of the target MT-1207 concentration achieved after 100 % release from the tablets in

500 mL 0.1 M acetate buffer pH 4.0 (0.06 mg/mL). Three replicates were prepared at each concentration level. As per the FDA guidelines, a method can be considered accurate for each level if the mean concentration of the accuracy samples is within 85 − 115 % of the nominal concentration value (226). A method is considered precise when the % RSD between the three accuracy samples analysed within a day and three samples analysed within different days is less than or equal to 15 % (226).

As seen in Table A-11, all accuracy values fell within 85 − 115 % of the nominal concentration range, therefore the method was considered validated in terms of accuracy for these drug concentration levels. Furthermore, in Tables A-11 and A-12, the % RSD values were quite lower than 15 % for both intra-day and between-day runs. Therefore, the method was considered validated in terms of intra-day and inter-day precision for these drug concentration levels.

4.3.8.2 *In vitro* dissolution study

In the previous *in vitro* release study reported in Chapter 3, 0.1 M phosphate pH 6.8 with 0.2% w/v SDS was used as the dissolution medium for the *in vitro* release testing. Based on that study results, single-layer A1 tablets containing HPMC K15M as the release retardant were selected as the optimised formulation. Even though a 24-hour release of MT-1207 from the tablets was demonstrated *in vitro*, the results in Beagle dogs indicated a much more rapid release of the API *in vivo* (255). Since the solubility of MT-1207 in the medium was 0.4 mg/mL, it was considered a potential limiting factor for drug release, although sink conditions were theoretically established, as per the USP guidelines (262). Therefore, the phosphate dissolution medium was replaced by 0.1 M acetate buffer pH 4.0 where MT-1207 had a solubility value of 6.5 mg/mL.

The A1 tablets were tested for their *in vitro* drug release in the new medium. As seen in Figure 4-10, MT-1207 was completely released from the tablets within 12 hours. This finding contrasts with the 24-hour release profile that was recorded in 0.1 M phosphate pH 6.8 with 0.2% w/v SDS. The release profile in the acetate buffer was closer to the *in vivo* data. Furthermore, the inability of HPMC K15M to retard the release of MT-1207 from the single-layer tablets over 24 hours in acetate pH 4.0 was demonstrated.

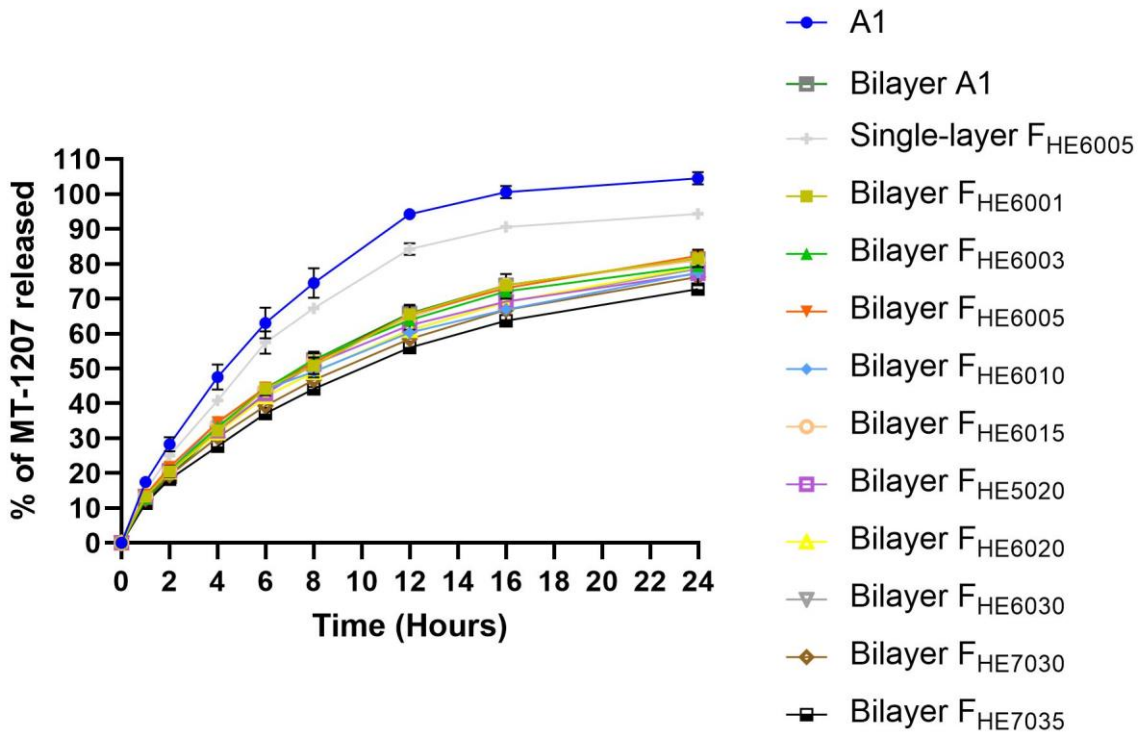


Figure 4-10: *In vitro drug release profiles of A1, single-layer F_{HE6005} and the bilayer tablet formulations in 0.1 M acetate pH 4.0 at 75 rpm (n = 3 tablets). Results are presented as mean ± standard deviation.*

As part of the once-a-day formulation optimisation, bilayer tablets were prepared and their *in vitro* drug release was assessed. Ethylcellulose 10 cps was incorporated as an additional release retardant in the drug layer, due to its hydrophobic polymer properties. HPMC K15M and ethylcellulose are intended to be able to retard the release of drugs from a

formulation in different ways. HPMC K15M swells upon contact with aqueous media and forms a thick gel layer that is able to slow drug diffusion through the polymer chain network (236, 237). Ethylcellulose can be effective in retarding drug release through a reduction in the penetration of solvent molecules into the matrix, due to the hydrophobicity of the polymer. This, in turn, could lead to reduced drug solubilisation and diffusion through the polymer matrix (83, 84).

The release profiles of MT-1207 from the different bilayer tablet formulations can be seen in Figure 4-10. The concentration of ethylcellulose varied from 0.5 to 19% w/w in the different formulations. Furthermore, bilayer A1 tablets were prepared and tested for their *in vitro* drug release. Incorporation of the gastroretentive layer into the formulation led to a statistically significant difference in the *in vitro* drug release profiles between the bilayer and single-layer A1 formulations ($f_1 = 40$, $f_2 = 36$). The bilayer A1 tablets were able to provide a 24-hour sustained release of MT-1207 *in vitro* with more than 80 % of the API released at the 24-hour timepoint. Therefore, it was deemed promising as a sustained-release tablet formulation for the once-a-day oral delivery of MT-1207. Additionally, there was no statistically significant difference in the *in vitro* release profiles between the bilayer A1 tablets and the bilayer tablets with the highest content of ethylcellulose (F_{HE7035}) ($f_1 = 13$, $f_2 = 59$). Therefore, the factor which significantly affected the release of MT-1207 from the tablets was not ethylcellulose, but the presence of the gastroretentive layer. This significant effect could be attributed to a much lower surface area of the drug layer that was exposed to the dissolution medium during the *in vitro* release testing. This was in contrast to previous studies which have reported the effectiveness of ethylcellulose as a release retardant, due to its very high hydrophobicity, compared to other hydrophobic polymers that have also been reported as release retardants. The relatively small particle size of ethylcellulose 10 cps (mean particle size of 100.6 μm; ethylcellulose of higher viscosities have particle sizes of 300

μm or more) could also have contributed to retardation of drug release (263, 264). Other reports have also attributed this capability of ethylcellulose to percolation theory, where a small particle size of polymeric release retardant(s), relative to drug particle size, contributed to lower polymer percolation thresholds, thus potentially resulting in slowing of drug release at lower polymer concentrations (265, 266). Finally, variations of the HPMC K15M content in the drug layer between different formulations did not seem to induce any statistically significant effects on the *in vitro* release profile of MT-1207 ($f_1 = 10$, $f_2 = 68$).

Even though ethylcellulose did not seem to have a significant effect on the *in vitro* drug release, it could potentially affect the release of MT-1207 *in vivo*. Despite the insignificant differences in the *in vitro* release profiles between the different ethylcellulose-containing formulations, F_{HE6015} and F_{HE6005} were the only formulations that provided a complete release of MT-1207, i.e., higher than 80 %, as per the EMA guidelines (267). F_{HE6005} was the only formulation where all three tablets released more than 80 % of MT-1207 over 24 hours. Based on this additional consideration, F_{HE6005} was selected as the optimised ethylcellulose-containing drug layer to be formulated into the gastroretentive bilayer tablets.

An *in vitro* release experiment using a paddle rotation speed of 200 rpm was conducted for bilayer F_{HE6005} and bilayer A1 tablets. This rotation speed has been reported to better simulate the *in vivo* conditions of fasted Beagle dogs (148). The results for both formulations demonstrated a sustained release of MT-1207 from the tablets over 24 hours even under those high shear conditions (Figure 4-11). For both formulations, the *in vitro* drug release profiles at 200 rpm were statistically similar to respective data recorded at 75 rpm ($f_1 = 2$ and $f_2 = 89$ for F_{HE6005} bilayer tablets, $f_1 = 6$ and $f_2 = 76$ for bilayer A1 tablets). Since the drug release was unaffected by conditions mimicking the Beagle dog destructive forces, it was probably largely independent of matrix erosion. Therefore, bilayer F_{HE6005} and bilayer A1

were selected as the optimised formulations. The details of the final optimised bilayer tablet formulations can be seen in Table 4-14.

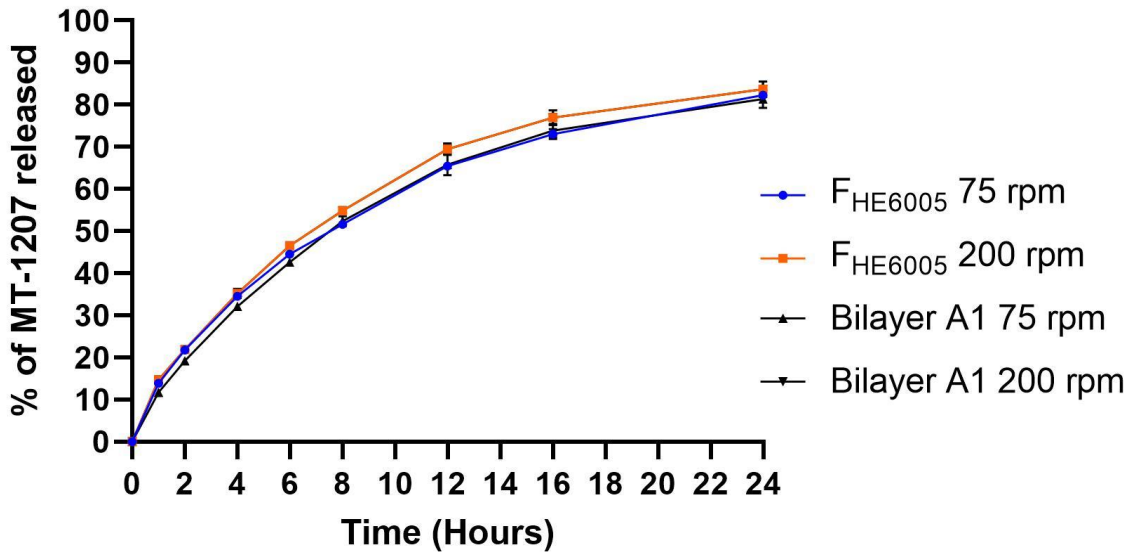


Figure 4-11: *In vitro release profiles of MT-1207 from bilayer F_{HE6005} and bilayer A1 tablets at paddle rotation speeds of 75 rpm and 200 rpm (n = 3 tablets). Results are presented as mean ± standard deviation.*

Table 4-14: *The optimised bilayer tablet formulation (F_{HE6005} and A1) details.*

Gastroretentive layer		
Components	Amount (mg)	
PEO 8M	380	
Spray-dried lactose	47	
Kollidon® SR	228	
HPMC K100M	16.2	
Colloidal silicon dioxide	1.5	
Magnesium stearate	1.5	
Total layer weight (mg)	**674.2**	
Drug layer	**F_{HE6005}**	**A1**
Components	Amount (mg)	Amount (mg)
MT-1207 Hydrochloride	30	30
Alpha-D-lactose monohydrate	65	99
Polyvinylpyrrolidone K30	20	20
HPMC K15M	60	70
Ethylcellulose 10 cps	5	-
Iron oxide	1	1
Colloidal silicon dioxide	6	6
Magnesium stearate	0.5	0.5
Total layer weight	**187.5**	**226.5**
Total tablet weight	**861.7**	**900.7**

4.3.9 Kinetics and mechanism of drug release from bilayer F_{HE6005} and bilayer A1 tablets

The release profiles of the bilayer F_{HE6005} and bilayer A1 tablets were plotted against different models to elucidate the kinetics of drug release from each formulation, while the Korsmeyer-Peppas model was used to obtain information on the potential mechanism of drug release. The release data that were plotted against the different models were those up to 60 % of the respective release curves (215, 218).

The release data of formulations bilayer F_{HE6005} and bilayer A1 were plotted in the first-order, zero-order, Higuchi, and Hixson-Crowell models. The highest R^2 value recorded was used to determine the best fit for each of the release profiles. The drug release from bilayer F_{HE6005} tablets followed a combination of first-order (R^2 = 0.9989) and Higuchi (R^2 = 0.9963) kinetics. When the data were plotted against the Korsmeyer-Peppas model, the *n*

value (calculated from the slope of the curve) was 0.66 (Table 4-15) which, despite the complex geometry of the drug layer and the tablets, most likely indicated a non-Fickian diffusion mechanism of release of MT-1207 from F_{HE6005}. Therefore, it can be proposed that the kinetics of drug release from bilayer F_{HE6005} is best described as the release of MT-1207 from an intact matrix the rate of which declined over time due to a reduction in the drug concentration within the tablet matrix. The mechanism of the release of MT-1207 from bilayer F_{HE6005} tablets hence resembles a combination of drug diffusion and polymer matrix erosion. The same assumptions on the kinetics and mechanism of drug release were also followed for the kinetic analysis of drug release from bilayer A1 tablets (Table 4-16). However, there was a statistically significant difference in the *n* values recorded for the different formulations when the data were plotted against the Korsmeyer-Peppas model (*t*-test, $p < 0.01$). Therefore, matrix erosion was more significant for the release of MT-1207 from bilayer A1 tablets than for its release from bilayer F_{HE6005} ones. The small percentage of ethylcellulose in F_{HE6005} may have contributed towards a more intact drug layer during dissolution, an attribute that was desirable since it could potentially further ensure the integrity of the drug layer *in vivo* and, consequently, a robust controlled drug release.

Table 4-15: *Bilayer F_{HE6005} kinetic analysis results.*

Models	Kinetic constant	Coefficient of determination (R^2)
First-order	0.0914	0.9989
Zero-order	0.0041	0.9729
Higuchi	22.4790	0.9963
Hixson-Crowell	0.1321	0.9593
Korsmeyer-Peppas		
Kinetic constant	Coefficient of determination (R^2)	Exponent (*n*)
1.0133	0.9992	0.66

Table 4-16: *Bilayer A1 kinetic analysis results.*

Models	Kinetic constant	Coefficient of determination (R^2)
First-order	0.0877	0.9997
Zero-order	0.0040	0.9825
Higuchi	22.3140	0.9971
Hixson-Crowell	0.1389	0.9569
Korsmeyer-Peppas		
Kinetic constant	Coefficient of determination (R^2)	Exponent (*n*)
0.0560	0.9999	0.72

4.4 Conclusions

The aim of the present study was to optimise the MT-1207 sustained-release formulation (A1) prepared in the study of the previous chapter. As part of the formulation optimisation, gastroretentive bilayer tablets were developed. The gastroretentive layer consisted of a combination of hydrophilic and hydrophobic polymers which had not been employed for gastric retention purposes before. The gastroretentive layer optimisation was performed through preliminary experiments, followed by a factorial experiment that demonstrated the factors significantly affecting the *in vitro* buoyancy behaviour of the tablets. Based on the data, an optimised gastroretentive layer was selected. The novel gastroretentive layer was prepared via a simple direct compression process and provided an immediate and robust tablet buoyancy that lasted longer than 24 hours in FaSSGF pH 1.6 *in vitro*. As part of the drug layer optimisation, ethylcellulose was incorporated as an additional release retardant. The optimised ethylcellulose-containing bilayer formulation, as well as bilayer A1 tablets, gave a robust 24-hour sustained release of MT-1207 which demonstrated the significance of the gastroretentive layer in achieving a 24-hour sustained release of the API *in vitro*, due to the much smaller surface area of the drug layer exposed to the dissolution medium. Furthermore, the fact that the floating lag time and total floating time values recorded for

bilayer tablets with different drug layers were similar demonstrated the versatility of the novel gastroretentive layer and its potential to maintain a robust tablet buoyancy that would not be affected by the drug layer. This finding, alongside the optimised gastroretentive layer *in vitro* buoyancy properties, demonstrated that the combination of hydrophilic and hydrophobic polymers could have promising gastroretentive tablet applications. Finally, the *in vitro* buoyancy testing of the optimised ethylcellulose-containing bilayer tablets in media of different pH values demonstrated the positive effect of increasing pH on the buoyancy of PEO-based non-effervescent gastroretentive formulations. Based on these results, PEO-based formulations should potentially be administered orally after a meal to encounter the weakly acidic to neutral pH of the stomach contents during the fed state.

The two optimised bilayer formulations from the present study (bilayer F_{HE6005}, bilayer A1) were forwarded to an *in vivo* study in Beagle dogs which was conducted during fed state conditions.

5 Chapter 5: *In Vivo* Pharmacokinetic Study of the Optimised Gastroretentive Bilayer Tablet Formulations in Beagle Dogs

Acknowledgement of research work done by collaborators

A special thanks to Professor Xijin Chen (School of Basic Medicine and Clinical Pharmacy, China Pharmaceutical University) for his help with the *in vivo* study on the pharmacokinetics of MT-1207.

5.1 Introduction

Beagle dogs are commonly selected to assess the *in vivo* performance of oral formulations, including gastroretentive systems (95, 106, 108, 114, 142, 268, 269).

5.1.1 Experimental aim

In Chapter 4, two promising non-effervescent gastroretentive bilayer tablet formulations of MT-1207 (bilayer F_{HE6005} and bilayer A1) were prepared and characterised in terms of their physicochemical, *in vitro* buoyancy and *in vitro* release properties.

In this study, the *in vivo* performance of these gastroretentive formulations was tested in Beagle dogs.

5.2 Methodology

An *in vivo* animal study was conducted in Beagle dogs with a body weight of (10 ± 2) kg) for MT-1207 30 mg gastroretentive bilayer F_{HE6005} and bilayer A1 tablets, and 10 mg immediate-release tablets. The study was conducted by researchers in China Pharmaceutical University (Nanjing, China) in collaboration with the author. It complied with the principles of Laboratory Animal Care and was approved by China Pharmaceutical University Animal Management and Ethics Committee.

Four healthy male Beagle dogs provided by Nanjing Chai Men Biotechnology Co., Ltd. (Nanjing, China) were used. Each time, the Beagle dogs were fasted overnight, and blank blood was collected shortly before the study. The Beagle dogs were then given free access to a meal and, after 30 minutes, one gastroretentive bilayer tablet or three immediate-release tablets were administered orally. 1.5 mL of venous blood were taken at 0.25 h, 0.5 h, 1 h, 2 h, 4 h, 6 h, 8 h, 12 h, 24 h and 32 h after administration and centrifuged in a tube with heparin. A one-week washout period was applied between the different dosing regimens. In all cases, each sample was placed in a test tube containing heparin, centrifuged and the plasma was separated and stored at -70 °C. The concentration of MT-1207 in plasma samples was determined using UPLC-MS/MS as detailed in Chapter 2.

5.3 Results and Discussion

The gastroretentive bilayer F_{HE6005} and bilayer A1 tablets were administered to four Beagle dogs after a meal. This choice was made as gastric pH is higher during the stomach fed state, which could potentially promote the gastric retention of the formulations, based on the SEM and viscosity findings from the *in vitro* buoyancy testing in media of different pH. Furthermore, the presence of food in the stomach disrupts the MMC and housekeeper waves, thereby leading to a prolonged gastric residence time of the stomach contents (103, 131, 140, 172).

Figure 5-1 illustrates the pharmacokinetic profiles of MT-1207 in the dog plasma after oral administration of one MT-1207 30 mg bilayer F_{HE6005} tablet, one MT-1207 30 mg bilayer A1 tablet, and three MT-1207 10 mg immediate-release tablets. The pharmacokinetic parameters recorded on the respective dosing regimens in Beagle dogs can be seen in Table 5-1. Sustained-release pharmacokinetic profiles of MT-1207 in dog plasma were recorded after oral administration of bilayer F_{HE6005} and bilayer A1 tablets. There was a statistically significant difference in the $t_{1/2}$ (one-way ANOVA, $p < 0.05$) and T_{max} values (one-way

ANOVA, $p < 0.01$) recorded between the different dosing regimens with pairwise comparisons demonstrating significant differences between each of the gastroretentive bilayer dosing regimens and the immediate-release one ($t_{1/2}$: *post hoc* Bonferroni, $p < 0.05$, T_{max}: *post hoc* Bonferroni, $p < 0.01$). There was no statistically significant difference between the $t_{1/2}$ values reported for the gastroretentive dosing regimens (*post hoc* Bonferroni, $p > 0.05$). Furthermore, there was no statistically significant difference in the C_{max} values recorded between the different dosing regimens (one-way ANOVA, $p > 0.05$). This could be attributed to the fact that, during fed state conditions, gastric emptying rates tend to be lower, compared to the fasted state (103, 140, 270, 271). Consequently, the amount of MT-1207 released in the stomach during the fed state was probably emptied gradually and at a slower rate, thereby resulting in smaller peak plasma concentration values. Additionally, the abovementioned parameter values were not statistically different to those recorded after oral administration of A1 tablets in our previous study (one-way ANOVA, $p > 0.05$) (255). With regard to clearance, there was no statistically significant difference between the values recorded for the different dosing regimens in the present pharmacokinetic study (one-way ANOVA $p > 0.05$).

Table 5-1: *Pharmacokinetic parameters of MT-1207 after oral administration of a single MT-1207 30 mg gastroretentive bilayer F_{HE6005} tablet (F_{HE6005} o.d.), a single MT-1207 30 mg gastroretentive bilayer A1 tablet (Bilayer A1 o.d.), and three MT-1207 10 mg immediate-release tablets administered at the same time (3 × 10 mg IR o.d.) to Beagle dogs (n = 4).*

Dosing Regimen	$t_{1/2}$ (h)	T_{max} (h)	C_{max} (ng/mL)	$AUC_{0\text{-}24h}$ (h*ng/mL)	$AUC_{0\text{-}\infty}$ (h*ng/mL)	V_d (L/kg)	CL (L/h/kg)	MRT (h)
F_{HE6005} o.d.	5.10±1.37	6.00±1.63	22.29±11.50	226.6±97.9	232.7±100.4	78.1±23.2	11.4±5.4	9.23±1.05
Bilayer A1 o.d.	4.76±1.13	6.50±1.00	31.74±18.92	288.9±167.5	295.1±169.7	60.6±19.1	9.7±4.9	8.71±0.32
3 × 10 mg IR o.d.	2.47±0.09	2.25±1.26	49.72±33.70	283.6±183.2	295.1±189.9	78.9±21.2	11.6±8.9	5.36±1.01

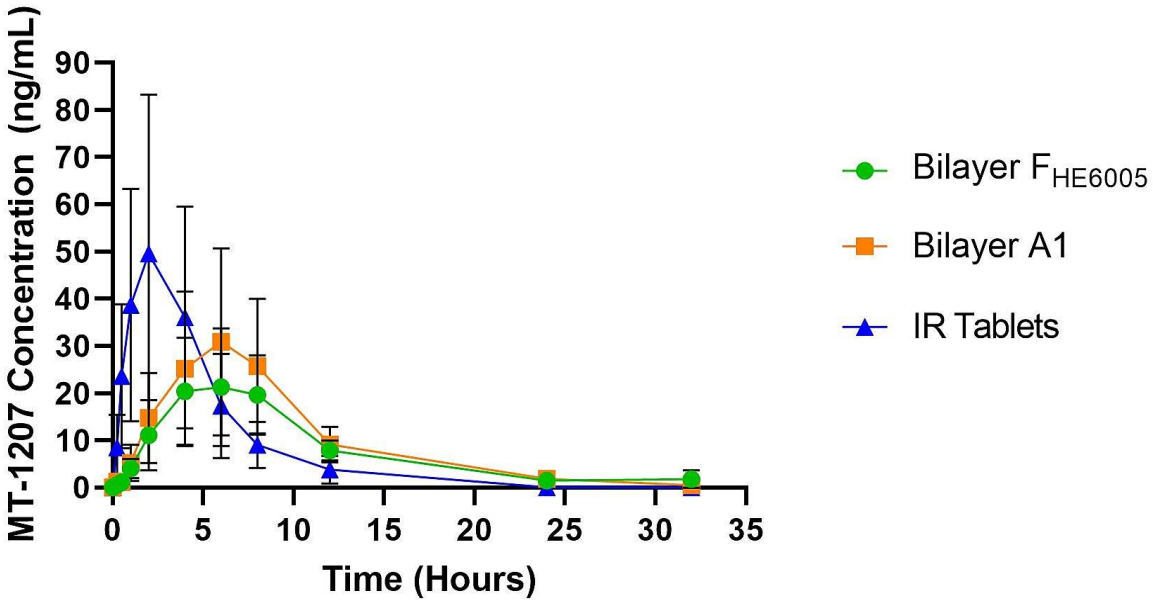


Figure 5-1: *Plasma concentration of MT-1207 in Beagle dogs after oral administration of bilayer F_{HE6005} tablet o.d., bilayer A1 tablet o.d., and 3 × 10 mg IR tablet o.d. (n = 4).*

The bioequivalence between the gastroretentive and immediate-release tablets was investigated by calculating the $AUC_{0\text{-}24h}$ ratio of each. The ratio values calculated for the bilayer F_{HE6005} and bilayer A1 formulations were 92.31 ± 29.33 % and 112.35 ± 35.20 %, respectively. These values fell within the 80.00 – 125.00 % range outlined in the EMA guidelines for the $AUC_{0\text{-}t}$ ratios that allows for bioequivalence to be established between the test and reference products (239). This is an indication that there can be bioequivalence between the gastroretentive formulations and the immediate-release tablets, and that MT-1207 was fully released from the former. However, the relatively high standard deviations linked to the $AUC_{0\text{-}24h}$ ratio values need to be considered. This variation in the AUC values between the different Beagle dogs could be attributed to the built-in subject variability of this animal model. Previous studies have demonstrated considerable inter- and intra-animal variations in the gastric pH of different Beagle dogs (272, 273). Such variations in the present study could potentially have noticeable effects on the solubility of MT-1207 in the stomach contents, thereby introducing inter-subject variability in its solubilisation, release, and consequent absorption and bioavailability.

The distribution of MT-1207 in the Beagle dog body was reflected by the V_d and MRT parameters. V_d indicated the extent of distribution of MT-1207 in the peripheral tissues, while MRT indicated the average time that the drug resided in the body. There was no statistically significant difference in the V_d values recorded for the different dosing regimens (one-way ANOVA, $p > 0.05$). All V_d values were sufficiently high to indicate extensive distribution of the API in the peripheral tissues. Additionally, there was a statistically significant difference between the MRT values of the three different dosing regimens (one-way ANOVA, $p < 0.001$) with pairwise comparisons demonstrating statistically significant differences between each of the gastroretentive dosing regimens and the immediate-release one (*post hoc* Bonferroni, $p < 0.001$). This indicates that the time during which the drug resided in the body

and, therefore, potentially provided antihypertensive action was significantly prolonged when MT-1207 was administered in the form of gastroretentive tablets, instead of immediate-release tablets. Furthermore, the MRT values of MT-1207 after administration of the gastroretentive formulations were significantly longer than the MRT value recorded after administration of single-layer A1 tablets in our previous study (one-way ANOVA, $p < 0.001$; *post hoc* Bonferroni, $p < 0.05$ for pairwise comparisons) (255).

This pharmacokinetic study demonstrated the ability of the gastroretentive formulations to provide a sustained release of MT-1207 *in vivo*, as indicated by the significantly prolonged $t_{1/2}$, T_{max} and MRT values, compared to the respective ones recorded after administration of the immediate-release tablets (145). Furthermore, the gastroretentive formulations were able to fully release the API within 24 hours. These findings, alongside the significant prolongation of MRT, compared to single-layer A1 tablets, indicate the significant role of the gastroretentive layer in retarding the release of MT-1207, potentially due to the reduced surface area of the drug layer that was exposed to the stomach contents, and prolonging the residence of the drug *in vivo*. Furthermore, the gastroretentive layer potentially ensured robust gastric retention that was long enough to provide a 24-hour complete release and absorption of MT-1207 in the upper part of the GIT. *In vivo* monitoring of the formulations could give a deeper insight into the ability of the gastroretentive formulations to remain in the Beagle dog stomach over 24 hours (140, 246), although, the pharmacokinetic study results provided promising indication towards this occurring. Additionally, the presence of ethylcellulose had only a minor effect on drug release *in vivo* which was in alignment with the *in vitro* release testing findings.

Another important factor that needs to be considered is the significantly higher average MT-1207 $t_{1/2}$ value of 7.28 – 7.38 hours recorded in humans after administration of 20 – 40 mg of the drug (206). Since MT-1207 is mainly biotransformed via S-methylation in the

liver, this inter-species discrepancy in the $t_{1/2}$ of the drug could be due to the higher hepatic metabolism of Beagle dogs, compared to humans (241). Therefore, it can be concluded that both gastroretentive bilayer F_{HE6005} and bilayer A1 formulations are promising for the once-a-day oral delivery of MT-1207.

5.4 Conclusions

In this chapter, a pharmacokinetic study was conducted in Beagle dogs for the gastroretentive bilayer F_{HE6005} and bilayer A1 tablet formulations that were selected based on the *in vitro* testing results reported in Chapter 4 of the thesis. The gastroretentive formulations provided a complete 24-hour sustained release of MT-1207 *in vivo* that could be inferred by its pharmacokinetic profile, the $AUC_{0\text{-}24h}$ values and the significantly prolonged $t_{1/2}$, T_{max}, and MRT values, compared to those recorded after administration of MT-1207 immediate-release tablets. Furthermore, the novel gastroretentive layer indicated robust 24-hour gastric retention capability *in vivo,* alongside its contribution to the sustained release of MT-1207 provided by the gastroretentive formulations. Even though its gastric retention capability should further be assessed in an *in vivo* monitoring study, this gastroretentive layer could have promising gastroretentive applications for the once-a-day delivery of different drugs in the form of either bilayer or single-layer controlled-release tablets. The gastroretentive bilayer F_{HE6005} and bilayer A1 formulations were deemed promising for the once-a-day oral delivery of MT-1207 and will, therefore, be forwarded to clinical development.

6 Chapter 6: General Conclusions

The aim of this thesis was the development of promising sustained-release tablet formulations for the once-a-day oral delivery of the novel antihypertensive drug MT-1207.

Initially, single-layer sustained-release HPMC matrix tablets were prepared and characterised *in vitro*. Based on the *in vitro* testing, a sustained-release tablet formulation (A1) containing 30 mg of MT-1207 was selected to be forwarded to a pharmacokinetic study in Beagle dogs. Even though the single-layer A1 tablets provided a sustained release of MT-1207 *in vivo*, it was not certain whether the plasma concentration of MT-1207 was maintained within therapeutic levels over 24 hours. Therefore, further formulation optimisation was conducted since the tablets released the API much faster *in vivo* than *in vitro*.

As part of the further formulation optimisation, gastroretentive bilayer tablets were prepared. The gastroretentive layer contained a novel combination of PEO and Kollidon® SR which, to the best of our knowledge, has not been reported before as a successful gastroretentive tablet application, even though the materials have been used for this purpose in previous reports. The gastroretentive layer optimisation was conducted via preliminary experiments and a subsequent factorial experiment. The optimised gastroretentive layer was easy to prepare using direct compression and ensured an immediate *in vitro* buoyancy of the bilayer tablets that lasted longer than 24 hours in FaSSGF pH 1.6 and was not affected by modifications in the drug layer. However, the floating capability of the bilayer tablets was affected by the pH of the medium in which they were immersed, despite them being non-effervescent. To the best of our knowledge, the potential pH effect on the total floating time of non-effervescent PEO-based gastroretentive tablets has not been reported in the literature. SEM imaging and viscosity testing of the gastroretentive layer of the tablets and the different

media in which they were immersed, respectively, indicated statistically significant variations in the total floating time of the tablets between the different media. This was linked to differences in the rate and extent of PEO degradation that mainly took place in strongly acidic conditions at temperatures above 36 °C. With regards to the drug layer, ethylcellulose was incorporated as an additional release retardant to provide a more sustained release of MT-1207 from the bilayer tablets, compared to single-layer A1 tablets. The *in vitro* testing results of the different bilayer ethylcellulose-containing and bilayer A1 formulations demonstrated that the significant factor affecting the release of MT-1207 was the presence of the gastroretentive layer in the formulation. The presence and/or content of ethylcellulose did not have a statistically significant effect on the *in vitro* drug release. The gastroretentive bilayer F_{HE6005} and bilayer A1 formulations provided a 24-hour sustained release of MT-1207 *in vitro* in 0.1 M acetate pH 4.0, in contrast to single-layer A1 tablets which released the API within 12 hours with a release profile that was closer to *in vivo* data of the respective pharmacokinetic study. The two gastroretentive formulations were, therefore, forwarded to a final pharmacokinetic study in Beagle dogs. Based on the findings reported in regard to the differences in the total floating time of the tablets in media of different pH, the tablets were administered in Beagle dogs orally after a meal, since fed conditions would ensure the exposure of the gastroretentive tablets to relatively high gastric pH values. The results demonstrated a complete, 24-hour sustained release of MT-1207 from the gastroretentive bilayer tablet formulations. Furthermore, the MRT values recorded during the gastroretentive tablet dosing regimens were significantly prolonged, compared to those of the single-layer A1 tablet dosing regimen in Chapter 3 of the thesis. This confirmed the superior ability of the gastroretentive formulations to retard the release of MT-1207 and prolong its residence *in vivo*, conferred by the presence of the gastroretentive layer in the formulation. The presence of the gastroretentive layer also ensured a robust retention of the tablets in the stomach that

was potentially long enough to ensure a complete 24-hour sustained release of MT-1207 in the upper part of the GIT. The *in vivo* buoyancy capability of the novel gastroretentive layer was, therefore, demonstrated. Overall, both gastroretentive formulations demonstrated promising capability for the once-a-day oral delivery of MT-1207.

7 Chapter 7: Limitations and Future Work

7.1 Limitations

The work that was conducted and reported in the present thesis comes with certain limitations.

Formulation development and manufacturing took place at a lab scale. Small amounts of API and excipients were each time used to produce a small number of tablets. The optimised MT-1207 gastroretentive tablets that were developed in the present study were not manufactured at an industrial scale. It is not yet known whether the lab-scale manufacturing process can be reproduced at a large scale. The tablets that will be forwarded to clinical development must be produced at an industrial scale reproducibly. Therefore, this is a crucial prerequisite for the continuation of their development.

The MT-1207 gastroretentive bilayer tablets that were selected as optimised, based on the *in vitro* testing results, were further assessed in terms of their *in vivo* performance in Beagle dogs. While certain inferences could be made regarding the ability of the tablets to remain in the Beagle dog stomach and release MT-1207 over 24 hours, and what this could mean for potential clinical application, there are certain limitations that need to be considered. To get a deeper insight into the gastric retention capability of the tablets, *in vivo* monitoring studies should be conducted in Beagle dogs and/or humans (140, 246). Furthermore, there are differences in the GIT environment between Beagle dogs and humans. More specifically, the gastric pH is higher in Beagle dogs than in humans (256, 272, 273). Additionally, the gastric mechanical destructive force of Beagle dogs has been estimated to be almost two times higher than that of humans (247, 248). These differences could cause inter-species discrepancies in the rate and/or extent of the release of MT-1207 from the tablets, linked to solubility differences (for gastric pH) and/or differences in the forces

applied to the tablets. Furthermore, hepatic metabolism tends to be higher in Beagle dogs than in humans (241). This could contribute to differences in the bioavailability and/or rate of elimination of MT-1207 since it is mainly biotransformed via S-methylation. Such a discrepancy has already been demonstrated for the $t_{1/2}$ of MT-1207 since its half-life in humans has been recorded to be significantly higher than that in Beagle dogs (208).

7.2 Future Work

In the present thesis, two MT-1207 gastroretentive bilayer formulations were prepared and characterised *in vitro* and *in vivo*. These formulations have been deemed promising for further development. A scale-up procedure should be initiated, and a large-scale manufacturing process should be developed and optimised, so that the tablets may be manufactured at an industrial scale reproducibly. Afterwards, this process can be used to prepare gastroretentive bilayer tablets that will be forwarded to human clinical trials.

Appendix

This section includes supplementary tables and figures containing results of the HPLC and dissolution method validation conducted in Chapters 3 and 4 of the thesis.

Chapter 3 HPLC and dissolution method validation

- **Linearity**

Table A-1: Concentration and peak area values of MT-1207 calibration curve in 0.1 M phosphate pH 6.8 with 0.2% w/v SDS:methanol 95:5 (% v/v) replicate 1.

Concentration (mg/mL)	Peak Area (mAU*min)
0.001	1.5872
0.002	2.6935
0.005	6.0083
0.007	9.0453
0.01	12.8738
0.02	25.9631
0.05	64.9897

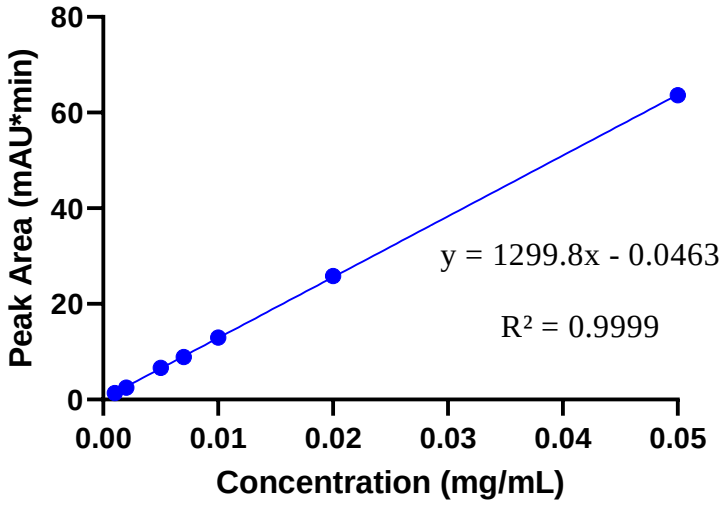


Figure A-1: *MT-1207 calibration curve in 0.1 M phosphate pH 6.8 with 0.2% w/v SDS:methanol 95:5 (%v/v) replicate 1 (Peak Area vs Concentration).*

Table A-2: *Concentration and peak area values of MT-1207 calibration curve in 0.1 M phosphate pH 6.8 with 0.2% w/v SDS:methanol 95:5 (% v/v) replicate 2.*

Concentration (mg/mL)	Peak Area (mAU*min)
0.001	1.4479
0.002	2.5809
0.005	6.1665
0.007	9.4091
0.01	13.4194
0.02	26.3017
0.05	65.5137

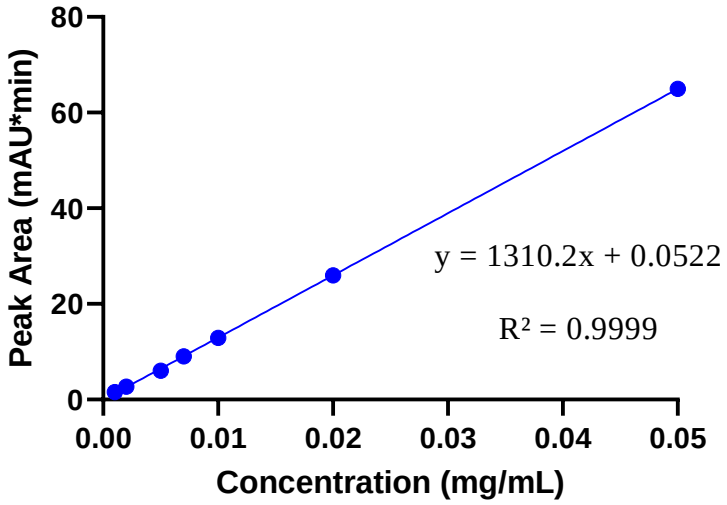


Figure A-2: *MT-1207 calibration curve in 0.1 M phosphate pH 6.8 with 0.2% w/v SDS:methanol 95:5 (% v/v) replicate 2 (Peak Area vs Concentration).*

Table A-3: *Concentration and peak area values of MT-1207 calibration curve in 0.1 M phosphate pH 6.8 with 0.2% w/v SDS:methanol 95:5 (% v/v) replicate 3.*

Concentration (mg/mL)	Peak Area (mAU*min)
0.001	1.3857
0.002	2.5248
0.005	6.6079
0.007	8.9321
0.01	12.9395
0.02	25.8331
0.05	63.6373

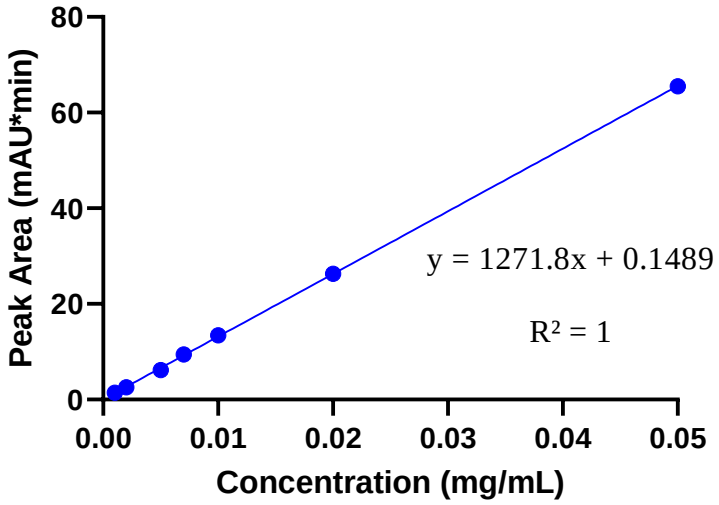


Figure A-3: *MT-1207 calibration curve in 0.1 M phosphate pH 6.8 with 0.2% w/v SDS:methanol 95:5 (% v/v) replicate 3 (Peak Area vs Concentration).*

- **LOD and LOQ determination**

Table A-4: *Data of the calibration curve that occurred from calculating the mean of the peak area values from the linearity calibration curves for the respective concentration points (n = 3). Peak area results are presented as mean ± standard deviation.*

Concentration (mg/mL)	Peak Area (mAU*min) (Mean ± Standard Deviation)
0.001	1.4736 ± 0.1032
0.002	2.5997 ± 0.0859
0.005	6.2609 ± 0.3107
0.007	9.1288 ± 0.2492
0.01	13.0776 ± 0.2979
0.02	26.0326 ± 0.2419
0.05	64.7136 ± 0.9682

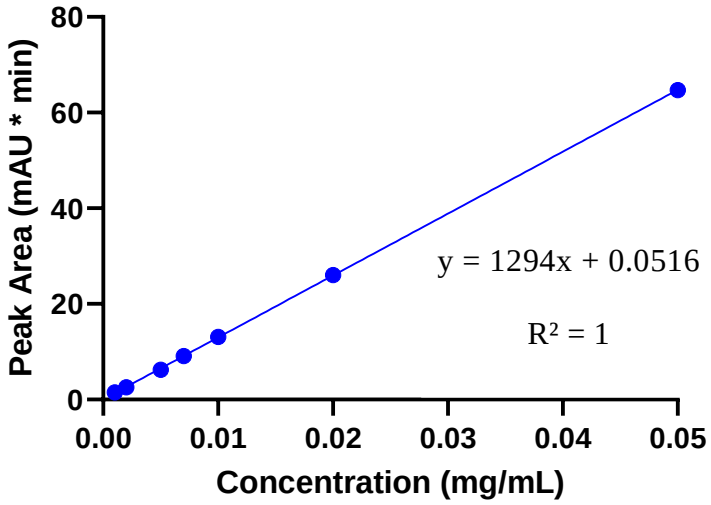


Figure A-4: *MT-1207 calibration curve in 0.1 M phosphate pH 6.8 with 0.2% w/v SDS:methanol 95:5 (% v/v) that was used for the LOD and LOQ determination (Peak Area vs Concentration). Peak area results are presented as mean ± standard deviation.*

- **Specificity**

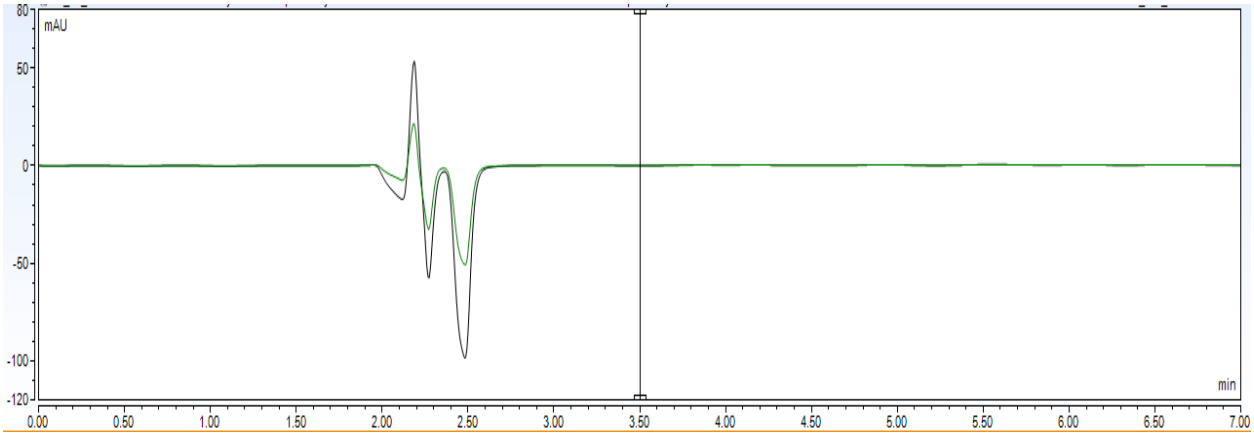


Figure A-5: *Chromatogram of specificity sample (n = 3).*

- **Accuracy, intra-day and inter-day precision**

Table A-5: *MT-1207 dissolution method accuracy and intra-day precision validation results at 20 %, 50 %, 80 %, 100 % and 120 % concentration level of MT-1207.*

Sample Name	Peak Area (mAU*min)	Concentration (mg/mL)	Initial Concentration (mg/mL)	Accuracy (%)	**Mean Accuracy (%)**	**Standard Deviation**	**% RSD**
Accuracy 20 % Rep 1	6.5848	0.00498	0.00443	112.5	**111.7**	**0.8**	**0.8**
Accuracy 20 % Rep 2	6.5456	0.00495	0.00443	111.8			
Accuracy 20 % Rep 3	6.4871	0.00491	0.00443	110.8			
Accuracy 50 % Rep 1	15.6082	0.01189	0.01105	107.6	**107.5**	**2.0**	**1.9**
Accuracy 50 % Rep 2	15.8952	0.01210	0.01105	109.5			
Accuracy 50 % Rep 3	15.3055	0.01165	0.01105	105.5			
Accuracy 80 % Rep 1	24.7493	0.01887	0.01762	107.1	**106.1**	**1.2**	**1.1**
Accuracy 80 % Rep 2	24.5957	0.01875	0.01762	106.4			
Accuracy 80 % Rep 3	24.2210	0.01846	0.01762	104.8			
Accuracy 100 % Rep 1	32.4177	0.02469	0.02198	112.3	**108.2**	**3.6**	**3.3**
Accuracy 100 % Rep 2	30.4709	0.02321	0.02198	105.6			
Accuracy 100 % Rep 3	30.7957	0.02346	0.02198	106.7			
Accuracy 120 % Rep 1	38.7459	0.02955	0.02632	112.3	**111.6**	**1.2**	**1.1**
Accuracy 120 % Rep 2	38.7953	0.02959	0.02632	112.4			
Accuracy 120 % Rep 3	38.0285	0.02900	0.02632	110.2			

Table A-6: *MT-1207 dissolution method inter-day precision validation results at 20 %, 50 %, 80 %, 100 % and 120 % concentration level of MT-1207.*

Sample Name	Accuracy (%)	**Mean Accuracy (%)**	**Standard Deviation**	**% RSD**
Precision 20 % Rep 1	109.0	**109.8**	**2.4**	**2.2**
Precision 20 % Rep 2	107.9			
Precision 20 % Rep 3	112.5			
Precision 50 % Rep 1	112.8	**110.9**	**4.8**	**4.3**
Precision 50 % Rep 2	114.6			
Precision 50 % Rep 3	105.5			
Precision 80 % Rep 1	112.2	**110.5**	**5.2**	**4.7**
Precision 80 % Rep 2	114.7			
Precision 80 % Rep 3	104.7			
Precision 100 % Rep 1	107.4	**108.3**	**2.7**	**2.4**
Precision 100 % Rep 2	106.1			
Precision 100 % Rep 3	111.3			
Precision 120 % Rep 1	111.1	**111.1**	**0.8**	**0.8**
Precision 120 % Rep 2	111.9			
Precision 120 % Rep 3	110.2			

- **Linearity**

Table A-7: *Concentration and peak area values of MT-1207 calibration curve in 0.1 M acetate buffer pH 4.0 replicate 1.*

Concentration (mg/mL)	Peak Area (mAU*min)
0.001	1.4017
0.002	2.7218
0.005	6.7316
0.007	9.0305
0.01	13.4500
0.02	27.2400
0.05	68.3314
0.07	94.9500
0.1	135.1867

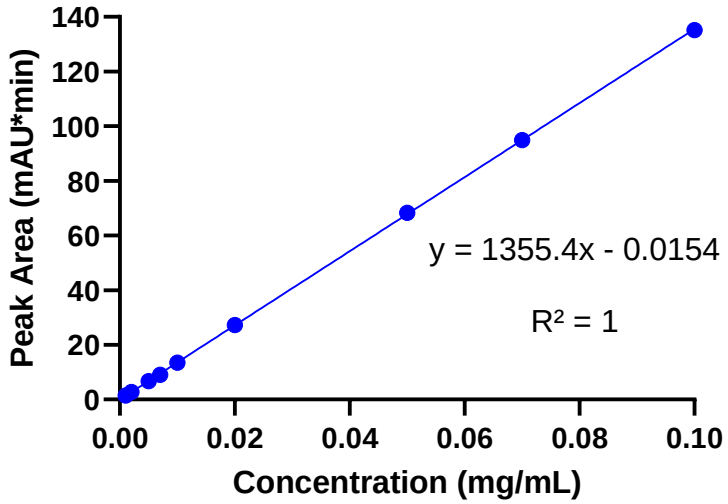


Figure A-6: *MT-1207 calibration curve in 0.1 M acetate buffer pH 4.0 replicate 1 (Peak Area vs Concentration).*

Table A-8: *Concentration and peak area values of MT-1207 calibration curve in 0.1 M acetate buffer pH 4.0 replicate 2.*

Concentration (mg/mL)	Peak Area (mAU*min)
0.001	1.3467
0.002	2.7383
0.005	6.6933
0.007	9.2500
0.01	13.4134
0.02	26.3217
0.05	67.2383
0.07	94.3816
0.1	134.3150

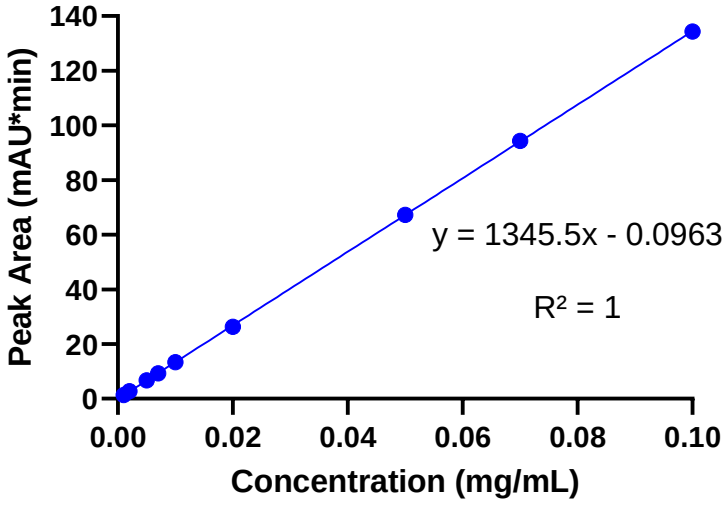


Figure A-7: *MT-1207 calibration curve in 0.1 M acetate buffer pH 4.0 replicate 2 (Peak Area vs Concentration).*

Table A-9: *Concentration and peak area values of MT-1207 calibration curve in 0.1 M acetate buffer pH 4.0 replicate 3.*

Concentration (mg/mL)	Peak Area (mAU*min)
0.001	1.3116
0.002	2.6164
0.005	6.4967
0.007	9.2950
0.01	13.2433
0.02	26.4300
0.05	67.0950
0.07	93.6051
0.1	132.7950

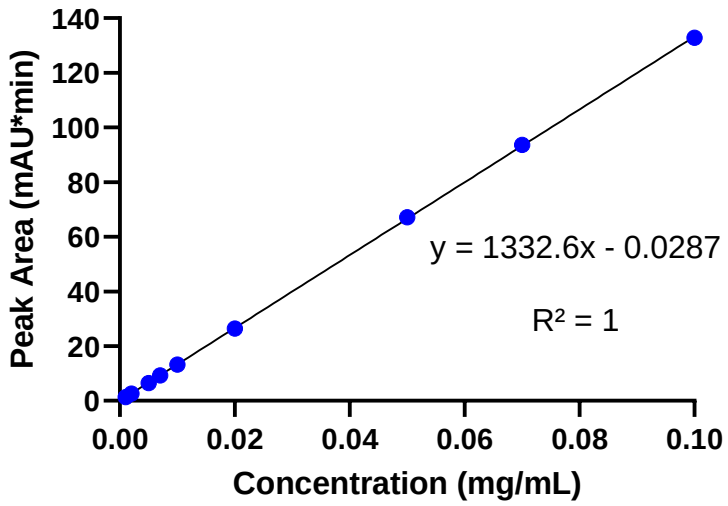


Figure A-8: *MT-1207 calibration curve in 0.1 M acetate buffer pH 4.0 replicate 3 (Peak Area vs Concentration).*

- **LOD and LOQ determination**

Table A-10: *Data of the calibration curve that occurred from calculating the mean of the peak area values from the linearity calibration curves for the respective concentration points (n = 3). Peak area results are presented as mean ± standard deviation.*

Concentration (mg/mL)	Peak Area (mAU*min)
0.001	1.3533 ± 0.0454
0.002	2.6922 ± 0.0660
0.005	6.6406 ± 0.1261
0.007	9.1918 ± 0.1415
0.01	13.3689 ± 0.1103
0.02	26.6639 ± 0.5019
0.05	67.5550 ± 0.6764
0.07	94.3122 ± 0.6752
0.1	134.0989 ± 1.2104

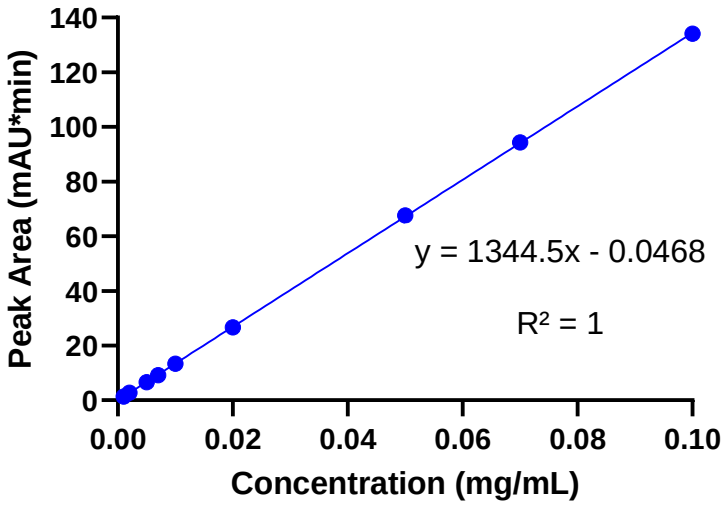


Figure A-9: *MT-1207 calibration curve in 0.1 M acetate buffer pH 4.0 that was used for the LOD and LOQ determination (Peak Area vs Concentration). Peak area results are presented as mean ± standard deviation.*

- **Specificity**

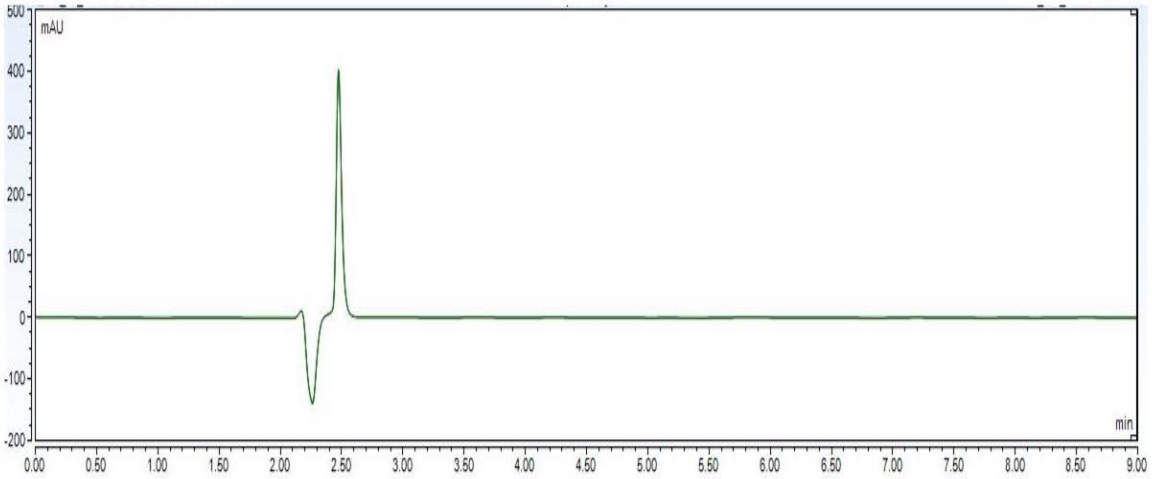


Figure A-10: *Chromatogram of specificity sample (n = 3).*

- **Accuracy, intra-day and inter-day precision**

Table A-11: *MT-1207 dissolution method accuracy and intra-day precision validation results at 20 %, 50 %, 80 %, 100 % and 120 % concentration level of MT-1207 (n = 3).*

	Peak Area (mAU*min)	Concentration (mg/mL)	Initial Concentration (mg/mL)	Accuracy (%)	**Mean Accuracy (%)**	**Standard Deviation**	**% RSD**
Accuracy 20 % R1	15.4103	0.01239	0.01200	103.2	**100.1**	**4.3**	**4.3**
Accuracy 20 % R2	15.2197	0.01224	0.01200	102.0			
Accuracy 20 % R3	14.1793	0.01142	0.01200	95.2			
Accuracy 50 % R1	40.4233	0.03204	0.03000	106.8	**101.9**	**7.6**	**7.4**
Accuracy 50 % R2	40.0211	0.03172	0.03000	105.7			
Accuracy 50 % R3	35.2270	0.02795	0.03000	93.2			
Accuracy 80 % R1	64.6137	0.05104	0.04800	106.3	**106.2**	**0.3**	**0.3**
Accuracy 80 % R2	64.2838	0.05078	0.04800	105.8			
Accuracy 80 % R3	64.6688	0.05109	0.04800	106.4			
Accuracy 100 % R1	76.6211	0.06048	0.06000	100.8	**103.7**	**2.7**	**2.6**
Accuracy 100 % R2	79.2104	0.06251	0.06000	104.2			
Accuracy 100 % R3	80.6419	0.06364	0.06000	106.1			
Accuracy 120 % R1	92.6152	0.07304	0.07200	101.4	**101.5**	**2.7**	**2.7**
Accuracy 120 % R2	95.2354	0.07510	0.07200	104.3			
Accuracy 120 % R3	90.2154	0.07116	0.07200	98.8			

Table A-12: *MT-1207 dissolution method inter-day precision validation results at 20 %, 50 %, 80 %, 100 % and 120 % concentration level of MT-1207 (n = 3).*

	Accuracy (%)	**Mean Accuracy (%)**	**Standard Deviation**	**% RSD**
20 % Rep 1	100.1	**99.1**	**1.6**	**1.6**
20 % Rep 2	100.0			
20 % Rep 3	97.3			
50 % Rep 1	101.8	**99.6**	**2.0**	**2.0**
50 % Rep 2	98.0			
50 % Rep 3	99.0			
80 % Rep 1	99.2	**103.9**	**4.4**	**4.3**
80 % Rep 2	108.0			
80 % Rep 3	104.6			
100 % Rep 1	104.7	**102.2**	**2.7**	**2.6**
100 % Rep 2	99.4			
100 % Rep 3	102.5			
120 % Rep 1	104.7	**105.1**	**0.9**	**0.8**
120 % Rep 2	104.5			
120 % Rep 3	106.1			

References

1. Katzung B, Masters S, Trevor A. Basic & Clinical Pharmacology: McGraw-Hill Medical (London); 2012.

2. [NICE] National Institute for Health and Care Excellence. Hypertension in adults: diagnosis and management. NICE Guideline [NG136]. 28 August 2019. [website] (https://www.nice.org.uk/guidance/ng136). Accessed: 17 November 2021.

3. [WHO] World Health Organization. Hypertension. Key facts. 25 August 2021 [website] (https://www.who.int/news-room/fact-sheets/detail/hypertension). Accessed: 17 November 2021.

4. Zhou B, Carrillo-Larco R, Danaei G, et al. Worldwide trends in hypertension prevalence and progress in treatment and control from 1990 to 2019: a pooled analysis of 1201 population-representative studies with 104 million participants. Lancet. 2021;398(10304):957-80.

5. Mills K, Stefanescu A, He J. The global epidemiology of hypertension. Nat Rev Nephrol. 2020;16(4):223-37.

6. Di Chiara T, Scaglione A, Corrao S, Argano C, Pinto A, Scaglione R. Education and hypertension: impact on global cardiovascular risk. Acta Cardiol. 2017;72(5):507-13.

7. Elliott W. Systemic Hypertension. Curr Probl Cardiol. 2007;32(4):201-59.

8. Thom J, Haase C, Rosamond C, Howard C, Rumsfeld C, Manolio C, et al. Heart Disease and Stroke Statistics—2006 Update: A Report From the American Heart Association Statistics Committee and Stroke Statistics Subcommittee. Circulation. 2006;113(6):e85-e151.

9. Carretero O, Oparil S. Essential Hypertension. Circulation. 2000;101(3):329-35.

10. Manaktala R, Tafur-Soto J, White C. Renal Artery Stenosis in the Patient with Hypertension: Prevalence, Impact and Management. Integr Blood Press Control. 2020;13:71-82.

11. Nakamura K, Stefanescu Schmidt A. Treatment of Hypertension in Coarctation of the Aorta. Curr Treat Options Cardiovasc Med. 2016;18(6):40.

12. Zuber S, Kantorovich V, Pacak K. Hypertension in pheochromocytoma: characteristics and treatment. Endocrinol Metab Clin North Am. 2011;40(2):295-vii.

13. Singh Y, Kotwal N, Menon A. Endocrine hypertension - Cushing's syndrome. Indian J Endocrinol Metab. 2011;15 Suppl 4(Suppl4):S313-S6.

14. Aronova A, Fahey TI, Zarnegar R. Management of hypertension in primary aldosteronism. World J Cardiol. 2014;6(5):227-33.

15. Pazoki R, Dehghan A, Evangelou E, Warren H, Gao H, Caulfield M, et al. Genetic Predisposition to High Blood Pressure and Lifestyle Factors: Associations With Midlife Blood Pressure Levels and Cardiovascular Events. Circulation. 2018;137(7):653-61.

16. Natekar A OR, Lau MW, Min K, Imoto K, Slavin TP. Elevated blood pressure: Our family's fault? The genetics of essential hypertension. World J Cardiol. 2014;6(5):327-37.

17. Gasperin D, Netuveli G, Dias-da-Costa J, Pattussi M. Effect of psychological stress on blood pressure increase: a meta-analysis of cohort studies. Cad Saude Publica. 2009;25(4):715-26.

18. Kokubo Y, Padmanabhan S, Iwashima Y, Yamagishi K, Goto A. Gene and environmental interactions according to the components of lifestyle modifications in hypertension guidelines. Environ Health Prev Med. 2019;24(1):19.

19. Williams B, Mancia G, Spiering W, Agabiti Rosei E, Azizi M, Burnier M, et al. 2018 ESC/ESH Guidelines for the management of arterial hypertension. Eur Heart J. 2018;39(33):3021-104.

20. Robinson R, Batisky D, Hayes J, Nahata M, Mahan J. Significance of heritability in primary and secondary pediatric hypertension. Am J Hypertens. 2005;18(7):917-21.

21. Cusi D, Barlassina C, Azzani T, Casari G, Citterio L, Devoto M, et al. Polymorphisms of alpha-adducin and salt sensitivity in patients with essential hypertension. Lancet. 1997;349(9062):1353-7.

22. Castellano M, Barlassina C, Muiesan M, Beschi M, Cinelli A, Rossi F, et al. Alpha-adducin gene polymorphism and cardiovascular phenotypes in a general population. J Hypertens. 1997;15(12 Pt 2):1707-10.

23. Barlassina C, Schork N, Manunta P, Citterio L, Sciarrone M, Lanella G, et al. Synergistic effect of alpha-adducin and ACE genes causes blood pressure changes with body sodium and volume expansion. Kidney Int. 2000;57(3):1083-90.

24. Pacanowski M, Gong Y, Cooper-Dehoff R, Schork N, Shriver M, Langaee T, et al. beta-adrenergic receptor gene polymorphisms and beta-blocker treatment outcomes in hypertension. Clin Pharmacol Ther. 2008;84(6):715-21.

25. Ott C, Schmieder R. Diagnosis and treatment of arterial hypertension 2021. Kidney Int. 2021.

26. Forouzanfar MH, Alexander L, Anderson HR, Bachman VF, Biryukov S, Brauer M, et al. Global, regional, and national comparative risk assessment of 79 behavioural, environmental and occupational, and metabolic risks or clusters of risks in 188 countries, 1990-2013: a systematic analysis for the Global Burden of Disease Study 2013. Lancet. 2015;386(10010):2287-323.

27. Eeftinck Schattenkerk DW, van Gorp J, Vogt L, Peters RJ, van den Born B. Isolated systolic hypertension of the young and its association with central blood pressure in a large multi-ethnic population. The HELIUS study. Eur J Prev Cardiol. 2018;25(13):1351-9.

28. Yano Y, Stamler J, Garside D, Daviglus M, Franklin S, Carnethon M, et al. Isolated systolic hypertension in young and middle-aged adults and 31-year risk for cardiovascular

mortality: the Chicago Heart Association Detection Project in Industry study. J Am Coll Cardiol. 2015;65(4):327-35.

29. Aronow WS FJ, Pepine CJ, Artinian NT, Bakris G, Brown AS, Ferdinand KC, Forciea MA, Frishman WH, Jaigobin C, Kostis JB, Mancia G, Oparil S, Ortiz E, Reisin E, Rich MW, Schocken DD, Weber MA, Wesley DJ. ACCF/AHA 2011 expert consensus document on hypertension in the elderly. A report of the American College of Cardiology Foundation Task Force on Clinical Expert Consensus Documents. Developed in collaboration with the American Academy of Neurology, American Geriatrics Society, American Society for Preventive Cardiology, American Society of Hypertension, American Society of Nephrology, Association of Black Cardiologists, and European Society of Hypertension. J Am Coll Cardiol. 2011;57:2037-114.

30. Virdis A, Giannarelli C, Neves M, Taddei S, Ghiadoni L. Cigarette smoking and hypertension. Curr Pharm Des. 2010;16(23):2518-25.

31. Mulè G, Calcaterra I, Nardi E, Cerasola G, Cottone S. Metabolic syndrome in hypertensive patients: An unholy alliance. World J Cardiol. 2014;6(9):890-907.

32. Halperin R, Sesso H, Ma J, Buring J, Stampfer M, Gaziano J. Dyslipidemia and the risk of incident hypertension in men. Hypertension (Dallas, Tex : 1979). 2006;47(1):45-50.

33. Tsimihodimos V, Gonzalez-Villalpando C, Meigs J, Ferrannini E. Hypertension and Diabetes Mellitus: Coprediction and Time Trajectories. Hypertension (Dallas, Tex : 1979). 2018;71(3):422-8.

34. Goldstein I, Shapiro D, Guthrie D. Ambulatory blood pressure and family history of hypertension in healthy men and women. Am J Hypertens. 2006;19(5):486-91.

35. Decker W, Godwin S, Hess E, Lenamond C, Jagoda A. Clinical policy: critical issues in the evaluation and management of adult patients with asymptomatic hypertension in the emergency department. Ann Emerg Med. 2006;47(3):237-49.

36. Chobanian A, Bakris G, Black H, Cushman W, Green L, Izzo JJ, et al. National Heart, Lung, and Blood institute Joint National Committee on Prevention, Detection, Evaluation, and Treatment of High Blood Pressure; National High Blood Pressure Education Program Coordinating Committee. The Seventh Report of the Joint National Committee on Prevention, Detection, Evaluation, and Treatment of High Blood Pressure. The JNC 7 Report. JAMA. 2003;289:2560-72.

37. Medical Research Council Working Party. MRC trial of mild hypertension: principal results. Br Med J. 1985;291:97-104.

38. Thomopoulos C, Parati G, Zanchetti A. Effects of blood pressure-lowering on outcome incidence in hypertension: 5. Head-to-head comparisons of various classes of antihypertensive drugs - overview and meta-analyses. J Hypertens. 2015;33(7):1321-41.

39. Thomopoulos C, Parati G, Zanchetti A. Effects of blood-pressure-lowering treatment on outcome incidence. 12. Effects in individuals with high-normal and normal blood pressure: overview and meta-analyses of randomized trials. J Hypertens. 2017;35(11):2150-60.

40. Tsioufis C, Thomopoulos C. Combination drug treatment in hypertension. Pharmacol Res. 2017;125(Pt B):266-71.

41. Nair A, Vyas H, Kumar A. Controlled release matrix uncoated tablets of enalapril maleate using hpmc alone. J Basic Clin Pharm. 2010;1(2):71.

42. Wen H, Park K. Oral controlled release formulation design and drug delivery : theory to practice / edited by Hong Wen, Kinam Park. Hoboken, N.J.: Hoboken, N.J. : Wiley; 2010.

43. Lee H-G, Park Y-S, Jeong J-H, Kwon Y-B, Shin D, Kim J-Y, et al. Physicochemical properties and drug-release mechanisms of dual-release bilayer tablet containing mirabegron and fesoterodine fumarate. Drug Des Devel Ther. 2019;13:2459-74.

44. Defang O, Shufang N, Wei L, Hong G, Hui L, Weisan P. In Vitro and In Vivo Evaluation of Two Extended Release Preparations of Combination Metformin and Glipizide. Drug Dev Ind Pharm. 2005;31(7):677-85.

45. Chen L, Wang F. Development of sustained-release matrix tablets of BKP-01-041 (tilorone derivative) containing Hypromellose. Pharmazie. 2013;68:796-9.

46. Merchant H, Shoaib H, Tazeen J, Yousuf R. Once-daily tablet formulation and in vitro release evaluation of cefpodoxime using hydroxypropyl methylcellulose: a technical note. AAPS PharmSciTech. 2006;7(3):78.

47. Santos J, Pina M, Marques M, de Carvalho L. New sustained release of Zidovudine Matrix tablets − cytotoxicity toward Caco-2 cells. Drug Dev Ind Pharm. 2013;39(8):1154-66.

48. Melia C. Hydrophilic matrix sustained release systems based on polysaccharide carriers. Crit Rev Ther Drug Carrier Syst. 1991;8(4):395-421.

49. Abd-Elbary A, Haider M, Sayed S. In vitro characterization and release study of Ambroxol hydrochloride matrix tablets prepared by direct compression. Pharm Dev Technol. 2012;17(5):562-73.

50. Chaibva F, Khamanga S, Walker R. Swelling, erosion and drug release characteristics of salbutamol sulfate from hydroxypropyl methylcellulose-based matrix tablets. Drug Dev Ind Pharm. 2010;36(12):1497-510.

51. Rowe R. Handbook of pharmaceutical excipients : edited by Raymond C. Rowe ... [et al.]. London: London : APhA/Pharmaceutical Press; 2009.

52. Phadtare D, Phadtare G, Nilesh B, Asawat M. Hypromellose – A Choice of Polymer in Extended Release Tablet Formulation. World J Pharm Pharm Sci. 2014;3(9):551-66.

53. Aulton M, Taylor K. Aulton's Pharmaceutics : the design and manufacture of medicines / edited by Michael E. Aulton, Kevin M.G. Taylor. 5th ed. ed. Edinburgh: Edinburgh : Elsevier; 2018.

54. Chaerunisaa AY, Ali R, Dashevskiy A. Release Adjustment of Two Drugs with Different Solubility Combined in a Matrix Tablet. AAPS PharmSciTech. 2019;20(4):1-8.

55. Maggi L, Bruni R, Conte U. High molecular weight polyethylene oxides (PEOs) as an alternative to HPMC in controlled release dosage forms. Int J Pharm. 2000;195(1-2):229-38.

56. Wen H, Li X, Li Y, Wang H, Wang Y, Wang T, et al. In vitro and in vivo evaluation of controlled-release matrix tablets of highly water-soluble drug applying different mw polyethylene oxides (PEO) as retardants. Drug Dev Ind Pharm. 2018;44(4):544-52.

57. Kim C-J. Effects of Drug Solubility, Drug Loading, and Polymer Molecular Weight on Drug Release from Polyox® Tablets. Drug Dev Ind Pharm. 1998;24(7):645-51.

58. Shojaee S, Kaialy W, Cumming K, Nokhodchi A. Comparative evaluation of drug release from aged prolonged polyethylene oxide tablet matrices: effect of excipient and drug type. Pharm Dev Technol. 2016;21(2):189-95.

59. Khizer Z, Nirwan J, Conway B, Ghori M. Okra (Hibiscus esculentus) gum based hydrophilic matrices for controlled drug delivery applications: Estimation of percolation threshold. Int J Biol Macromol. 2020.

60. Karemore MN, Avari JG. Formulation, Optimization, and In vivo Evaluation of Gastroretentive Drug Delivery System of Nifedipine for the Treatment of Preeclampsia. AAPS PharmSciTech. 2019;20(5):200.

61. El-Zahaby S, Kassem A, El-Kamel A. Formulation and in vitro evaluation of size expanding gastro-retentive systems of levofloxacin hemihydrate. Int J Pharm. 2014;464(1-2):10-8.

62. Tønnesen H, Karlsen J. Alginate in Drug Delivery Systems. Drug Dev Ind Pharm. 2002;28(6):621-30.

63. Murata Y, Maeda T, Miyamoto E, Kawashima S. Preparation of chitosan-reinforced alginate gel beads — effects of chitosan on gel matrix erosion. Int J Pharm. 1993;96(1-3):139-45.

64. Savaşer A, Taş C, Bayrak Z, Özkan CK, Özkan Y. Effect of different polymers and their combinations on the release of metoclopramide HCl from sustained-release hydrophilic matrix tablets. Pharm Dev Technol. 2013;18(5):1122-30.

65. Velasco M, Ford J, Rowe P, Rajabi-Siahboomi A. Influence of drug:hydroxypropylmethylcellulose ratio, drug and polymer particle size and compression force on the release of diclofenac sodium from HPMC tablets. J Control Release. 1999;57(1):75-85.

66. Mitchell K, Ford J, Armstrong D, Elliott P, Hogan J, Rostron C. The influence of the particle size of hydroxypropylmethylcellulose K15M on its hydration and performance in matrix tablets. Int J Pharm. 1993;100(1):175-9.

67. Jamzad S, Fassihi R. Development of a robust once-a-day glipizide matrix system. J Pharm Pharmacol. 2007;59(6):769.

68. Jain A, Söderlind E, Viridén A, Schug B, Abrahamsson B, Knopke C, et al. The influence of hydroxypropyl methylcellulose (HPMC) molecular weight, concentration and effect of food on in vivo erosion behavior of HPMC matrix tablets. J Control Release. 2014;187:50-8.

69. Schiller C, Frohlich C, Giessmann T, Siegmund W, Monnikes H, Hosten N, et al. Intestinal fluid volumes and transit of dosage forms as assessed by magnetic resonance imaging. Aliment Pharmacol Ther. 2005;22(10):971-9.

70. Maggi L, Segale L, Torre M, Ochoa Machiste E, Conte U. Dissolution behaviour of hydrophilic matrix tablets containing two different polyethylene oxides (PEOs) for the

controlled release of a water-soluble drug. Dimensionality study. Biomaterials. 2002;23(4):1113-9.

71. Körner A, Larsson A, Piculell L, Wittgren B. Molecular Information on the Dissolution of Polydisperse Polymers: Mixtures of Long and Short Poly(ethylene oxide). J Phys Chem B. 2005;109(23):11530-7.

72. Khan G, Meidan V. Drug Release Kinetics from Tablet Matrices Based Upon Ethylcellulose Ether-Derivatives: A Comparison Between Different Formulations. Drug Dev Ind Pharm. 2007;33(6):627-39.

73. Desai R, Neau S, Pather S, Johnston T. Fine-Particle Ethylcellulose as a Tablet Binder in Direct Compression, Immediate-Release Tablets. Drug Dev Ind Pharm. 2001;27(7):633-41.

74. Palmieri G, Wehrle A. Evaluation of Ethylcellulose-Coated Pellets Optimized Using the Approach of Taguchi. Drug Dev Ind Pharm. 1997;23(11):1069-77.

75. RC R. The effect of the molecular weight of ethyl cellulose on the drug release properties of mixed films of ethyl cellulose and hydroxypropylmethylcellulose. Int J Pharm. 1986;29(1):37-41.

76. Khan GM, Zhu JB. Evaluation of Ethocel® Premium Ethylcellulose Ether Derivatives with Different Molecular Weights as Controlled-release Matrix Forming Functional Polymers for Ibuprofen. J Med Sci. 2001;1(6).

77. Shaikh N, Abidi S, Block L. Evaluation of Ethylcellulose as A Matrix for Prolonged Release Formulations. I. Water Soluble Drugs: Acetaminophen and Theophylline. Drug Dev Ind Pharm. 1987;13(8):1345-69.

78. Shaikh N, Abidl S, Block L. Evaluation of Ethylcellulose as a Matrix for Prolonged Release Formulations. II. Sparingly Water-Soluble Drugs: Ibuprofen and Indomethacin. Drug Dev Ind Pharm. 1987;13(14):2495-518.

79. Shlieout G, Zessin G. Investigation of Ethylcellulose as a Matrix Former and a New Method to Regard and Evaluate the Compaction Data. Drug Dev Ind Pharm. 1996;22(4):313-9.

80. Upadrashta S, Katikaneni P, Hileman G, Keshary P. Direct Compression Controlled Release Tablets Using Ethylcellulose Matrices. Drug Dev Ind Pharm. 1993;19(4):449-60.

81. Siddique S, Bose A, Khanam J. Modulation of drug (metoprolol succinate) release by inclusion of hydrophobic polymer in hydrophilic matrix. Drug Dev Ind Pharm. 2011;37(9):1016-25.

82. Yadav K, Yadav D, Srivastava A. Evaluation of hydrophilic, hydrophobic and waxy matrix excipients for sustained release tablets of Venlafaxine hydrochloride. Drug Dev Ind Pharm. 2013;39(8):1197-206.

83. Patra C, Kumar A, Pandit H, Singh S, Devi M. Design and evaluation of sustained release bilayer tablets of propranolol hydrochloride. Acta Pharm. 2007;57(4):479.

84. Tiwari S, Murthy T, Raveendra Pai M, Mehta P, Chowdary P. Controlled release formulation of tramadol hydrochloride using hydrophilic and hydrophobic matrix system. AAPS PharmSciTech. 2003;4(3):18-23.

85. Afrasiabi Garekani H, Faghihnia Torshizi M, Sadeghi F. Surelease as granulating liquid in preparation of sustained release matrices of ethylcellulose and theophylline. Drug Dev Ind Pharm. 2015;41(10):1655-60.

86. Thakral S, Thakral N, Majumdar D. Eudragit®: a technology evaluation. Expert Opin Drug Deliv. 2013;10(1):131-49.

87. Kawashima Y, Niwa T, Handa T, Takeuchi H, Iwamoto T, Itoh K. Preparation of controlled-release microspheres of ibuprofen with acrylic polymers by a novel quasi-emulsion solvent diffusion method. J Pharm Sci. 1989;78(1):68-72.

88. Boyapally H, Nukala R, Douroumis D. Development and release mechanism of diltiazem HCl prolonged release matrix tablets. Drug Deliv. 2009;16(2):67-74.

89. Siepmann F, Siepmann J, Walther M, MacRae R, Bodmeier R. Polymer blends for controlled release coatings. J Control Release. 2008;125(1):1-15.

90. Notario-Pérez F, Martín-Illana A, Cazorla-Luna R, Ruiz-Caro R, Peña J, Veiga M. Improvement of Tenofovir vaginal release from hydrophilic matrices through drug granulation with hydrophobic polymers. Eur J Pharm Sci. 2018;117:204-15.

91. Sudha B, Sridhar B, Srinatha A. Modulation of Tramadol Release from a Hydrophobic Matrix: Implications of Formulations and Processing Variables. AAPS PharmSciTech. 2010;11(1):433-40.

92. El-Shanawany S. Sustained release of nitrofurantoin from inert wax matrixes. J Control Release. 1993;26(1):11-9.

93. Lee B, Choe J, Kim C. Preparation and characterization of melatonin-loaded stearyl alcohol microspheres. J Microencapsul. 1998;15(6):775-87.

94. Nokhodchi A, Raja S, Patel P, Asare-Addo K. The Role of Oral Controlled Release Matrix Tablets in Drug Delivery Systems. Bioimpacts. 2012;2(4):175-87.

95. Yin L, Qin C, Chen K, Zhu C, Cao H, Zhou J, et al. Gastro-floating tablets of cephalexin: Preparation and in vitro/in vivo evaluation. Int J Pharm. 2013;452(1-2):241-8.

96. Tatavarti A, Mehta K, Augsburger L, Hoag S. Influence of methacrylic and acrylic acid polymers on the release performance of weakly basic drugs from sustained release hydrophilic matrices. J Pharm Sci. 2004;93(9):2319-31.

97. Makhija S, Vavia P. Once daily sustained release tablets of venlafaxine, a novel antidepressant. Eur J Pharm Biopharm. 2002;54(1):9-15.

98. Gröning R, Heun G. Oral Dosage Forms with Controlled Gastrointestinal Transit. Drug Dev Ind Pharm. 1984;10(4):527-39.

99. Moës A. Gastroretentive dosage forms. Crit Rev Ther Drug Carrier Syst. 1993;10(2):143-95.

100. Deshpande A, Rhodes C, Shah N, Malick A. Controlled-Release Drug Delivery Systems for Prolonged Gastric Residence: An Overview. Drug Dev Ind Pharm. 1996;22(6):531-9.

101. Bardonnet P, Faivre V, Pugh W, Piffaretti J, Falson F. Gastroretentive dosage forms: Overview and special case of Helicobacter pylori. J Control Release. 2006;111(1-2):1-18.

102. Lopes C, Bettencourt C, Rossi A, Buttini F, Barata P. Overview on gastroretentive drug delivery systems for improving drug bioavailability. Int J Pharm. 2016;510(1):144-58.

103. Tripathi J, Thapa P, Maharjan R, Jeong S. Current State and Future Perspectives on Gastroretentive Drug Delivery Systems. Pharmaceutics. 2019;11(4):193.

104. Rouge N, Buri P, Doelker E. Drug absorption sites in the gastrointestinal tract and dosage forms for site-specific delivery. Int J Pharm. 1996;136(1-2):117-39.

105. Darbasizadeh B, Motasadizadeh H, Foroughi-Nia B, Farhadnejad H. Tripolyphosphate-crosslinked chitosan/poly (ethylene oxide) electrospun nanofibrous mats as a floating gastro-retentive delivery system for ranitidine hydrochloride. J Pharm Biomed Anal. 2018;153:63-75.

106. Kim S, Hwang K-M, Park Y, Nguyen T-T, Park E-S. Preparation and evaluation of non-effervescent gastroretentive tablets containing pregabalin for once-daily administration and dose proportional pharmacokinetics. Int J Pharm. 2018;550(1-2):160-9.

107. Hwang K-M, Cho C-H, Tung N-T, Kim J-Y, Rhee Y-S, Park E-S. Release kinetics of highly porous floating tablets containing cilostazol. Eur J Pharm Biopharm. 2017;115:39-51.

108. Klausner EA, Lavy E, Friedman M, Hoffman A. Expandable gastroretentive dosage forms. J Control Release. 2003;90(2):143-62.

109. Thapa P, Jeong S. Effects of Formulation and Process Variables on Gastroretentive Floating Tablets with A High-Dose Soluble Drug and Experimental Design Approach. Pharmaceutics. 2018;10(3):161.

110. Jiménez-Martínez I, Quirino-Barreda T, Villafuerte-Robles L. Sustained delivery of captopril from floating matrix tablets. Int J Pharm. 2008;362(1):37-43.

111. El-Zahaby S, Kassem A, El-Kamel A. Design and evaluation of gastroretentive levofloxacin floating mini-tablets-in-capsule system for eradication of Helicobacter pylori. Saudi Pharm J. 2014;22(6):570-9.

112. Sarkar D, Nandi G, Changder A, Hudati P, Sarkar S, Ghosh L. Sustained release gastroretentive tablet of metformin hydrochloride based on poly (acrylic acid)-grafted-gellan. Int J Biol Macromol. 2017;96:137-48.

113. Sarparanta M, Bimbo L, Mäkilä E, Salonen J, Laaksonen P, Helariutta A, et al. The mucoadhesive and gastroretentive properties of hydrophobin-coated porous silicon nanoparticle oral drug delivery systems. Biomaterials. 2012;33(11):3353-62.

114. He W, Li Y, Zhang R, Wu Z, Yin L. Gastro-floating bilayer tablets for the sustained release of metformin and immediate release of pioglitazone: Preparation and in vitro/in vivo evaluation. Int J Pharm. 2014;476(1):223-31.

115. Michelson E. Calcium antagonists in cardiology: Update on sustained-release drug delivery systems. Clin Cardiol. 1991. p. 947-50.

116. Hutton J, Morris J. Long-acting carbidopa-levodopa in the management of moderate and advanced Parkinson's disease. Neurology. 1992;42(1 Suppl 1):51-6; discussion 7-60.

117. Wagstaff A, Goa K. Once-weekly fluoxetine. Drugs. 2001;61(15):2221-8; discussion 9-30.

118. Michel M. A Benefit-Risk Assessment of Extended-Release Oxybutynin. Drug Saf. 2002;25(12):867-76.

119. Pieper J. Understanding niacin formulations. Am J Manag Care. 2002;8(12 Suppl):S308.

120. McCarberg B. Tramadol extended-release in the management of chronic pain. Ther Clin Risk Manag. 2007;3(3):401.

121. Desai N, Purohit R. Development of Novel High Density Gastroretentive Multiparticulate Pulsatile Tablet of Clopidogrel Bisulfate Using Quality by Design Approach. AAPS PharmSciTech. 2017;18(8):3208-18.

122. Patil H, Tiwari R, Repka M. Recent advancements in mucoadhesive floating drug delivery systems: A mini-review. J Drug Deliv Sci Technol. 2016;31:65-71.

123. Shtenberg Y, Goldfeder M, Prinz H, Shainsky J, Ghantous Y, Abu El-Naaj I, et al. Mucoadhesive alginate pastes with embedded liposomes for local oral drug delivery. Int J Biol Macromol. 2018;111:62-9.

124. Andrews GP, Laverty TP, Jones DS. Mucoadhesive polymeric platforms for controlled drug delivery. Eur J Pharm Biopharm. 2009;71(3):505-18.

125. Wang J, Tauchi Y, Deguchi Y, Morimoto K, Tabata Y, Ikada Y. Positively Charged Gelatin Microspheres as Gastric Mucoadhesive Drug Delivery System for Eradication of H. pylori. Drug Deliv. 2000;7(4):237-43.

126. Bhalla S, Nagpal M. Comparison of Various Generations of Superporous Hydrogels Based on Chitosan-Acrylamide and *In Vitro* Drug Release. ISRN Pharm. 2013;2013:624841.

127. Omidian H, Rocca J, K P. Advances in superporous hydrogels. J Control Release. 2005;102(1):3-12.

128. Fujimori J, Machida Y, Tanaka S, Nagai T. Effect of magnetically controlled gastric residence of sustained release tablets on bioavailability of acetaminophen. Int J Pharm. 1995;119(1):47-55.

129. Gröning R, Berntgen M, Georgarakis M. Acyclovir serum concentrations following peroral administration of magnetic depot tablets and the influence of extracorporal magnets to control gastrointestinal transit. Eur J Pharm Biopharm. 1998;46(3):285-91.

130. Zhou Y, Gu N, Yang F. In situ microbubble-assisted, ultrasound-controlled release of superparamagnetic iron oxide nanoparticles from gastro-retentive tablets. Int J Pharm. 2020;586:119615-.

131. Prajapati V, Jani G, Khutliwala T, Zala B. Raft forming system—An upcoming approach of gastroretentive drug delivery system. J Control Release. 2013;168(2):151-65.

132. Choi B, Park H, Hwang S, Park J. Preparation of alginate beads for floating drug delivery system: effects of CO2 gas-forming agents. Int J Pharm. 2002;239(1-2):81-91.

133. Rossi A, Conti C, Colombo G, Castrati L, Scarpignato C, Barata P, et al. Floating modular drug delivery systems with buoyancy independent of release mechanisms to sustain amoxicillin and clarithromycin intra-gastric concentrations. Drug Dev Ind Pharm. 2016;42(2):332-9.

134. Nguyen T-T, Hwang K-M, Kim S-H, Park E-S. Development of novel bilayer gastroretentive tablets based on hydrophobic polymers. Int J Pharm. 2020;574.

135. Dorożyński P, Kulinowski P, Mendyk A, Jachowicz R. Gastroretentive drug delivery systems with l-dopa based on carrageenans and hydroxypropylmethylcellulose. Int J Pharm. 2011;404(1-2):169-75.

136. Verma A, Dubey J, Verma N, Nayak AK. Chitosan-Hydroxypropyl Methylcellulose Matrices as Carriers for Hydrodynamically Balanced Capsules of Moxifloxacin HCl. Curr Drug Deliv. 2017;14(1):83-90.

137. Nayak A, Das B, Maji R. Gastroretentive hydrodynamically balanced systems of ofloxacin: In vitro evaluation. Saudi Pharm J. 2013;21(1):113-7.

138. Reddy L, Murthy R. Floating Dosage Systems in Drug Delivery. Crit Rev Ther Drug Carrier Syst. 2002;19(6):36.

139. Hwang S, Park H, Park K. Gastric retentive drug-delivery systems. Crit Rev Ther Drug Carrier Syst. 1998;15(3):243-84.

140. Vrettos N-N, Roberts C, Zhu Z. Gastroretentive Technologies in Tandem with Controlled-Release Strategies: A Potent Answer to Oral Drug Bioavailability and Patient Compliance Implications. Pharmaceutics. 2021;13(10).

141. Nayak A, Malakar J. Formulation and in vitro evaluation of Hydrodynamically balanced system for theophylline delivery. J Basic Clin Pharm. 2011;2(3):133-7.

142. Qin C, Wu M, Xu S, Wang X, Shi W, Dong Y, et al. Design and optimization of gastro-floating sustained-release tablet of pregabalin: In vitro and in vivo evaluation. Int J Pharm. 2018;545(1-2):37-44.

143. Mehta D, Parejiya P, Patel H, Trivedi P, Suthar D, Shelat P. Design, optimization and pharmacokinetics of novel prolonged gastroretentive drug delivery system of quetiapine fumarate. J Pharm Investig. 2016;46(5):453-65.

144. Lin H-L, Chen L-C, Cheng W-T, Cheng W-J, Ho H-O, Sheu M-T. Preparation and Characterization of a Novel Swellable and Floating Gastroretentive Drug Delivery System (sfGRDDS) for Enhanced Oral Bioavailability of Nilotinib. Pharmaceutics. 2020;12(2):137.

145. Raza A, Hayat U, Wang HJ, Wang JY. Preparation and evaluation of captopril loaded gastro-retentive zein based porous floating tablets. Int J Pharm. 2020;579:119185.

146. Oh J-H, Eun Lee J, Jeong Kim Y, Oh T-O, Han S, Jeon E, et al. Designing of the fixed-dose gastroretentive bilayer tablet for sustained release of metformin and immediate release of atorvastatin. Drug Dev Ind Pharm. 2016;42(2):340-9.

147. Oh T-O, Kim J-Y, Ha J-M, Chi S-C, Rhee Y-S, Park C-W, et al. Preparation of highly porous gastroretentive metformin tablets using a sublimation method. Eur J Pharm Biopharm. 2013;83(3):460-7.

148. Sako K, Mizumoto T, Kajiyama A, Ohmura T. Influence of physical factors in gastrointestinal tract on acetaminophen release from controlled-release tablets in fasted dogs. Int J Pharm. 1996;137(2):225-32.

149. Hajare P, Rachh P. Gastroretentive microballoons: a novel approach for drug delivery. Int J Pharm Sci & Res. 2020;11(3):1075-83.

150. Maghsoodi M, Hemati E, Qadermazi B, Yari Z. Hollow microspheres for gastroretentive floating- pulsatile drug delivery: preparation and in vitro evaluation. Adv Pharm Bull. 2011;1(2):55-61.

151. Kawashima Y, Niwa T, Takeuchi H, Hino T, Itoh Y. Hollow microspheres for use as a floating controlled drug delivery system in the stomach. J Pharm Sci. 1992;81(2):135-40.

152. Jayanthi G, Jayaswal S, Srivastava A. Formulation and evaluation of terfenadine microballoons for oral controlled release. Pharmazie. 1995;50(11):769-70.

153. Sato Y, Kawashima Y, Takeuchi H, Yamamoto H. In vivo evaluation of riboflavin-containing microballoons for floating controlled drug delivery system in healthy human volunteers. J Control Release. 2003;93(1):39-47.

154. Sato Y, Kawashima Y, Takeuchi H, Yamamoto H. In vitro and in vivo evaluation of riboflavin-containing microballoons for a floating controlled drug delivery system in healthy humans. Int J Pharm. 2004;275(1):97-107.

155. Sato Y, Kawashima Y, Takeuchi H, Yamamoto H, Fujibayashi Y. Pharmacoscintigraphic evaluation of riboflavin-containing microballoons for a floating controlled drug delivery system in healthy humans. J Control Release. 2004;98(1):75-85.

156. Rahim S, Carter P, Elkordy A. Influence of calcium carbonate and sodium carbonate gassing agents on pentoxifylline floating tablets properties. Powder Technol. 2017;322:65-74.

157. Qi X, Chen H, Rui Y, Yang F, Ma N, Wu Z. Floating tablets for controlled release of ofloxacin via compression coating of hydroxypropyl cellulose combined with effervescent agent. Int J Pharm. 2015;489(1-2):210-7.

158. Baumgartner S, Kristl J, Vrečer F, Vodopivec P, Zorko B. Optimisation of floating matrix tablets and evaluation of their gastric residence time. Int J Pharm. 2000;195(1-2):125-35.

159. Raza A, Shen N, Li J, Chen Y, Wang J-Y. Formulation of zein based compression coated floating tablets for enhanced gastric retention and tunable drug release. Eur J Pharm Sci. 2019;132:163-73.

160. Hwang K-M, Nguyen T-T, Seok S, Jo H-I, Cho C-H, Hwang K-M, et al. Swellable and porous bilayer tablet for gastroretentive drug delivery: Preparation and in vitro-in vivo evaluation. Int J Pharm. 2019;572:118783.

161. Han D, Steckl A. Triaxial Electrospun Nanofiber Membranes for Controlled Dual Release of Functional Molecules. ACS Appl Mater Interfaces. 2013;5(16):8241-5.

162. Han D, Yu X, Chai Q, Ayres N, Steckl A. Stimuli-Responsive Self-Immolative Polymer Nanofiber Membranes Formed by Coaxial Electrospinning. ACS Appl Mater Interfaces. 2017;9(13):11858-65.

163. Hu X, Liu S, Zhou G, Huang Y, Xie Z, Jing X. Electrospinning of polymeric nanofibers for drug delivery applications. J Control Release. 2014;185:12-21.

164. Palo M, Kogermann K, Laidmäe I, Meos A, Preis M, Heinämäki J, et al. Development of Oromucosal Dosage Forms by Combining Electrospinning and Inkjet Printing. Mol Pharm. 2017;14(3):808-20.

165. Adibkia K, Hamedeyazdan S, Javadzadeh Y. Drug release kinetics and physicochemical characteristics of floating drug delivery systems. Expert Opin Drug Deliv. 2011;8(7):891-903.

166. Malik R, Garg T, Goyal A, Rath G. Polymeric nanofibers: targeted gastro-retentive drug delivery systems. J Drug Target. 2015;23(2):109-24.

167. Abou Youssef N, Kassem A, El-Massik M, Boraie N. Development of gastroretentive metronidazole floating raft system for targeting Helicobacter pylori. Int J Pharm. 2015;486(1):297-305.

168. Kerdsakundee N, Mahattanadul S, Wiwattanapatapee R. Development and evaluation of gastroretentive raft forming systems incorporating curcumin-Eudragit® EPO solid dispersions for gastric ulcer treatment. Eur J Pharm Biopharm. 2015;94:513-20.

169. Lambert J, Korman M, Nicholson L, Chan J. In-vivo anti-reflux and raft properties of alginates. Aliment Pharmacol Ther. 1990;4(6):615-22.

170. Hampson F, Jolliffe I, Bakhtyari A, Taylor G, Sykes J, Johnstone L, et al. Alginate-antacid combinations: raft formation and gastric retention studies. Drug Dev Ind Pharm. 2010;36(5):614-23.

171. Abouelatta S, Aboelwafa A, El-Gazayerly O. Gastroretentive raft liquid delivery system as a new approach to release extension for carrier-mediated drug. Drug Deliv. 2018;25(1):1161-74.

172. Shaha S, Jayvadan P, Pundarikakshudu K. An overview of a gastro-retentive floating drug delivery system. Asian J Pharm. 2009;4(1):65-80.

173. Clarke G, Newton J, Short M. Gastrointestinal transit of pellets of differing size and density. Int J Pharm. 1993;100(1):81-92.

174. Sharma A, Goyal A, Rath G. Development and Characterization of Gastroretentive High-Density Pellets Lodged With Zero Valent Iron Nanoparticles. J Pharm Sci. 2018;107(10):2663-73.

175. Garg R, Gupta G. Progress in Controlled Gastroretentive Delivery Systems. Trop J Pharm Res. 2008;7(3).

176. Kinloch A. The science of adhesion. J Mater Sci. 1982;17(3):617-51.

177. Su C-Y, Ho H-O, Chen Y-C, Yu Y-T, Liu D-Z, Chao F-C, et al. Complex Hydrogels Composed of Chitosan with Ring-opened Polyvinyl Pyrrolidone as a Gastroretentive Drug Dosage Form to Enhance the Bioavailability of Bisphosphonates. Sci Rep. 2018;8(1):8092.

178. Illum L. Chitosan and its use as a pharmaceutical excipient. Pharm Res. 1998;15(9):1326-31.

179. Nakatsuka S, Andrady A. Permeability of vitamin B-12 in chitosan membranes. Effect of crosslinking and blending with poly(vinyl alcohol) on permeability. J Appl Polym Sci. 1992;44(1):17-28.

180. Vishal Gupta N, Shivakumar H. Preparation and characterization of superporous hydrogels as gastroretentive drug delivery system for rosiglitazone maleate. Daru. 2010;18(3):200-10.

181. Alvarez-Lorenzo C, Blanco-Fernandez B, Puga A, Concheiro A. Crosslinked ionic polysaccharides for stimuli-sensitive drug delivery. Adv Drug Deliv Rev. 2013;65(9):1148-71.

182. Inouye K, Machida Y, Sannan T, Nagai T. Buoyant sustained release tablets based on chitosan. Drug Des Deliv. 1988;2(3):165-75.

183. Chandy T, Sharma C. Chitosan matrix for oral sustained delivery of ampicillin. Biomaterials. 1993;14(12):939-44.

184. Patel V, Amiji M. Preparation and Characterization of Freeze-dried Chitosan-Poly(Ethylene Oxide) Hydrogels for Site-Specific Antibiotic Delivery in the Stomach. Pharm Res. 1996;13(4):588-93.

185. Gupta K, Ravi Kumar M. Drug release behavior of beads and microgranules of chitosan. Biomaterials. 2000;21(11):1115-9.

186. Souza M, Sábio R, Ribeiro T, Santos A, Meneguin A, Chorilli M. Highlighting the impact of chitosan on the development of gastroretentive drug delivery systems. Int J Biol Macromol. 2020;159:804-22.

187. Khattab A, Zaki N. Optimization and Evaluation of Gastroretentive Ranitidine HCl Microspheres by Using Factorial Design with Improved Bioavailability and Mucosal Integrity in Ulcer Model. AAPS PharmSciTech. 2017;18(4):957-73.

188. Hou J, Gao L, Meng F, Cui Y. Mucoadhesive microparticles for gastroretentive delivery: preparation, biodistribution and targeting evaluation. Mar Drugs. 2014;12(12):5764-87.

189. Ruiz-Caro R, Gago-Guillan M, Otero-Espinar F, Veiga M. Mucoadhesive tablets for controlled release of acyclovir. Chem Pharm Bull. 2012;60(10):1249.

190. Lele B, Hoffman A. Mucoadhesive drug carriers based on complexes of poly(acrylic acid) and PEGylated drugs having hydrolysable PEG–anhydride–drug linkages. J Control Release. 2000;69(2):237-48.

191. Salonen J, Kaukonen A, Hirvonen J, Lehto V. Mesoporous silicon in drug delivery applications. J Pharm Sci. 2008;97(2):632-53.

192. Prestidge C, Barnes T, Lau C, Barnett C, Loni A, Canham L. Mesoporous silicon: a platform for the delivery of therapeutics. Expert Opin Drug Deliv. 2007;4(2):101-10.

193. Streubel A, Siepmann J, Bodmeier R. Drug delivery to the upper small intestine window using gastroretentive technologies. Curr Opin Pharmacol. 2006;6(5):501-8.

194. Salessiotis N. Measurement of the diameter of the pylorus in man: Part I. Experimental project for clinical application. Am J Surg. 1972;124(3):331-3.

195. Lalloo A, McConnell E, Jin L, Elkes R, Seiler C, Wu Y. Decoupling the role of image size and calorie intake on gastric retention of swelling-based gastric retentive formulations: Pre-screening in the dog model. Int J Pharm. 2012;431(1-2):90-100.

196. Mandal U, Chatterjee B, Senjoti F. Gastro-retentive drug delivery systems and their in vivo success: A recent update. Asian J Pharm Sci. 2016;11(5):575-84.

197. Sivaneswari S, Karthikeyan E, Chandana P. Novel expandable gastro retentive system by unfolding mechanism of levetiracetam using simple lattice design – Formulation optimization and in vitro evaluation. Bull Fac Pharm Cairo Univ. 2017;55(1):63-72.

198. Dey S, Chattopadhyay S, Mazumder B. Formulation and Evaluation of Fixed-Dose Combination of Bilayer Gastroretentive Matrix Tablet Containing Atorvastatin as Fast-Release and Atenolol as Sustained-Release. BioMed Res Int. 2014;2014:396106-12.

199. Chen Y-C, Ho H-O, Lee T-Y, Sheu M-T. Physical characterizations and sustained release profiling of gastroretentive drug delivery systems with improved floating and swelling capabilities. Int J Pharm. 2013;441(1-2):162-9.

200. Chen J, Park H, Park K. Synthesis of superporous hydrogels: hydrogels with fast swelling and superabsorbent properties. J Biomed Mater Res. 1999;44(1):53-62.

201. Askari F, Nafisi S, Omidian H, Hashemi S. Synthesis and characterization of acrylic-based superabsorbents. J Appl Polym Sci. 1993;50(10):1851-5.

202. Awasthi R, Kulkarni G. Decades of research in drug targeting to the upper gastrointestinal tract using gastroretention technologies: where do we stand? Drug Deliv. 2016;23(2):378-94.

203. Murphy C, Pillay V, Choonara Y, du Toit L. Gastroretentive Drug Delivery Systems: Current Developments in Novel System Design and Evaluation. Curr Drug Deliv. 2009;6(5):451-60.

204. Li S, Lin S, Daggy B, Mirchandani H, Chien Y. Effect of HPMC and Carbopol on the release and floating properties of Gastric Floating Drug Delivery System using factorial design. Int J Pharm. 2003;253(1):13-22.

205. Xu T, Wang P, Tian J, Qing S, Wang S, Huang Y, et al. Pharmacological characterization of MT-1207, a novel multitarget antihypertensive agent. Acta Pharmacol Sin. 2021;42(6):885-97.

206. Zhang H, Wu M, Hu Y, Li C, Zheng W, Liu J, et al. Pharmacokinetics and pharmacodynamics of MT-1207, a novel multitarget blocker of α1 receptor, 5-HT2A receptor, and calcium channel, in healthy subjects. Expert Opin Investig Drugs. 2021;30(3):271-8.

207. Shenyang Haiwang Biotechnology Co. Ltd. MT-1207 physicochemical information (internal document). 2016.

208. Shenyang Haiwang Biotechnology Co. Ltd. Summary of MT-1207 DMPK study results in Beagle dogs and rats (internal document). 2017.

209. Patel P, Koli D, Maitra N, Sheth T, Vaishnav P. Comparison of Efficacy and Safety of Intravenous Labetalol Versus Hydralazine for Management of Severe Hypertension in Pregnancy. J Obstet Gynaecol India. 2018;68(5):376-81.

210. The United States Pharmacopoeia. 2016. <905> Uniformity of Dosage Units. Rockville (MD).

211. The United States Pharmacopoeia 35. 2015. <616> Bulk Density and Tapped Density of Powders. Rockville (MD).

212. The United States Pharmacopoeia 35. 2012. <1217> Tablet Breaking Force. Rockville (MD).

213. The United States Pharmacopoeia 35. 2012. <1216> Tablet Friability. Rockville (MD).

214. Korsmeyer R, Gurny R, Doelker E, Buri P, Peppas N. Mechanisms of solute release from porous hydrophilic polymers. Int J Pharm. 1983;15(1):25-35.

215. Peppas N. Analysis of Fickian and non-Fickian drug release from polymers. Pharm Acta Helv. 1985;60(4):110-1.

216. Siepmann J, Peppas N. Modeling of drug release from delivery systems based on hydroxypropyl methylcellulose (HPMC). Adv Drug Deliv Rev. 2001;48(2-3):139-57.

217. Alkhatib HS, Aiedeh KM, Bustanji Y, Hamed S, Mohammad MK, Alkhalidi B, et al. Modulation of buspirone HCl release from hypromellose matrices using chitosan succinate: Implications for pH-independent release. Eur J Pharm Biopharm. 2008;70(3):804-12.

218. Saurí J, Millán D, Suñé-Negre J, Colom H, Ticó J, Miñarro M, et al. Quality by Design approach to understand the physicochemical phenomena involved in controlled release of captopril SR matrix tablets. Int J Pharm. 2014;477(1-2):431-41.

219. Mašková E, Kubová K, Raimi-Abraham B, Vllasaliu D, Vohlídalová E, Turánek J, et al. Hypromellose - A traditional pharmaceutical excipient with modern applications in oral and oromucosal drug delivery. J Control Release. 2020;324:695-727.

220. Baka E, Comer J, Takacs-Novak K. Study of equilibrium solubility measurement by saturation shake-flask method using hydrochlorothiazide as model compound. J Pharm Biomed Anal. 2008;46(2):335-41.

221. The United States Pharmacopoeia 40. 2017. <467> Residual Solvents. Rockville (MD).

222. The United States Pharmacopoeia 35. 2012. <1174> Powder Flow. Rockville (MD).801-3.

223. [FDA] United States Food and Drug Administration. 1997. Guidance for Industry: Dissolution Testing of Immediate-Release Solid Oral Dosage Forms. Rockville (MD). USA.

224. International Conference on Harmonisation of Technical Requirements for Registration of Pharmaceuticals for Human Use (ICH). Validation of Analytical Procedures: Text and Methodology. Q2 (R1). 1995.

225. [FDA] United States Food and Drug Administration 2018. Bioanalytical Method Validation Guidance for Industry. Rockville, MD, USA.

226. [FDA] United States Food and Drug Adminstration. 2018. Bioanalytical Method Validation Guidance for Industry. Center for Drug Evaluation and Research.

227. Jinno J-I, Kamada N, Miyake M, Yamada K, Mukai T, Odomi M, et al. Effect of particle size reduction on dissolution and oral absorption of a poorly water-soluble drug, cilostazol, in beagle dogs. J Control Release. 2006;111(1-2):56-64.

228. Loh Z, Samanta A, Sia Heng P. Overview of milling techniques for improving the solubility of poorly water-soluble drugs. Asian J Pharm Sci. 2015;10(4):255-74.

229. Chu K, Lee E, Jeong S, Park E-S. Effect of particle size on the dissolution behaviors of poorly water-soluble drugs. Arch Pharm Res. 2012;35(7):1187-95.

230. Marinko N, Zámostný P. Meloxicam Carrier Systems Having Enhanced Release and Aqueous Wettability Prepared Using Micro-suspensions in Different Liquid Media. AAPS PharmSciTech. 2020;21(5):155.

231. Carr R. Evaluating flow properties of solids. Chem Eng. 1965b:163-8.

232. Hausner H. Friction condition in a mass of metal powders. Int J Powder Metall. 1967;3:7-13.

233. Chowhan ZT. Role of Binders in Moisture-Induced Hardness Increase in Compressed Tablets and Its Effect on In Vitro Disintegration and Dissolution. J Pharm Sci. 1980;69(1):1-4.

234. Soare AC, Meltzer V, Colbea C, Stanculescu I, Pincu E. Compatibility of Drotaverine Hydrochloride with Ibuprofen and Ketoprofen Nonsteroidal Anti-Inflammatory Drugs Mixtures. Materials (Basel). 2022;15(3).

235. Pani N, Nath L, Acharya S. Compatibility studies of nateglinide with excipients in immediate release tablets. Acta Pharm. 2011;61(2):237-47.

236. Hiremath P, Saha R. Controlled Release Hydrophilic Matrix Tablet Formulations of Isoniazid: Design and In Vitro Studies. AAPS PharmSciTech. 2008;9(4):1171-8.

237. Jamzad S, Fassihi R. Development of a controlled release low dose class II drug-Glipizide. Int J Pharm. 2006;312(1-2):24-32.

238. Gao P, Skoug JW, Nixon PR, Ju TR, Stemm NL, Sung KC. Swelling of hydroxypropyl methylcellulose matrix tablets. 2. Mechanistic study of the influence of formulation variables on matrix performance and drug release. J Pharm Sci. 1996;85(7):732-40.

239. [EMA] European Medicines Agency 2010. CPMP/EWP/QWP/1401/98 Rev. 1/Corr Guideline on the Investigation of Bioequivalence. London.

240. Shargel L, Wu-Pong S, Yu A. Applied biopharmaceutics & pharmacokinetics. 6th ed. ed: McGraw-Hill; 2012.

241. Boxenbaum H. Interspecies Scaling, Allometry, Physiological Time, and the Ground Plan of Pharmacokinetics. J Pharmacokinet Biopharm. 1982;10(2):201-27.

242. Kuksal A, Tiwary A, Jain N, Jain S. Formulation and in vitro, in vivo evaluation of extended- release matrix tablet of Zidovudine: Influence of combination of hydrophilic and hydrophobic matrix formers. AAPS PharmSciTech. 2006;7(1):E1-E9.

243. Tamilvanan S, Venkatesh Babu R, Nappinai A, Sivaramakrishnan G. In vitro and in vivo evaluation of hydrophilic and hydrophobic polymers-based nicorandil-loaded peroral tablet compared with its once-daily commercial sustained-release tablet. Drug Dev Ind Pharm. 2011;37(4):436-45.

244. El-Zahaby SA, Kassem AA, El-Kamel AH. Design and evaluation of gastroretentive levofloxacin floating mini-tablets-in-capsule system for eradication of Helicobacter pylori. Saudi Pharmaceutical Journal. 2014;22(6):570-9.

245. Sharma O, Shah M, Parikh D, Mehta T. Formulation optimization of gastroretentive drug delivery system for allopurinol using experimental design. Expert Opin Drug Deliv. 2015;12(4):513-24.

246. Schneider F, Koziolek M, Weitschies W. In Vitro and In Vivo Test Methods for the Evaluation of Gastroretentive Dosage Forms. Pharmaceutics. 2019;11(8):416.

247. Kamba M, Seta Y, Kusai A, Nishimura K. Evaluation of the mechanical destructive force in the stomach of dog. Int J Pharm. 2001;228(1):209-17.

248. Kamba M, Seta Y, Kusai A, Ikeda M, Nishimura K. A unique dosage form to evaluate the mechanical destructive force in the gastrointestinal tract. Int J Pharm. 2000;208(1):61-70.

249. Timmermans J, Moës A. The Cutoff Size for Gastric Emptying of Dosage Forms. J Pharm Sci. 1993;82(8):854.

250. Aguilar-de-Leyva Á, Cifuentes C, Rajabi-Siahboomi A, Caraballo I. Study of the critical points and the role of the pores and viscosity in carbamazepine hydrophilic matrix tablets. Eur J Pharm Biopharm. 2012;80(1):136-42.

251. Acharya S, Patra S, Pani N. Optimization of HPMC and carbopol concentrations in non-effervescent floating tablet through factorial design. Carbohydr Polym. 2014;102:360-8.

252. Kosir D, Ojstersek T, Vrecer F. Does the performance of wet granulation and tablet hardness affect the drug dissolution profile of carvedilol in matrix tablets? Drug Dev Ind Pharm. 2018;44(9):1543-50.

253. Goole J, Vanderbist F, Amighi K. Development and evaluation of new multiple-unit levodopa sustained-release floating dosage forms. Int J Pharm. 2007;334(1-2):35-41.

254. Munk J, Gannaway R, Hoare M, Johnson A. H.L Duthie (Ed.), Gastrointestinal Motility in Health and Disease. MTP Press. Lancaster. pp. 349–359. 1978.

255. Vrettos N-N, Wang P, Zhou Y, Roberts C, Xu J, Yao H, et al. In vitro and in vivo evaluation of a sustained-release once-a-day formulation of the novel antihypertensive drug MT-1207. Pharm Dev Technol. 2021;26(3):349-61.

256. Dressman J, Berardi R, Dermentzoglou L, Russell T, Schmaltz S, Barnett J, et al. Upper Gastrointestinal (GI) pH in Young, Healthy Men and Women. Pharm Res. 1990;7(7):756-61.

257. McGary Jr C. Degradation of poly(ethylene oxide). J Polym Sci. 1960;46(147):51-7.

258. Crowley M, Zhang F, Koleng J, McGinity J. Stability of polyethylene oxide in matrix tablets prepared by hot-melt extrusion. Biomaterials. 2002;23(21):4241-8.

259. Yang B, Guo C, Chen S, Ma J, Wang J, Liang X, et al. Effect of Acid on the Aggregation of Poly(ethylene oxide)−Poly(propylene oxide)−Poly(ethylene oxide) Block Copolymers. J Phys Chem B. 2006;110(46):23068-74.

260. Iyer S. Study of the crystallization behavior of polyethylene oxide in compatibilized and uncompatibilized polypropylene/polyethylene oxide blends. RIT Scholar Works Rochester Institute of Technology New York (USA). 2002.

261. Anta L, Luisa Marina M, García M. Simultaneous and rapid determination of the anticarcinogenic proteins Bowman-Birk inhibitor and lectin in soybean crops by perfusion RP-HPLC. J Chromatogr A. 2010;1217(45):7138-43.

262. The United States Pharmacopoeia. 2005. <1088> In vitro and in vivo evaluation of dosage forms. Rockville (MD).

263. Reddy K, Mutalik S, Reddy S. Once-daily sustained-release matrix tablets of nicorandil: formulation and in vitro evaluation. AAPS PharmSciTech. 2003;4(4):E61-E.

264. Cifuentes C, Aguilar-de-Leyva A, Rajabi-Siahboomi A, Caraballo I. Critical points in ethylcellulose matrices: influence of the polymer, drug and filler properties. Acta Pharm. 2013;63(1):115-29.

265. Miranda A, Millán M, Caraballo I. Investigation of the influence of particle size on the excipient percolation thresholds of HPMC hydrophilic matrix tablets. J Pharm Sci. 2007;96(10):2746-56.

266. Millán M, Caraballo I, Rabasco A. The role of the drug/excipient particle size ratio in the percolation model for tablets. Pharm Res. 1998;15(2):216-20.

267. [EMA] European Medicines Agency. 2013. EMA/CHMP/QWP/428693/2013 Guideline on quality of oral modified release products. London.

268. Ma J, Wang J, Cheng Z, Yin T, Teng H, Xu H, et al. Sustained-release pellets of nifedipine using microcrystals combined with MCC-based matrix. Drug Dev Ind Pharm. 2013;41(2):307-14.

269. Wang Y, Yang J, Qian Y, Yang M, Qiu Y, Huang W, et al. Novel ethylcellulose-coated pellets for controlled release of metoprolol succinate without lag phase: characterization, optimization and in vivo evaluation. Drug Dev Ind Pharm. 2014;41(7):1120-9.

270. Wickham M, Faulks R, Mann J, Mandalari G. The Design, Operation, and Application of a Dynamic Gastric Model. Dissolution Technol. 2012;19(3):15-22.

271. Talukder R, Fassihi R. Gastroretentive delivery systems: a mini review. Drug Dev Ind Pharm. 2004;30(10):1019-28.

272. Polentarutti B, Albery T, Dressman J, Abrahamsson B. Modification of gastric pH in the fasted dog. J Pharm Pharmacol. 2010;62(4):462-9.

273. Zane P, Guo Z, MacGerorge D, Vicat P, Ollier C. Use of the pentagastrin dog model to explore the food effects on formulations in early drug development. Eur J Pharm Sci. 2014;57:207-13.